Universitetet
i Stavanger

FACULTY OF SCIENCE AND TECHNOLOGY

MASTER'S THESIS

Study programme/specialisation: Environmental Engineering / Water Science and Technology	[✓ Spring] / Autumn semester, 2018.. Open/[✓ Confidential]
Author: Hans Kristian Tangen	H.K.T (signature of author)

Programme coordinator: Torleiv Bilstad

Supervisor(s): Sindre Åse Lunde

Title of master's thesis:

Treatment of oily water using a submerged Silicon Carbide flat-sheet membrane:
Technology evaluation and design of a full-scale treatment unit

Credits: 30

Keywords: Submerged membrane filtration, ceramic, SiC, flat-sheet, slop water treatment, oily wastewater flux performance, backwashing, air-scouring	Number of pages: 75 + supplemental material/other: 8 Stavanger, July 13 / 2018 date/year

Abstract

Offshore activity in the oil and gas industry generates high quantities of wastewater. It is of interest for the operators to treat this water offshore to limit shipment costs to onshore treatment facilities, in addition to lower environmental concerns. To be able to treat the water offshore, robust technology with high treatment capacity and low footprint is required. Submerged membrane technology using ceramic flat-sheet membranes is a relatively new technology and has not previously been tested on slop water treatment. A collaboration was established with Norwegian Technology AS, which had an interest in testing submerged ceramic membrane technology with air-scouring, on slop water treatment.

Four different slop water types were tested, labelled as S1, S2, S3 and S4. Based on flux performance, S1 was considered as light, S2 was considered as medium and S3 and S4 was considered as heavy slop. Different filtration/backwashing frequencies were tested, and it was found that more frequent backwashing was frequent backwashing was required for more heavier slop than for the light slop.

Permeate fluxes were found to be highly affected by the frequencies of backwashing. Testing S1 water, 1 second of backwash per minute gave 130% higher permeate flux than 10 seconds per 600 seconds.

Net flux of permeate of up to 114 LMH was obtained on the S2 water, with 3 seconds of backwash per minute. Though a net flux of around 30 LMH was mostly obtained over longer filtration periods.

The S3 water was considered heavy, with a net flux of only 3 LMH. Pretreatment significantly increased the flux by 40%, and addition of coagulant increased the flux by 25%.

The membrane was also able to process highly oil-contaminated water. Indication testing performed on the S4 water resulted in an average permeate flux of 49 LMH and a net flux of 17 LMH, with 3 seconds backwashing per minute.

With the produced data from this research, a design of a mobile slop water treatment unit was suggested. The design shows that most of the obtained fluxes was sustainable in this design due to its compactness. The possibility for upscaling the membrane treatment method for slop water was therefore considered feasible, though further studies on long-term durability would be recommended.

The technology was considered promising due to compact and robust structure, suitable on light slop without pre-treatment and on heavy slop in combination with pre-treatment.

Keywords:

Submerged membrane filtration, ceramic flat-sheet, slop water treatment, oily wastewater, flux performance, backwash, fouling, air scouring

Acknowledgements

I will first like to express my gratitude to Professor Torleiv Bilstad for providing the facilities and necessary resources for this project. I will also give my sincere appreciation to Norwegian Technology and Sindre Åse Lunde for sharing his enthusiasm and time, providing helpful guidance and engaging in constructive criticism in discussions. Thanks also to Remya Nair for helpful guidance on analytical procedures and Evgenia Protasova for constructive criticism on the thesis. Finally, I would like to thank my wife Møyfrid and my two kids Helle Tonette and Olivia for being patient and understanding during this semester of long days at the university, I would not be able to complete the project without their support.

List of figures

Figure 1: Norwegian technology logo www.norwegiantech.com 12
Figure 2: Membrane characteristics of MF, UF, NF and RO (Pentair) 15
Figure 3: Hollow fibre module (Process-Technology) 18
Figure 4: Tubular membranes (Liqtech) 18
Figure 5: Flat sheet module (Cembrane) 19
Figure 6: Cross-flow (left) and dead-end filtration (El–Safty & Hoa, 2012) 19
Figure 7:Flat sheet concept with outside-in filtration, with air scouring(Tianjin-Motimo) 21
Figure 8: Schematic of a submerged membrane filtration (SMF) system (Tianjin-Motimo) 21
Figure 9: Membrane element cross section (Meidensha) 22
Figure 10: Complete single flat-sheet alumina element (Meidensha) 22
Figure 11: Meidensha complete module of stacked flat-sheets 22
Figure 12: Simple schematic of the feed streams and membrane separation principle 23
Figure 13: Schematic representation of the concentration-polarization model near a porous membrane (Gitis & Rothenberg, 2016) 25
Figure 14: Schematic representation of fouling; adsorption, pore blocking and cake formation in pressure driven membrane filtration (Gitis & Rothenberg, 2016) 25
Figure 15: Principle of coagulation (Mazille & Spuhler) 26
Figure 16: Principle of flocculation (Mazille & Spuhler) 27
Figure 17: Schematic of a typical dissolved air flotation tank (Körting-Hannover) 28
Figure 18: Concept of micellar enhanced filtration (Deriszadeh, Husein, & Harding, 2010) 28
Figure 19: Cross-section of the SiC membrane layers (Cembrane) 31
Figure 20: Membrane pilot unit schematic 32
Figure 21: DAF pressure chamber 35
Figure 22: DAF setup 36
Figure 23: Total absorbance spectrum in MicroLab software 38
Figure 24: Reference concentration lines for 0,0 (dark brown), 0,1 (red), 0,2 (light green), 0,3 (purple), 0,4 (grey), 0,5 (green) and 0,6 (green) ml crude oil/liter sample 39
Figure 25: Model for predicting oil concentration 39
Figure 26: Clean water flux at increasing temperatures 42
Figure 27: S1 – Bioreactor wastewater 43
Figure 28: Visual representation of S2 - slop water 44
Figure 29: S3 - Slop water (batch 2) 45
Figure 30: S4 – Flowback water 46
Figure 31: Graphical representation of the removed compounds (VFA, TSS and COD) from the S1 water 47
Figure 32: Average permeate flux for each of the performed backwashing frequencies and BW durations 48
Figure 33: Flux decline in filtration cycles between each backwash, for different filtration/backwash frequencies (600/10, 300/10, 300/5 and 120/5) 49
Figure 34: Membrane relaxation. Cycles of 60 seconds of filtration followed by 10 seconds of relaxation (filtration-stop), without BW 49
Figure 35: Flux and pressure measurements after 1 hour with 10 second of CWP each minute + 5 seconds of CWP every 30 second 50
Figure 36: Graphical representation of the amount of permeate consumed by excessive backwashing, 300/10 configuration on S1 water 51

Figure 37: Backwash volume (ml) per backwash (blue) and per second (orange) for 1, 2, 3, 5 and 10 second BW durations with 50% applied BW-pump intensity. 52
Figure 38: Liters of BW volume per hour of operation for different configurations at 50% BW pump intensity. Backwash durations (s) are represented by different colors at filtration time scenarios of 30, 60, 120, 300 and 600 seconds 53
Figure 39: Backwash volume (ml) per BW cycle (blue) and per second of BW (orange) for 1, 2, 3, 5 and 10 second durations with 30% applied BW-pump intensity. 54
Figure 40: Graphical representation of the BW volume prediction model in liters per hour. Backwash durations are represented by different colors at filtration time scenarios of 30, 60, 120, 300 and 600 seconds. 55
Figure 41: Permeate flux and pressure during a 600/10 configuration on S2-water 56
Figure 42: Net flux and pressure development in 600/10 configuration, 50% BW-pump intensity on S2 water 56
Figure 43: Permeate flux for S2 slop over 7 hours 57
Figure 44: 60/3 configuration with increased membrane surface area on S2 filtration. 58
Figure 45: Permeate flux during a 60/3 configuration of S3 water 59
Figure 46: Sludge and clear phase after DAF treatment 60
Figure 47: 60/10 configuration using DAF processed S3 water as feed 61
Figure 48: Permeate flux of the S3 water after mixing the sludge and clear phase from the DAF treatment, the first 10 minutes, 60/3 configuration 61
Figure 49: Extension of figure 48, continued filtration on sludge and clear phase from DAF, S3 water, 60/3 configuration 62
Figure 50: S4 permeate flux with a 60/3 configuration using 50% BW pump intensity 63
Figure 51: S4 permeate flux at 30% BW intensity, 60/3 configuration 63
Figure 52: Type 1D ISO-container (common name 10 foot container) 67
Figure 53: Concept of the membrane unit shown from the long side. Container/membrane tower ratio are drawn in scale relative to each other 68
Figure 54: Membrane unit shown from short side Container/membrane tower ratio are drawn in scale relative to each other. 69
Figure 55: Permeate buffer tank container (concept) 69
Figure 56: Dissolved air flotation module (concept) 69
Figure 57: NF/RO (concept) separation container for complete purification 69
Figure 58: Permeate production with 100 s relaxation of membrane and 600 s filtration cycles 78
Figure 59: Accumulated volume of permeate vs. Accumulated volume of permeate consumed for BW 82

List of tables

Table 1: MF, UF, NF and RO pore size rages, applications and operating pressures (Cheryan, 1998; Gitis & Rothenberg, 2016) 15
Table 2: Typical ceramic membrane materials (Biesheuvel & Verweij, 1999; Castricum et al., 2008; Gitis & Rothenberg, 2016) 16
Table 3: Examples of industries and function of ceramic MF membranes (Gitis & Rothenberg, 2016; Lenntech) 17
Table 4: Corrosion of advanced ceramics in liquids (Ghali, Sastri, & Elboujdaini, 2007) 30
Table 5: Membrane properties according to the manufacturer (Cembrane) 31
Table 6: Permeate and backwash pump details 32
Table 7: Filtration/backwash configurations tested 33

Table 7: Backwash configurations baseline to construct a tabulated model to predict permeate consumed for backwashing 34
Table 9: Color coded overview of the four different wastewaters used in the experiments 40
Table 10: Parameter values for the bioreactor effluent wastewater 43
Table 10: Measured characteristics of the S2 slop water 43
Table 12: Measured characteristics of the S3 slop water 44
Table 12: Measured characteristics of the S4 Flowback water 45
Table 14: Parameter values of the wastewater before and after membrane separation 47
Table 15: Model 1: Predicting BW-flux (permeate loss) (LMH) at different filtration/BW configurations (50% BW-pump intensity) 53
Table 16: Model 2: Predicting BW-flux (LMH) at different filtration/backwash configurations (30% BW-pump intensity) 55
Table 17: Removal efficiency in the S3 water 58
Table 20: Removal rates from the S4-water 62
Table 19: Energy consumption during 600/10, 60/1 and 60/3 configurations on the S2 water 64
Table 21: Internal dimensions of a 1D container 67
Table 22: Membrane module specifications retrieved from the manufacturer (Cembrane) 67
Table 22: Membrane module/tower specifications retrieved from the manufacturer (Cembrane) 67
Table 24: Collected data in Figure 42 used to calculate the amount of backwash consumed 82
Table 25: : Volume of BW (ml) per backwash cycle and per second in each BW configuration at 50% BW pump intentsity 82
Table 26: Volume of BW (ml) per backwash cycle and per second in each BW configuration at 30% BW pump intentsity 82
Table 27: Baseline for the BW model (50% pump intensity) 83
Table 28: Baseline for the BW model (30% pump intensity) 84
Table 29: S2 water, 600/10 85

Abbreviations

CAGR	Compound Annual Growth Rate
CFF	Cross-flow filtration
CIP	Cleaning in Place
COD	Chemical Oxygen Demand
CWP	Cleaning without pressure
DAF	Dissolved Air Flotation
FBW	Flowback water
HMI	Human Machine Interface
LMH	Unit of flux; liter per square meter per hour $(\frac{liter}{m^2\times hour})$
MBR	Membrane Bioreactor
MF	Microfiltration
NF	Nanofiltration

PLC	Programmable Logic Controller
ppm	Parts per million
R&D	Research & Development
RO	Reverse Osmosis
SMF	Submerged membrane filtration
UF	Ultrafiltration
VFA	Volatile Fatty Acids

Table of contents

- Abstract 2
- Acknowledgements 3
- List of figures 4
- List of tables 5
- Abbreviations 6

1 Introduction 11

- 1.1 Background 11
- 1.2 The Norwegian Activity Regulations (Aktivitetsforskriften) 11
- 1.3 Objective 12
- 1.4 Collaboration with the industry 12
- 1.5 Focus of experimental work 13
- 1.6 Thesis outline 14

2 Theoretical aspects 15

- 2.1 Membrane filtration 15
  - 2.1.1 Basics of membrane filtration 15
  - 2.1.2 Membrane materials 16
  - 2.1.3 Ceramic vs. polymeric membranes 17
  - 2.1.4 Ceramic microfiltration (MF) 17
  - 2.1.5 Membrane configurations 18
  - 2.1.7 Submerged membrane filtration 20
  - 2.1.8 Large scale SMF 21
- 2.2 Membrane operational parameters 22
  - 2.2.1 Flow streams and flux 22
  - 2.2.2 Trans membrane pressure 23
  - 2.2.3 Membrane resistance 24
  - 2.2.4 Separation efficiency 24
  - 2.2.5 Clean water flux 24
  - 2.2.6 Flux decline and fouling 24
  - 2.2.8 Cleaning 25
- 2.3 Coagulation and flocculation 26
- 2.4 Dissolved Air Flotation (DAF) 27
- 2.5 Technologies for membrane enhancement 28
  - 2.5.1 Micellar enhanced filtration 28

    - 2.5.2 Hybrid flotation-membrane filtration ... 29
    - 2.5.3 CFD Computational fluid dynamics (CFD) ... 29
    - 2.5.4 Artificial neural network ... 29
  - 2.6 Silicon Carbide ... 30
- 3 Materials & Methods ... 31
  - 3.1 The SiC membrane ... 31
  - 3.2 The membrane unit system ... 31
  - 3.3 Measuring membrane performance ... 32
    - 3.3.1 Pressure, flux and temperature ... 32
    - Backwash configurations ... 33
    - 3.3.2 Flux measurements ... 33
    - 3.3.3 Membrane relaxation ... 33
    - 3.3.4 Filtration/backwash cycles ... 34
    - 3.3.5 Backwash volume model ... 34
  - 3.4 The Dissolved Air Flotation unit ... 35
  - 3.5 Analytical methods ... 36
    - 3.5.1 Turbidity ... 36
    - 4.5.2 pH ... 36
    - 4.5.3 Energy consumption ... 36
    - 4.5.3 Solids classification ... 37
    - 4.5.4 Oil concentration measurement: Infrared spectroscopy (IR) ... 37
  - 3.6 Wastewater used in the experiments ... 40
  - 3.6.1 S1 - Bioreactor effluent ... 40
  - 3.6.2 S2 - Slop water from tank 2, Stavanger slop (batch 1) ... 40
  - 3.6.3 S3 - Slop water (batch 2) ... 40
  - 3.6.4 S4 - Flowback water ... 41
- 4 Results & Discussion: Slop water treatment with SiC flat sheet membranes ... 42
  - 4.1 Clean water flux ... 42
  - 4.2 Wastewater feed analysis of S1, S2, S3 and S4 ... 43
    - 4.2.1 S1 Feed analysis ... 43
    - 4.2.2 S2 Feed analysis ... 43
    - 4.2.3 S3 Feed analysis ... 44
    - 4.2.4 S4 Feed analysis ... 45
  - 4.3 - S1 Results ... 47
    - 4.3.1 Removal degree ... 47

4.3.3 Backwash frequency and fouling 48
4.3.5 Membrane relaxation 49
4.3.4 Loss of permeate to backwashing 50
4.2 Results for S2 water 51
4.2.1 Removal rates 51
4.2.2 Model for predicting backwashing volume (50% BW pump intensity) 51
4.2.3 Model for predicting backwashing volume (30% BW-pump intensity) 53
4.2.4 Flux performance 55
4.2.7 Increased membrane surface area 57
4.5 Results for S3 water 58
4.5.1 S3 Removal rates 58
4.5.2 Flux performance 58
4.5.3 Dissolved air flotation as pre-treatment 59
4.5.4 Membrane performance after DAF pre-treatment 60
4.5.5 Sludge addition to feed 61
4.6 Results for S4 water 62
4.6.1 Removal rates 62
4.6.2 Flux performance 63
4.7 Additional remarks 64
4.7.1 Cleaning 64
4.8 Energy analysis 64
5 Conceptual design: Development of a submerged flat-sheet slop water treatment unit 66
Module framework 66
Membrane module 68
Additional container modules 69
Module flowchart 71
Flowrate 72
Cleaning 72
6 Conclusions 73
References 75
Appendices 78

1 Introduction

1.1 Background

Slop water is a highly contaminated waste stream that is produced from activities such as cleaning of equipment and tanks offshore. Large amounts of water can be emulsified in the oil due to excess emulsifiers. Typical sources for the ingredients of slop are oily water from cleaning, residual drilling fluids, rain water, various cleaning chemicals and other chemical residuals and hydraulic oil from leakages (McCosh, Kapila, Dixit, Way, & Phipps, 2009; Sorbwater, 2014). The slop water is collected in tanks and regarded as special waste in environmental reports.

Management of slop water is an expensive and time-consuming activity, though a necessary part of offshore operations to prevent discharge of harmful compounds leading to environmental pollution (Carlin, 2002). Traditionally, such wastewater is shipped and treated onshore (Jones & Pujadó, 2006), for example by biological treatment, such as at the facilities of Stavanger Slop in Mekjarvik. The economic interest from oil companies for treating the slop offshore is mainly due to the high costs related to shipping and disposal onshore. An effective way of lowering these costs is to concentrate the hazardous wastewater by separating clean water from the solution for disposal or re-use at site, before transporting the concentrated waste onshore.

With a globally increasing energy demand, extraction of natural resources such as oil and gas will be important to sustain for many years to come. Even with the developments of renewables which is increasingly taking its share of the energy mix, 44% of the total energy mix is still expected to be hydrocarbons by year 2050 (DNV-GL, 2017). Along with increasingly stringent regulations and environmental concern, it is therefore of utmost importance to continue developing more environmental friendly and energy efficient methods for managing oily wastewater offshore.

In Norway, regulations related to discharge limits are stated in the Activity Regulations (Aktivitetsforskriften):

1.2 The Norwegian Activity Regulations (Aktivitetsforskriften)

The Norwegian activity regulations are compiled by the Norwegian Petroleum Safety Authority (Petroleumstilsynet), Norwegian Environment Agency (Miljødirektoratet), Norwegian Directorate of Health (Helsedirektoratet), Norwegian Food Safety Authority (Mattilsynet) and the Norwegian Radiation Protection Authority (Statens strålevern). It contains regulations related to petroleum activities.

It is stated that discharge of slop and other oily wastewaters offshore are imposed to being treated to obtain an oil content as low as possible before discharging it into the sea ("Aktivitetsforskriften," 2010). Treatment facilities should be able to operate well below the permissible discharge limits, targeted for the least possible environmental load. The maximum oil content is never to exceed 30 ppm as a monthly average, though the operators demand is often 10 ppm. The operator is also responsible for performing comprehensive environmental assessments to find the best solution for treating slop and other oil-containing wastewaters ("Aktivitetsforskriften," 2010).

The activity regulation is partly based on the OSPAR convention for the protection of the marine environment of the North-East Atlantic. OSPAR is a legally binding agreement between 15 governments and the EU to reduce marine dumping and pollution (Miljødirektoratet, 2017). This cooperating mechanism is a result of the early 70’s Oslo and Paris (hence the name OSPAR) conventions against dumping and marine pollution, later followed by other governments. Two of the main guiding principles behind the OSPAR strategies are:

- ***Polluter Pays Principle:*** The polluter has the responsibility to pay for activities related to prevention, control and reduction measures of pollution.
- ***Best Available Techniques (BAT) & Best Available Practices (BEP):*** Contracting parties are required to apply both BAT and BEP, including clean technology if possible. These principles changes over time as scientific knowledge and technology advances. BAT is defined as: "the latest stage of development (state of the art) of processes, of facilities or of methods of operation which indicate practical suitability of a particular measure for limiting discharges, emissions and waste". BEP is defined as "the application of the most appropriate combination of environmental control measures and strategies" (OSPAR, 2015).

In accordance to the above-mentioned principles and regulations, the work done in this thesis will investigate the use of ceramic membrane technology for offshore treatment of oily wastewater by the following objectives.

1.3 Objective

The objective of this thesis is to test the efficiency of a flat-sheet Silicon Carbide membrane in a submerged membrane pilot unit for treating slop water from offshore operation, with focus on further development and upscaling.

The feasibility for upscaling this technology to a full-scale unit, potentially in combination with dissolved air flotation, will be evaluated as a conceptual design. This will be done based on results, relevant literature and insight from collaboration with Norwegian Technology AS.

Focus areas in accordance to the objective are listed below:

- Flux performance, in terms of permeate flux, backwash flux and net flux.
- Oil and solids removal degree
- Total suspended solids removal
- Effect of dissolved air flotation as pre-treatment
- Energy efficiency.

1.4 Collaboration with the industry

Norwegian Technology (NT) is a company located in Mekjarvik Stavanger, developing by their own words: "Technologies for the global green economy", mainly providing products and services based on the use of proprietary chemicals to wastewaters such as municipal wastewater, produced water, fracking fluids, completion fluids or any other industrial wastewater source. As an established and experienced company of wastewater treatment they have contributed to the perspective of this thesis with their insight to current important issues and needs in this industry. NT also have ownership in the company Stavanger Slop, which has supplied the slop wastewater used for this thesis.

Figure 1: Norwegian technology logo www.norwegiantech.com

With its experience with several customers in the oil and gas industry, NT have access to information about current challenges and needs related to offshore wastewater purification. Based on feedback from oil companies, NT have in recent time had an increased interest for submerged membrane filtration (SMF) using ceramic membranes, which is a relatively new type of technology. This thesis will be NT's experimental foundation on the technology and its applications for slop treatment by using new pilot unit delivered by Atec Neu-Ulm from Germany. Below are listed the key reasons why submerged membrane filtration technology (SMF) was chosen for these experiments based on feedback from oil companies:

- *Membrane erosion limitation:* Even though membrane technology has proved to be successful in many areas, the prevailing configuration is by tubular cross-flow, which is not always sustainable. NT Customers have reported vast erosion even of ceramic membranes which is a result of the fine particles combined with high shear forces that is produced under cross-flow. This is not the case regarding SMF technology as further explained in chapter 2.1.7.
- *Footprint and uniform transmembrane pressure:* SMF also ensures uniform transmembrane pressure (UTP), resulting in full utilization of the membrane surface area. The flat-sheet structure is beneficial regarding space requirements, as the plates can be stacked closely. The packing density can be up to 200 m^2 of active membrane surface per m^2 of floor space in one tower of modules of full height (2,69 m).
- *Energy efficient:* SMF is also highly energy efficient compared to tubular cross-flow.

1.5 Focus of experimental work

The bulk of the experimental work in this thesis have been to strategically gain as much information as possible in a limited period of time about SMF technology and the new pilot unit which was used in the experiments. Therefore, testing have been done on a set of different wastewaters to get a broader view of the units' functionality. Using this range of difference for the experimental part was considered to be be beneficial, as one important quality of the designed treatment unit in chapter 5 is flexibility in area of usage.

Based on early experiences with the unit, as well as conversations with the manufacturer, it has been assumed that the first hour of operation with a new type of water or unit configuration gives a good indication on how the unit would work over longer periods of time.

- Indication testing removal efficiency
- Gross permeate flux measurements using different backwash configuration
- Measurement and calculation of the net flux by considering the reverse flux (permeate consumed for backwashing).
- Construction of a model for prediction of net flux
- Design of a full-scale treatment unit based on the based on theoretical knowledge and practical experienced gained from the experimental process

The goal has been to evaluate the flat sheet membranes and the approach to the design have been to create a compact and generalized solution.

Planning of the whole experimental process was not practical, since the membrane unit was new and no experience-based knowledge was available. The experimental part was therefore proceeded based on a "learning by doing" approach.

Increased surface area (two extra membranes) was not added from the beginning because only one membrane element was available from the beginning of the experiments.

1.6 Thesis outline

Theoretical aspects of the work in the thesis are found in chapter 2. Materials and methods used in the experiments are found in chapter 3 and the results are presented and discussed in chapter 4. The full-scale design is found in chapter 5, and the conclusion of the thesis is presented in chapter 6.

2 Theoretical aspects

2.1 Membrane filtration

This section explains the basics of what membrane filtration is and what it is used for.

2.1.1 Basics of membrane filtration

A membrane is a barrier that selectively permits the passage of certain compounds while retaining others, and the modern membrane definition is an extension of the Latin word “membrana”, meaning skin (Nath, 2017). Membrane technology has emerged to be an environmental friendly alternative in separating solids from liquid streams, including wastewater. For pressure-driven porous membranes such as MF, UF and NF, the process utilizes pore size exclusion to selectively reject compounds by size, in an isothermal process. Membranes for water separation are usually classified by their pore size, material and shape. By pore size, membranes are divided into microfiltration (MF), ultrafiltration (UF), nanofiltration (NF) or as a reverse osmosis (RO, utilizes the concept of solution and diffusion) (Figure 2) (Table 1).

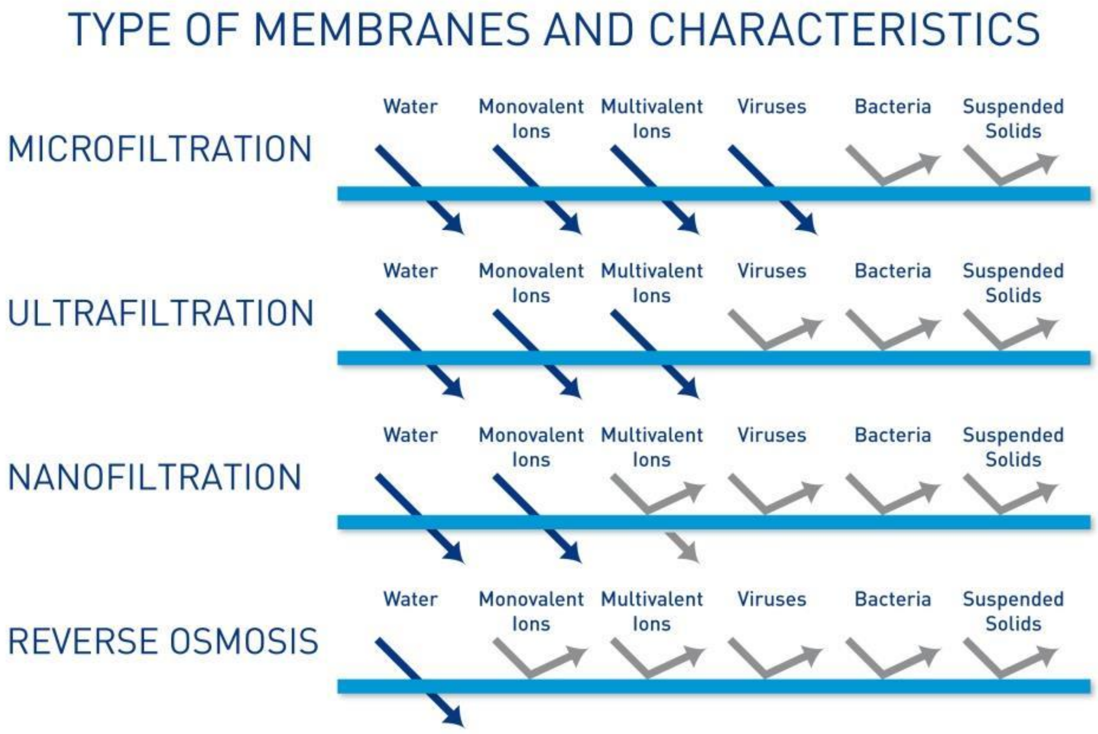

Figure 2: Membrane characteristics of MF, UF, NF and RO (Pentair)

Table 1: MF, UF, NF and RO pore size rages, applications and operating pressures (Cheryan, 1998; Gitis & Rothenberg, 2016)

Membrane class	Pore size, µm	Application/removal	Operating pressure, bar
Microfiltration (MF)	1 – 0,1	Suspended solids, bacteria and large viruses	< 5

Ultrafiltration (UF)	0,1 – 0,01	Macromolecules, fine solids, viruses, dye, proteins and starches	< 10
Nanofiltration (NF) (tight UF, loose RO)	0,01 – 0,001	Molecules and multivalent ions	< 40
Reverse osmosis (RO)	Permeation by solution-diffusion	Monovalent ion separation	< 100

2.1.2 Membrane materials

Independent from pore size, membranes are categorized by their building material and can roughly be divided into either ceramic (inorganic) or polymeric. The morphology of the membrane is either dense or porous where dense membranes separates by solution-diffusion across the membrane such as for gas separation and RO. Dense ceramic membranes are used mostly gas separation and is still being developed and positioned in the market (Gitis & Rothenberg, 2016). The second and most mature type regarding ceramic membranes is the porous structure used for MF and UF applications in industries such as the food, beverage, potable water and wastewater. They are usually composed of a porous internal structure with a thin microporous coating layer with rigid pores and is the type focused on in this thesis. Typical ceramic membrane materials are listed in Table 2.

Table 2: Typical ceramic membrane materials (Biesheuvel & Verweij, 1999; Castricum et al., 2008; Gitis & Rothenberg, 2016)

Material	Properties and use
Alumina (Aluminum oxide, AlO_3)	Most used material, has several allotropes
Silica (Silicon dioxide, SiO_2)	Thin coating layers applicable for gas separation
Titania (Titanium dioxide, TiO_2)	Coating with high pH variation resistance
Zirconia (Zirconium dioxide, ZrO_2)	Coating especially alkali resistant coating material
Silicon Carbide (SiC)	Hydrophilic, versatile, especially alkali resistance

2.1.2.1 Development of ceramic membranes

Humans have utilized ceramics for thousands of years, with the oldest man-made ceramic artifact found by archeologists dating back 26000 years from today (Owoeye, Olokode, Aiyedun, & Anyanwu, 2012). Ceramic materials typically consists of metal oxides or silicates and oxides such as Alumina (Al_2O_3) are often referred to as “technical ceramics” (Boch & Niepce, 2010). They can be found naturally occurring in minerals and clays and be processed into shapes by heating and subsequent cooling. Archeological discoveries show that the history of ceramics applications has expanded from simple tools and pottery for storage of food around 9000 BC, to water purification by ceramic filters in the Roman Empire 800 BC, where the drinking water was transported through air-open aqueducts (Griffin, 2003). We still use ceramics as simple tools such as dinnerware, bricks and bathroom sinks, but in the last century the ceramic technology has also developed into more technological purposes. In addition to membranes, we use it in a range of advanced applications such as artificial bones and teeth, electronic devices and other applications where long-term robustness and inertness is required. During the second world war, uranium isotopes were separated for nuclear weapons production, using semipermeable oxide membranes which were the only membranes capable of withstanding the high temperature and corrosive environments required for this process (Gillot, 1991). In the 1960's, the development of ceramic membranes advanced when the idea of a skin-layer surface on the porous membrane body was introduced, first for polymeric membranes (Loeb & Sourirajan, 1962). Ceramic membranes were commercialized in the beginning of the 1980s' and considered as a major step in membrane technology development (Cheryan, 1998). It was through the 1980s and 1990s adapted for applications such as gas separation (De Vos & Verweij, 1998), biotechnology (Shackleton, 1987), food and beverage processing. Around year 2000, ceramic membranes were already in use at Japanese water and wastewater treatment plants, but have in recent years also started to reach Europe and the USA, and is today considered as an established separation technology in this field (Gitis & Rothenberg, 2016).

2.1.3 Ceramic vs. polymeric membranes

Ceramic membranes have several advantages over polymers. The typical ones found in literature are:

- Higher flux due to high porosity, narrow pore size distribution and higher hydrophilicity
- Higher mechanical and chemical stability makes cleaning more convenient
- Better fouling resistance
- Long lifetime
  (Gitis & Rothenberg, 2016; Lin, Kumakiri, Nair, & Alsyouri, 2002; Van Gestel et al., 2003)

Although ceramic materials have been known for longer than polymers and despite the above-mentioned advantages, polymeric membranes dominate the market. The obvious reason for this is the price. On average, ceramic membranes cost 3-5 times more than a polymer (Yacou et al., 2013), which makes polymers the obvious choice for many new installations. However, in recent years many companies all over the world have found interest in the potential of ceramic membranes. The possibility of high temperature cleaning-in-place (CIP) with almost any chemical cleaning agent is especially important in the industry. Companies such as Cembrane (Denmark), Jiangsu Jiuwu Hitech Co. (China), Filtox (Switzerland), TAMI Industries (France), LiquiTech (Denmark), Corning (USA), Atech Innovations (Germany) and many more deliver full-scale installations. The global interest has led to increased R&D in the field and the obstacle of high cost is gradually being resolved and is expected to have increasing market share over the next years, with a forecasted compound annual growth-rate (CAGR) Of 10-15% (Gitis & Rothenberg, 2016; Pabby, Rizvi, & Requena, 2008)

2.1.4 Ceramic microfiltration (MF)

MF membranes have a pore size between 0,1 – 10 μm and has been used for a range of applications, including oily wastewater treatment in recent years (Abadi, Sebzari, Hemati, Rekabdar, & Mohammadi, 2011). Some common applications of MF membranes are listed below in Table 3.

Table 3: Examples of industries and function of ceramic MF membranes (Gitis & Rothenberg, 2016; Lenntech)

Treatment/industry	Function
Wastewater treatment	Turbidity removal and disinfection, often in combination with coagulants to remove soluble contaminants. Oil-water separation.
Potable water	Clarification, disinfection and pre-treatment prior to UF/NF/RO
Cold sterilization	Removal of bacteria and suspended solids from pharmaceuticals or beverages
Dairy processing	Separation of casein from whey proteins

Petroleum refining	Removal of particulates in flue gases

2.1.5 Membrane configurations

Membrane elements come in different shapes and technical configurations, each with their own advantages and disadvantages. Each membrane is typically connected in a module, which can further be connected into larger production units often called trains or towers. For ceramic membranes the most relevant modules are stacked flat-membranes (plate-and frame or flat sheets module), tubular and hollow fiber. Each membrane is commercially produced either as plates (flat sheets) assembled into plate-and-frame/flat-sheet modules, or in tubular form assembled into tubular or hollow fiber modules. (Gitis & Rothenberg, 2016)

Figure 3: Hollow fibre module (Process-Technology)

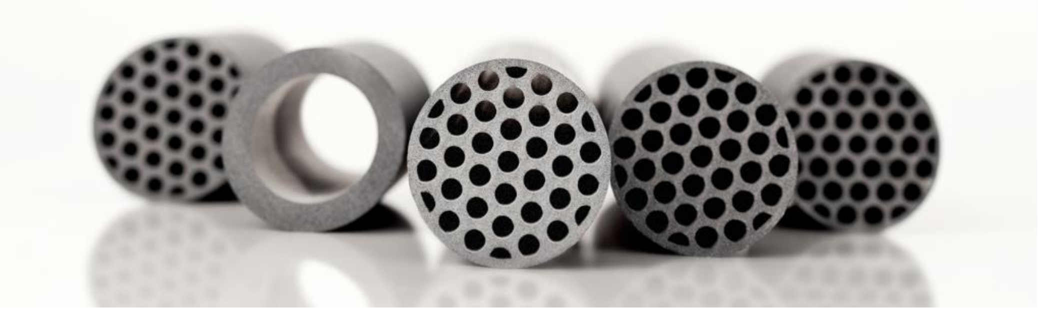

Figure 4: Tubular membranes (Liqtech)

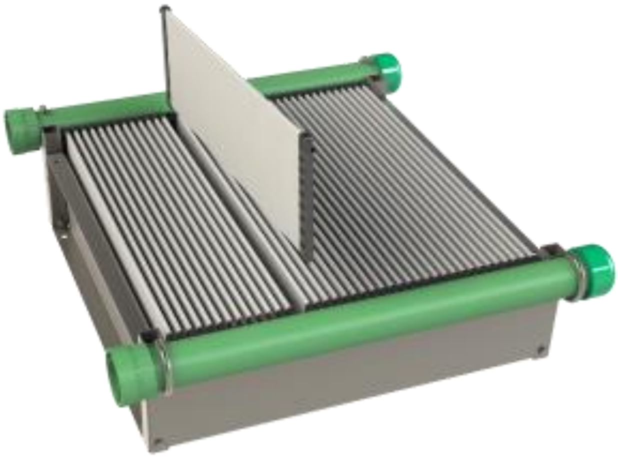

Figure 5: Flat sheet module (Cembrane)

2.1.6 Dead-end vs. Cross-flow filtration

There are two general concepts for the operation mode in membrane filtration; dead-end and cross-flow filtration (CFF) (Figure 6). Dead-end filtration is the oldest and most intuitive kind, where the fluid is directed perpendicular to the surface of the membrane, comparable to a filter in a vacuum cleaner. In CFF mode, the feed water is transported parallel to the membrane surface. It can go in loops for the retentate/concentrate to be recycled. Shear forces generated by the cross-flow velocity (CFV) reduces the amount of fouling. However, CFF demands high amounts of energy to operate to maintain the CFV. Even though fouling is not prevented by the cross-flow type of shear in dead end filtration, other methods can be used to prevent fouling such as frequent backwashing, spinning, air scouring and other forms of turbulence inducing functions (Figure 7).

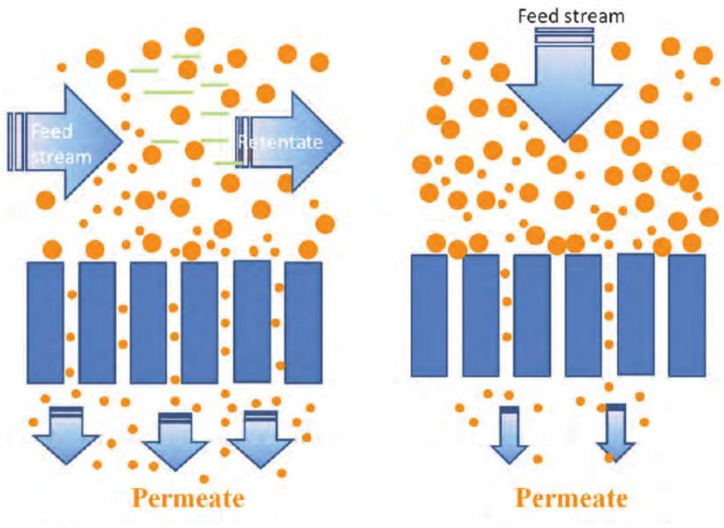

Figure 6: Cross-flow (left) and dead-end filtration (El–Safty & Hoa, 2012)

2.1.7 Submerged membrane filtration

Submerged membrane filtration (SMF) is a relatively new approach to membrane filtration where ultra-low negative pressure is applied for continuous outside-in, dead-end filtration. SMF represents a cheaper alternative to the conventional cross-flow membrane system. The SMF membranes are either of flat-sheet or hollow fiber configurations, submerged into an open feed water, usually vertically (*Management agency revised basin management plan project*, 2003; Tianjin-Motimo). Air bubbles/air scouring is usually supplied from the bottom of the feed tank by an air diffuser to provide shear (and oxygen in membrane bioreactor applications) across the vertically mounted membrane. A small transmembrane pressure of < 1 bar is generated hydrostatically, enhanced by a vacuum suction pump. The permeate flux per area is generally smaller than in cross flow, which requires a larger surface area, but the flat membranes can be stacked together and fitted as boxed modules containing over 70 m^2/m^3 (Cembrane). The power consumption is also significantly lower. Conventional cross-flow often requires over 10 kWh/m^3 to maintain the flux, due to the cross-flow velocity required to limit flux decrease (polarization concentration and cake layer formation) on the membrane. In SMF, gas sparging is used to gain a similar effect on the membrane surface but with a significantly lower power consumption, below 3kWh/m^3 (down to 0,02 kWh/m^3 for brackish groundwater (Cerafiltec)), less than 1/3 of cross-flow (Koltuniewicz, 2015). Though in cases such as for wastewater, CIP (cleaning-in-place) and backflushing must be added.

Gas/air sparging along with critical flux theory are two of the concepts taken advantage of in SMF technology. Critical flux is defined as the highest flux obtainable without fouling over time (Li & Li, 2015). Cleaning procedures are somewhat different than regular CFF and individual consideration for cleaning and maintenance for each membrane and feed flow is essential. In MF, turbulence such as with gas sparging is necessary to remove concentration polarization and buildup of cake layer and initiation of fouling. Whereas in UF, only stopping the filtration periodically (membrane relaxation) can be sufficient to transfer the polarizing layer back to the bulk (Koltuniewicz, 2015; Tianjin-Motimo).

As an example of large scale SMF, Tianjin Motimos' SMF module system can treat almost all kinds of wastewater. These systems can be integrated with online control, surveillance and cleaning possibilities, so that in case of a problem with the membrane it can quickly be judged and isolated even from a remote location (Tianjin-Motimo). According to several manufacturers of SMF systems, the economic factors supporting SMF is the relatively low investment cost due to simple design, easy installation/retrofitting, small footprint and low power consumption and maintenance (Cembrane; Meidensha; Tianjin-Motimo).

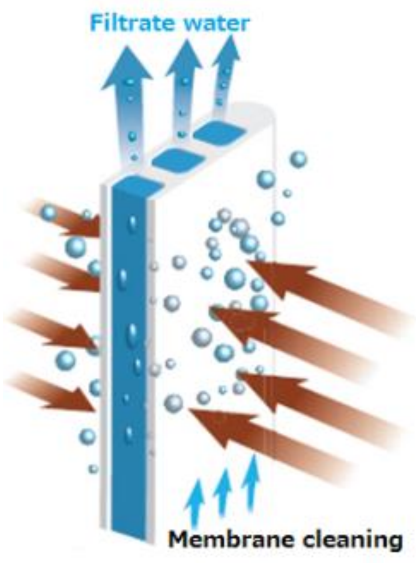

Figure 7:Flat sheet concept with outside-in filtration, with air scouring(Tianjin-Motimo)

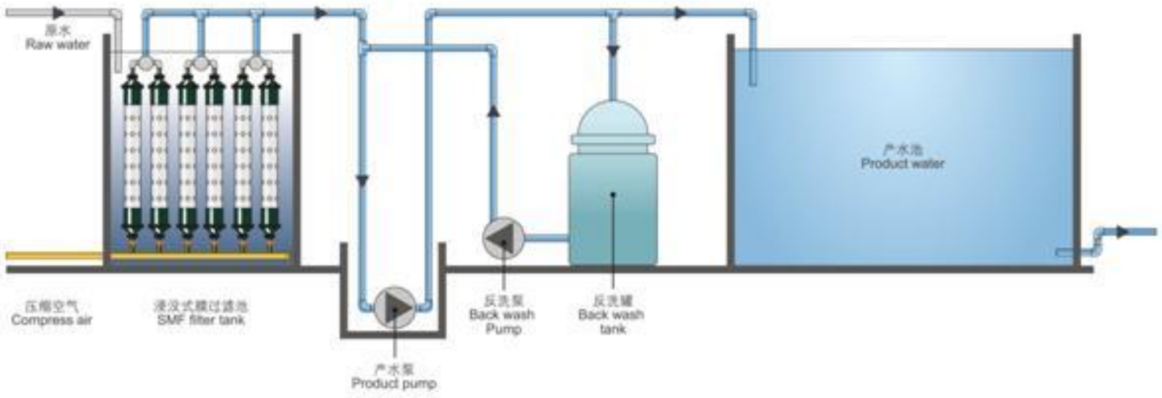

Figure 8: Schematic of a submerged membrane filtration (SMF) system (Tianjin-Motimo)

2.1.8 Large scale SMF

Ceramic SMF are already used in big scale. Meidensha, a well-established 120 years old Japanese company with long experience on wastewater treatment and membranes are producing flat-sheet alumina elements for outside-in filtration suitable for industrial treatment including oil, chemicals and suspended solids. Figure 11 shows a stacked module consisting of 400 alumina sheets with a total membrane surface of 200 m^2. It was installed in 2014 as Singapores' first ceramic MBR plant, to treat and recycle over 4500 m3/d of industrial wastewater (Kekre et al., 2015). Treatment of miscellaneous wastewater from a hotel using this module type was also commercially initiated in 2014, with a flow around 300 m^3/d. The water was successfully reused for toilet washing water while reducing loading on downstream plant (Meidensha). Cembrane has also recently delivered its flat-sheet ceramic to several large-scale facilities such as for produced water reuse (RO pre-treatment), on-site bilge water (containing oil, suspended solids, sea water, micro-organisms and various other accumulated waste) treatment in a cruise-ship. Cembranes' flat-sheet module was even implemented for thickening of waste activated sludge from 15000 mg/l up to 45000 mg/l (Cembrane). Figure 9,10 and 11 shows how a typical submerged membrane module is constructed.

Figure 11: Meidensha complete module of stacked flat-sheets

Figure 9: Membrane element cross section (Meidensha)

Figure 10: Complete single flat-sheet alumina element (Meidensha)

The successful integration of ceramic flat sheet membranes in a wide range of both treatment volume and wastewater type, done by leading corporations like Meidensha and Cembrane shows that the use of ceramic submerged membrane technology is increasing and is likely to have a promising future of water processing engineering. No documented results are found in the case of slop water treatment, as most conventional membrane treatment plants are based on tubular cross-flow filtration. As mentioned in the Objectives of the thesis, the baseline for the experimental part of this thesis is to investigate the potential utility of using submerged membrane technology combined with dissolved air flotation to design a smart unit for slop water treatment. The SMF technology is proven to be mature enough for upscaling, but still seems not to be overly established in the market, which makes it an interesting technology to investigate potential wider areas of applications.

2.2 Membrane operational parameters

2.2.1 Flow streams and flux

For porous ceramic MF/UF liquid filtration, the feed stream (**Q_f**) is divided into two separate streams; permeate (**Q_p**) and retentate (**Q_r**). If the purpose of the filtration is purification, the permeate is the product with retentate as by-product. In other cases, the retentate will be considered the product for example when up-concentration of a mixture is the purpose. This balance can be expressed mathematically as in Equation 1:

$$Q_f = Q_r + Q_p$$

Equation 1: Flow balance of the feed (Q_f), retentate (Q_r) and permeate (Q_p) volumes

Where the flow rate of Q (***Q_q*, *Q_r*, *Q_f***) is measured in volume (liter) over time (hour):

$$Q = \frac{V}{t}$$

Equation 2: Flow rate

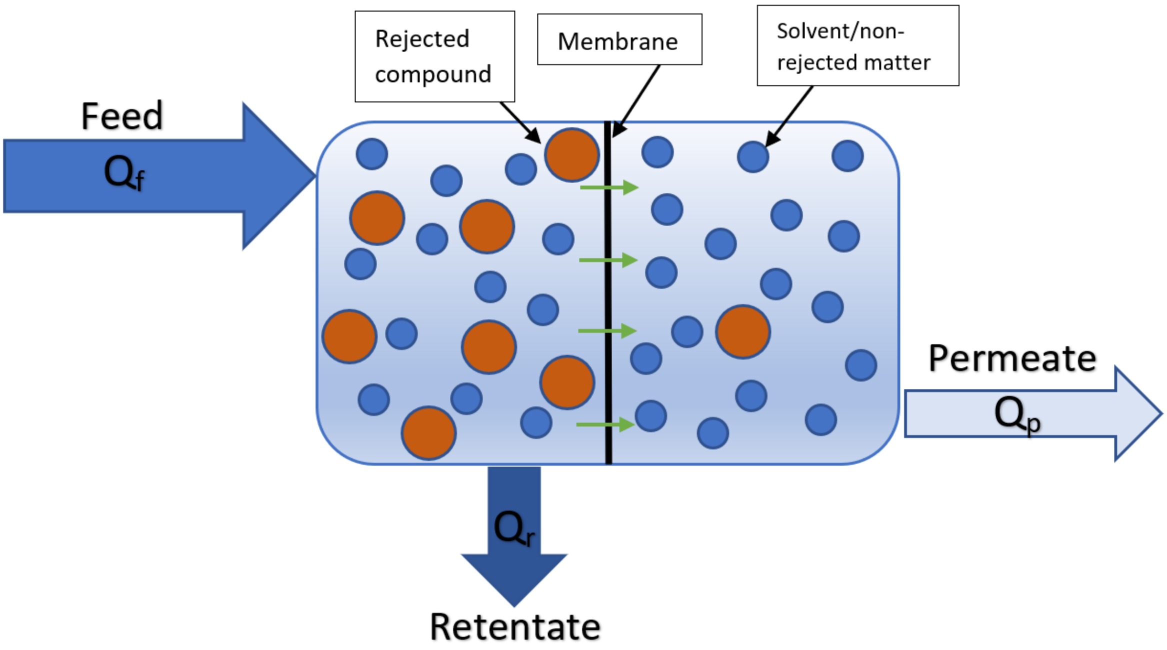

Figure 12: Simple schematic of the feed streams and membrane separation principle

The flowrate or flux (J_p) of permeate through the membrane is one of the most important parameters in industrial use of membranes. The flowrate is logically dependent on the size of the membrane surface area and is in this thesis as well as in much of the literature displayed by the unit of LMH (liter per square meter per hour) (Equation 2), mathematically expressed as:

$$J_p = \frac{Q_p}{A_m} = \frac{V_p}{A_m \times t} = LMH$$

Equation 3: Measured flux

Where ***J_p*** is the permeate flux ($l/m^2/h$), ***V*** is the volume of produced permeate (liters), ***A_m*** is the active surface area of the membrane (m^2) and ***t*** is the time (hours) (Gitis & Rothenberg, 2016).

2.2.2 Trans membrane pressure

Since membrane separation does not happen spontaneously, a driving force is required. Pressure, temperature, concentration and electrical potential can be used in different applications, but for liquid-liquid separation using MF or UF membranes pressure is most commonly used. The net pressure over the membrane is referred to as trans membrane pressure (TMP) and is for dead-end filtration expressed as:

$$TMP = P_f - P_p$$

Equation 4: Trans membrane pressure for dead-end filtration

Where P_f and P_p is the acting pressures on the feed and permeate side of the membrane, respectively.

2.2.3 Membrane resistance

Liquid permeation is impeded by the membrane resistance by which it must overcome to produce any permeate. The total membrane resistance (R_t) is the sum of the intrinsic resistance of the membrane itself (R_m) in addition to any accumulated matter or fouling resulting in flux decrease:

$$R_t = R_m + R_f$$

Equation 5: Membrane resistance

To express membrane performance independent of pressure, membrane permeability (***M***) can also be expressed by calculating amount of flux per unit of TMP:

$$M = \frac{J_p}{P_T}$$

Equation 6: Permeability

2.2.4 Separation efficiency

To evaluate the degree of purification, the retention ratio (R) is expressed dimensionless by calculating the ratio between C_p and C_f, which are the concentrations of the compound in focus in the permeate and feed, respectively. Whereas perfect separation gives an R value equal to 1:

$$R = 1 - \frac{C_p}{C_f}$$

Equation 7: Separation efficiency/retention

2.2.5 Clean water flux

The flux of clean water through the membrane, “clean water flux” (CWF), is measured before any fouling has occurred and is used as a reference value for the performance throughout the membrane lifetime to detect flux retardation. Significant decline in CWF (given that temperature and pressure are the same in both measurements) after physical cleaning indicates irreversible fouling, hence chemical cleaning should be performed to restore the flux. It is usually not expected to gain back 100% of the original clean water flux after every chemical cleaning, though the restoration is often higher for ceramic than polymeric membranes since ceramic materials can handle stronger cleaning chemicals. Significant CWF or permeability reduction after thorough chemical cleaning indicates that it is time to replace the membrane (Cheryan, 1998; Gitis & Rothenberg, 2016).

2.2.6 Flux decline and fouling

Depression in membrane performance is mostly the result of either concentration-polarization (CP) (Figure 13) or fouling (Figure 14). CP is the result of insufficient back-transfer of accumulated solutes, which causes a concentration gradient near the membrane surface and can in some cases result in gel or cake layer formation. The CP can be controlled by lowering TMP and flux or by turbulence created from air diffusers in submerged filtration. If the solute is physically attached to the membrane, fouling arises. Fouling can be described as “The process resulting in loss of performance of a membrane due to the deposition of suspended or dissolved substances in its external surfaces, at its pore openings, or within its pores" (McNaught & Wilkinson, 1997). Naturally, fouling is unwanted as it results in increased membrane resistance, hence more energy is required to perform the separation. Periodic backwash and chemical cleaning are therefore essential for maintaining a sustainable membrane operation over time.

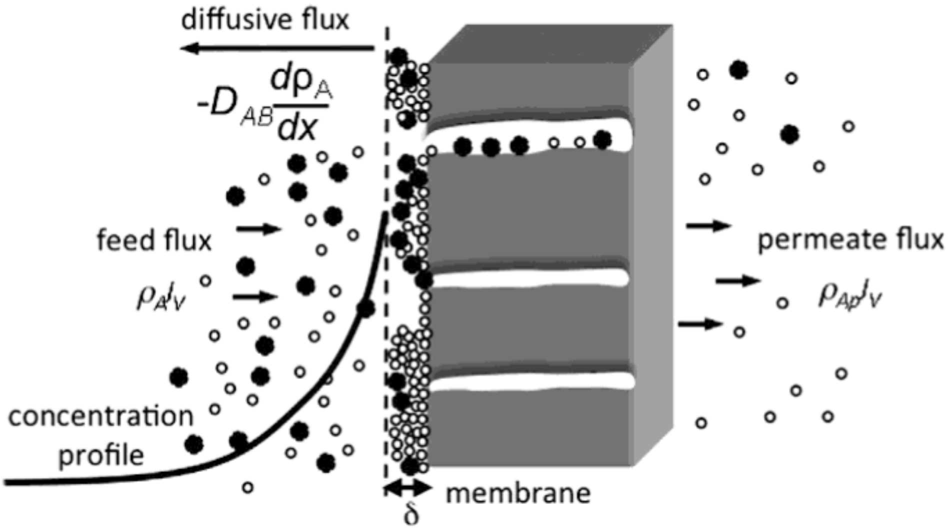

Figure 13: Schematic representation of the concentration-polarization model near a porous membrane (Gitis & Rothenberg, 2016)

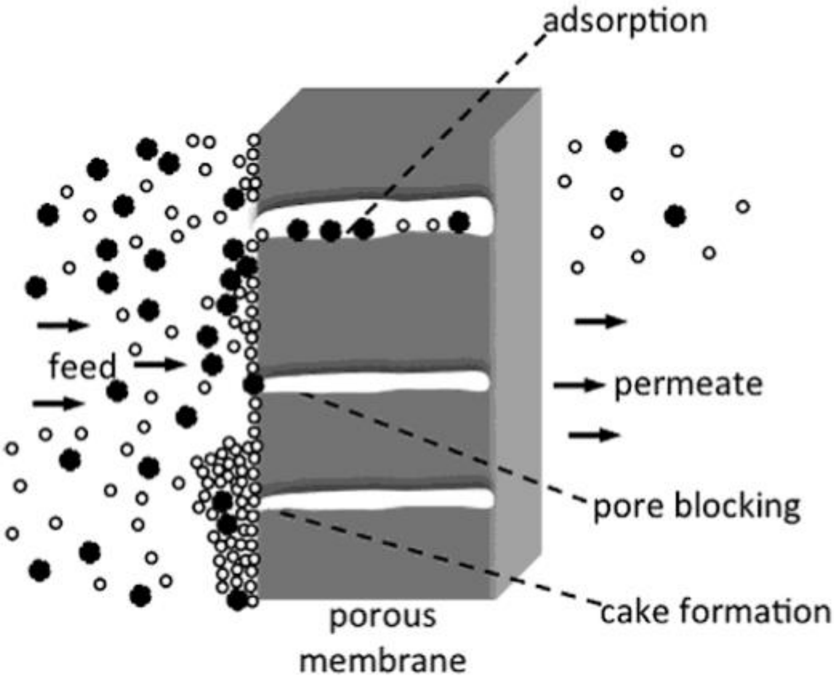

Figure 14: Schematic representation of fouling; adsorption, pore blocking and cake formation in pressure driven membrane filtration (Gitis & Rothenberg, 2016)

2.2.8 Cleaning

Foulants must be regularly removed from the membrane to prevent severe fouling. This can be done either physically or chemically. Physical cleaning such as hydraulic backwashing is more cost-efficient than chemical cleaning, but some foulants require chemical cleaning to be removed. The degree of cleaning efficiency is controlled by comparing the flux ratio of the clean water flux after cleaning with the original clean water flux from before the membrane had undergone any separation. A clean membrane should be free from physical, chemical and microbial matter. Fouling that can be physically removed is considered reversible while fouling which requires chemicals to be removed is considered irreversible fouling. Chemicals for cleaning are determined based on the type of fouling. Depending on the feed, fouling has different characteristics and can be categorized as organic, inorganic (scaling), colloidal or biofouling.

2.3 Coagulation and flocculation

Colloids in colloidal suspensions carry a net electrical charge (in its stationary fluid layer on the particle) which will usually have a potential difference from the bulk liquid, referred to as zeta potential. This leads to dispersion of colloids given they are small enough not to be controlled by gravitational forces. The particles also repel similarly charged colloids and is more stable in the bulk liquid. The higher zeta potential, the more stable mix. To gather the colloids together, as in wastewater purification, the particle charge needs to be neutralized to destabilize the mix and for the particles to bond together eventually into flocs which can then be separated from the solution (Figure 15) (Metcalf & Eddy, 2014; Ødegård, 2014)

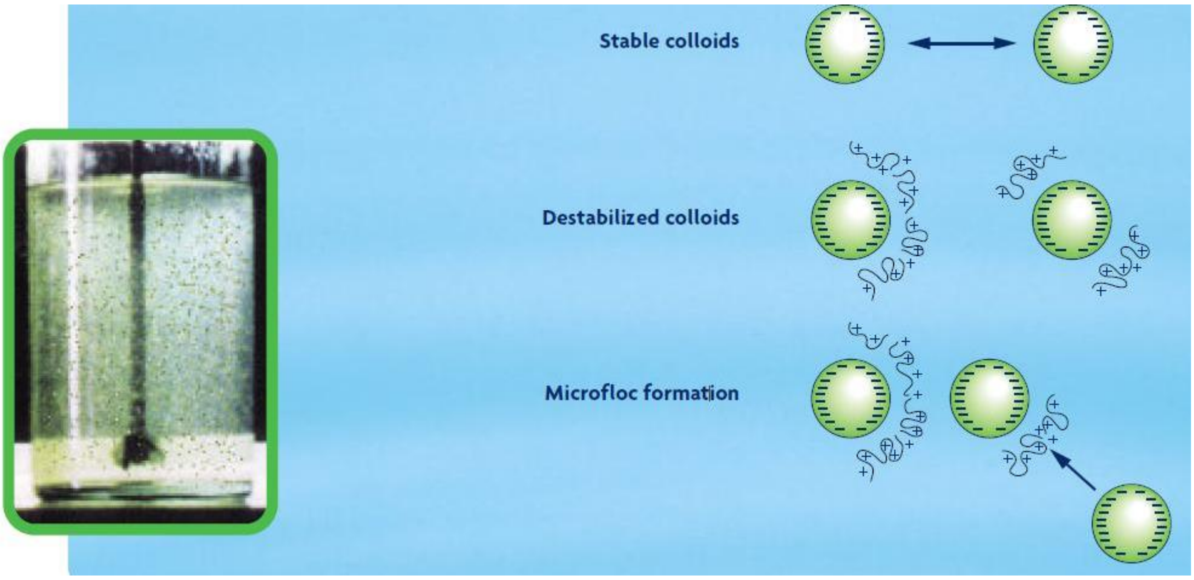

Figure 15: Principle of coagulation (Mazille & Spuhler)

The added coagulant must be of the opposite charge of the particle charge. For a negative zeta potential, a positively charged coagulant, for example a trivalent metallic salt such as Al^{3+} (in the form of aluminium sulphate, $Al_2(SO_4)_3$) is added to gain an electro-kinetic potential near zero. Van der Waals forces then can act between the particles to form flocs. A flocculant polymer can also be added to enhance the floc stability. The polymer acts as a bridge between the destabilized colloids or flocs (Figure 16) and can be used either after coagulation or in some cases as a primary coagulant. Anionic/cationic, inorganic/organic polymers are tailored to meet the requirements of achieving flocculation depending on the characteristics of the wastewater. (Metcalf & Eddy, 2014; Ødegård, 2014)

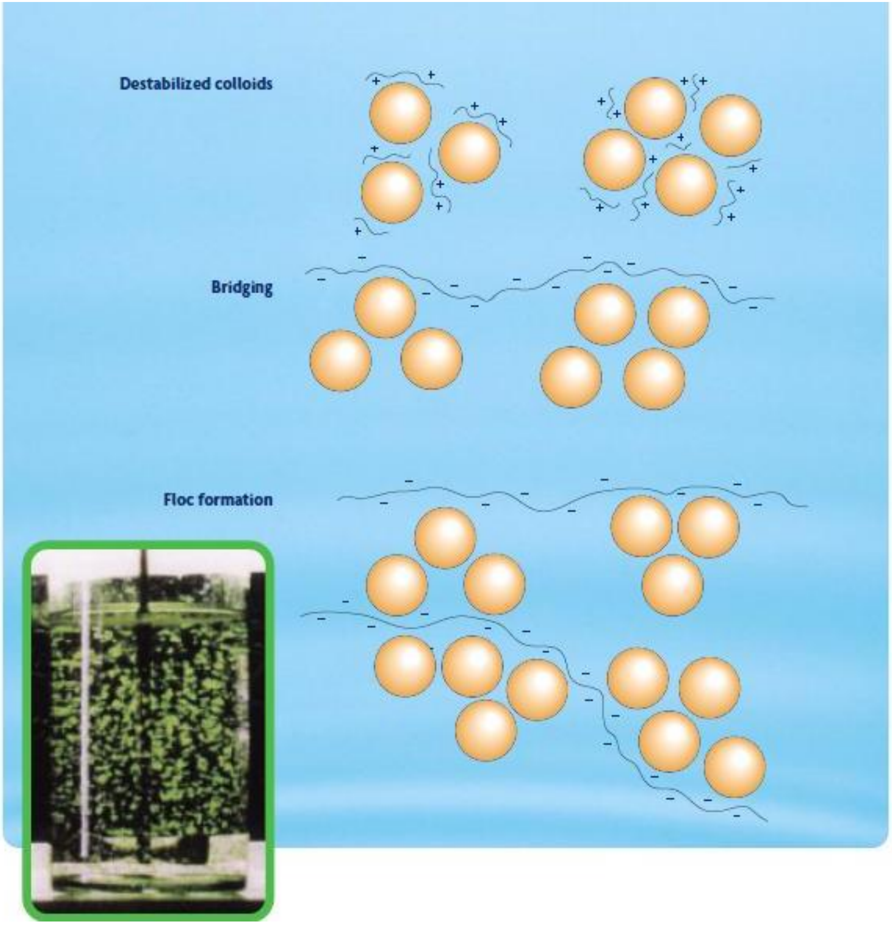

Figure 16: Principle of flocculation (Mazille & Spuhler)

2.4 Dissolved Air Flotation (DAF)

Dissolved air flotation is a treatment process where particles are separated by altering the settling velocity of the pollutant particles based on Stoke's Law (Equation 1) using water supersaturated by air, according to Henrys' Law (Equation 2):

$$v_c = \frac{d^2 g(\rho_p - \rho_f)}{18\mu}$$

Equation 1: Stokes law

Where $\boldsymbol{v_c}$ is the settling velocity of the particle (m/s), $\boldsymbol{d}$ is the diameter of the particle, $\boldsymbol{g}$ is the gravitational acceleration (m/s^2), $\boldsymbol{\rho_f}$ and $\boldsymbol{\rho_p}$ are the mass densities of the fluid and particle, respectively (kg/m^3) and $\boldsymbol{\mu}$ is the dynamic fluid viscosity (kg/m×s). The settling particle is assumed to be spherical. Henry's law explains the saturation of air according to pressure:

$$C_s = p_g \times H_g$$

Equation 2: Henrys' law

Where C_s is the concentration of a particular gas in the liquid at equilibrium, p_g is the partial pressure of the gas over the liquid and H_g is the Henry's constant for the particular gas.

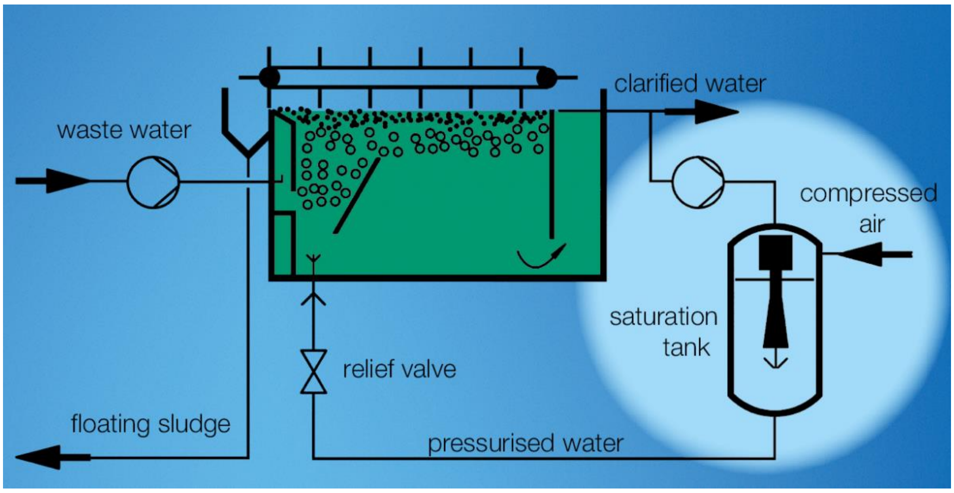

Figure 17: Schematic of a typical dissolved air flotation tank (Körting-Hannover)

According to Stokes law, particles that are either big (high *d*) and/or have a high mass density (ρ_p) will increase the settling velocity. But if the density is similar to the fluid and/or the diameter is small, the settling velocity approaches zero. Altering ρ_p with air bubbles, which have a low mass density, the particle will float to the surface instead of being dispersed in the solution. Introducing air by diffusers will not help because of high turbulence by the big bubbles. Instead, air is saturated into a batch of water in an external pressurized tank, then released into the DAF tank (Figure 17). Based on Henrys' Law (Equation 2) the pressure-drop results in tiny bubbles forming and interacting with the particles or flocs, resulting in negative settling velocity floating them onto the surface where sludge is formed and separated from the tank. The feed water can be dosed with a coagulant and/or a flocculant to enhance the process (Aarestrup, 2018).

2.5 Technologies for membrane enhancement

In this subchapter, theoretically researched technologies considered as valuable for improvement of membrane filtration processes are presented.

2.5.1 Micellar enhanced filtration

Micellar enhanced filtration (MEF) is the combination of surfactant addition to the feed and membrane filtration, to collect small compounds into larger particles or micelles, which can then be separated by the membrane. This allows separation of compounds that would normally require significantly smaller pore size in the membrane. Micelle formation also reduces the interactions between the membrane surface and the contaminants which leads to reduced fouling. (Deriszadeh et al., 2010)

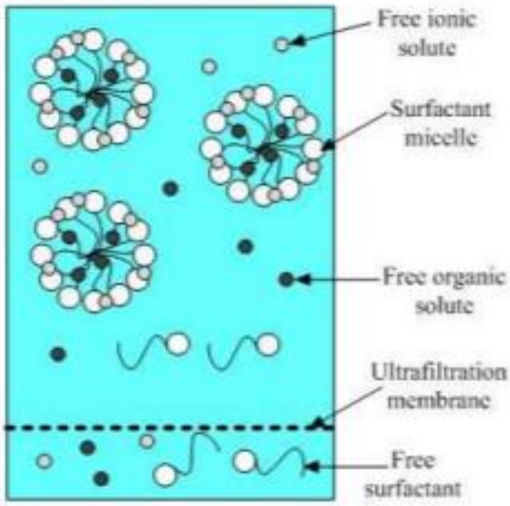

Figure 18: Concept of micellar enhanced filtration (Deriszadeh, Husein, & Harding, 2010)

2.5.2 Hybrid flotation-membrane filtration

Tests have shown that dissolved air flotation can be implemented and combined directly with membrane filtration. The flotation and membrane filtration process is then done from the same tank by submerging specially designed MF or UF modules directly into the reactor, allowing a compact design, which also have shown to be cost efficient for a broad range of wastewaters, compared to DAF or membrane filtration alone (Al-Zoubi, Al-Thyabat, & Al-Khatib, 2009).

2.5.3 CFD Computational fluid dynamics (CFD)

CFD is powerful software tool, able to predict flow and performance in fluid systems during the design process of the product. Digital prototyping saves time on prototype building and in the end extends the product lifetime and reduces maintenance costs by reaching more optimal solutions. In recent years, CFD software has in some cases been applied in membrane optimization by data-simulation of the fluid on the membrane surface, mass transfer modelling and prediction of fouling layer buildup. This can be a useful and effective tool in optimizing the design process. (Rahimi, Madaeni, Abolhasani, & Alsairafi, 2009; Sengur et al., 2015)

2.5.4 Artificial neural network

Artificial neural networks (ANN) are computational systems that can be implemented in a range of processes, with an increasing area of applications. The technology is inspired by biological neural networks, which feeds information from sensors to a computational “brain” that can be programmed to interpret the automatically collected data and use it to control operational parameters to reach optimal process configurations any time through the process. The ANN system progressively improves by learning after tailored learning algorithms are installed, but not requiring task specific programming. ANN technology has shown promising results in combination with membrane filtration in MBR trials, and is an area of great potential for optimization of membrane filtration processes (Schmitt & Do, 2017).

2.6 Silicon Carbide

Silicon carbide (SiC) is a thermally and chemically stable material with useful properties such as high hardness, strength, corrosion and erosion resistance. Pure Silicon Carbide is one of the hardest minerals on earth based on “Mohs scale of mineral hardness”(Cembrane). Because of its durability and strength, it is a versatile material used for a wide range of applications such as high-end brake discs, bullet proof vests and industrial heating elements. It is also used as abrasive in polishing and water-jet cutting, in graphene production, steel production, LED lighting and semiconductors. (Abderrazak & Hmida, 2011; Miyahara et al., 2015). It has a high corrosion resistance compared to other materials related to membranes, are summarized in Table 4 below.

Table 4: Corrosion of advanced ceramics in liquids (Ghali, Sastri, & Elboujdaini, 2007)

	Corrosive weight loss (mg × cm^{-2} × year^{-1})			
Test envirionment (wt % reagent)	Silicon carbide	Aluminium oxide	Si/SiC composites	Tungsten Carbide
98% H_2SO_4	1,8	65,0	55,0	> 1000
50% NaOH	2,5	75,0	> 1000	5,0
53% HF	< 0,2	20,0	7,9	8,0
70% HNO_3	< 0,2	7,0	> 1000	> 1000
45% KOH	< 0,2	60,0	> 1000	3,0
25% HCl	< 0,2	72,0	0,9	85,0
57% HNO_3	< 0,2	16,0	> 1000	> 1000
85% H_3PO_4	< 0,2	> 1000	8,8	55,0

3 Materials & Methods

3.1 The SiC membrane

The SiC membrane used in the experiments was manufactured by Cembrane, with a flat-sheet shape with an asymmetric internal structure, built for vacuum driven outside-in filtration. The surface layer (to the left in Figure 19) has a thickness of 0,1 mm supported by an 8 mm more porous body structure for support. The membrane material is highly hydrophilic allowing high wettability of the membrane inducing good water flux through the membrane, with a water droplet contact angle of only 10°, which is relatively low compared to aluminum oxide (30°) or cellulose UF (55°). Extensive membrane properties and limitations are listed in Table 5.

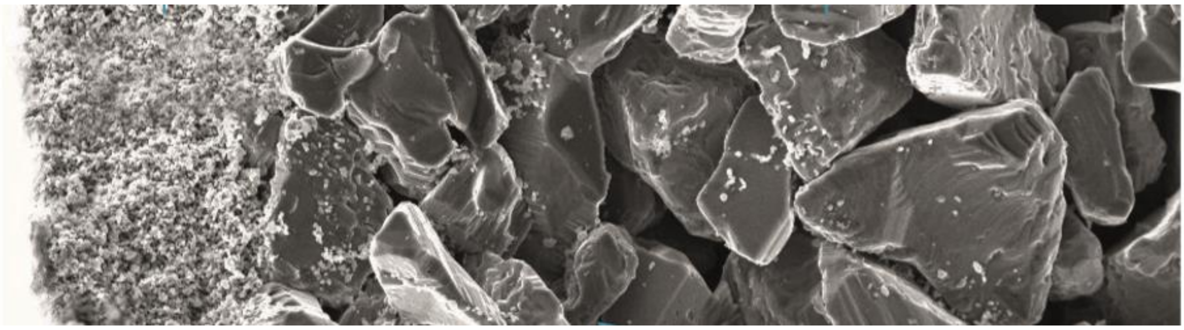

Figure 19: Cross-section of the SiC membrane layers (Cembrane)

Table 5: Membrane properties according to the manufacturer (Cembrane)

Specifications and properties	
Membrane material	Silicon Carbide (SiC)
Cap material	Glass fiber/PPS (NSF61)
Active membrane surface per membrane	0,065 m^2
Number of available membrane slots	4
Pore size	0,1 µm
pH range	1-14
Isoelectric point	pH 2,7
Clean water permeability	15000 LMH/bar
Suction pressure, max.	-0,700 bar
Backwash pressure, max.	2 bar
Operating temperature	5 – 80 °C
Cleaning methods	Backwash, ozone, high pressure jet, chemical cleaning

3.2 The membrane unit system

The membrane unit was delivered by Atec Neu-Ulm (Germany). The unit was programmed and controlled using an integrated HMI (Human Machine Interface) where backwash frequencies and pump intensity (for both backwash and filtration pumps) was programmed to the preferred choice. The surface area of one membrane element was 0,065 m^2 and there was 4 available slots to insert membrane. Due to practical limitations only one membrane was used during most of the experiments. A total of 3 elements (0,195 m^2) was used for the last part of the experiments (noted in the Results & Discussion chapter.

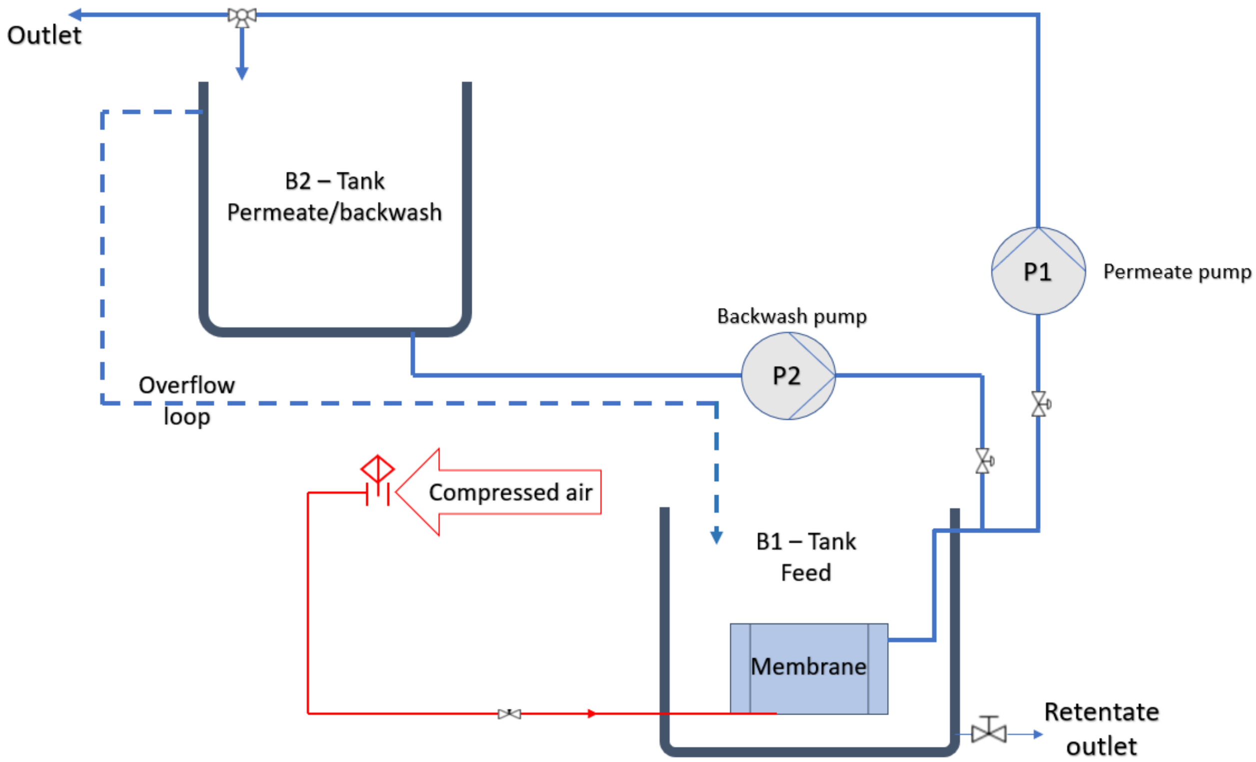

Figure 20: Membrane pilot unit schematic

Table 6: Permeate and backwash pump details

	Type	Brand	Motor size
P1 – Permeate pump	Peristaltic	Verderflex Rapide R17S	0,37 kW
P2 – Backwash pump	Centrifugal	Ebora 3-2T/0,45M	0,45 kW

3.3 Measuring membrane performance

This subchapter explains some of the reasons and practical circumstances behind how and why membrane performance measurements were done.

3.3.1 Pressure, flux and temperature

The HMI allowed to program the unit to have either constant flow, constant pressure or constant pump frequency. Though fixed pressure or flow was preferred, fixed pump intensity was used in all experiments because of the units' inability to maintain either stable pressure or flow. To limit concentration polarization and cake layer buildup near the membrane surface, air was continually injected at a constant rate of 2 m^3/h via an air diffuser at the bottom of the membrane to create turbulence mixing and shear. This was done in all trials. The filtration pump intensity was held constant at 25% which was the minimal effect. The BW pump was set to 50% and in some cases 30% of max effect.

Backwash configurations

Even though membrane separation reliably produces a stable permeate quality, being able to maintain a satisfactory flux of permeate is just as important for industrial purposes but can be far less predictable. Since the submerged flat sheet module does not have the advantage of the shear forces of cross-flow mode such as most conventional membrane setups, backwashing interval and length are crucial factors for the flux optimization and energy efficiency of the separation. Backwash was tested at different frequencies and durations, as presented in Table 7.

Table 7: Filtration/backwash configurations tested

Filtration time between each backwash (s)	Backwash duration (s)
600	10
300	10
300	5
120	5
60	10
60	5
60	3
60	2
60	1

3.3.2 Flux measurements

Permeate flux is referred to the actual output of permeate through the membrane. *Net flux* refers the total amount of produced flux after subtracting the reverse flux which is lost while backwashing.

The membrane unit had a built-in flow-meter but due to the pulsating flow of the peristaltic pump it was not able to give correct measurements. Permeate flux was therefore measured manually by directing the permeate outlet into a volumetric flask using equation 3 and equation 4 for to find the flux. The duration of the measurement was done according to the programmed filtration cycles, for example for a 10-minute filtration cycle, permeate volume was collected over 10 minutes to get the average flux of each filtration cycle because of big variations within each cycle.

Net flux was measured by emptying the B2-tank (where permeate is collected and BW-water is being withdrawn) and measure the accumulated volume.

3.3.3 Membrane relaxation

Hydraulic backwashing is an effective and necessary action to take for maintaining high permeate flux, but the downside is consumption of permeate used for backwashing which decreases the overall net flux. By periodically stopping filtration, it is possible for the CP-layer to be partially transported back into the bulk by the aid of air scouring and diffusion. This can be an effective tool to long-term flux sustainability (Howell, Chua, & Arnot, 2004). This is often referred to as membrane relaxation, intermittent permeation or cleaning without pressure (CWP).

3.3.4 Filtration/backwash cycles

Little information was available on how to operate the membrane pilot system, therefore it was not self-evident how to plan the experiments. The key thought and approach at start was that more backwashing would result in better permeate flux, but that too much would be limiting the overall net flux. This idea was also confirmed in literature (Hwang, Chan, & Tung, 2009).

The programmed cycles of filtration are referred to as "filtration time (s)/backwash duration (s)" in the text. For example, if the filtration time is set to 60 seconds and the duration of the backwash is set to 3 seconds, this configuration is referred to as a "60/3" configuration.

3.3.5 Backwash volume model

A tabulated model of the consumed amount of permeate for backwash was constructed. This was done by the following procedure:

1. Insert a quantified volume of permeate into the B2 tank.
2. Direct the permeate outlet away from the B2 tank into an external container.
3. Choose a configuration (BW duration and intensity) and start the unit.
4. Stop the unit after 10-20 cycles of BW.
5. Measure the amount of permeate left in the B2 tank.
6. Calculate the amount of permeate consumed for backwash according to Equation 10 and Equation 11.
7. Repeat for each configuration listed in Table 8:

Table 8: Backwash configurations baseline to construct a tabulated model to predict permeate consumed for backwashing

Backwash duration (s)	Backwash pump intensity (%)
1	30
2	30
3	30
5	30
10	30
1	50
2	50
3	50
5	50
10	50

$$V_{BW} = \frac{V_2 - V_1}{N_{BW}}$$

Equation 10: Calculation of consumed permeate volume per backwash cycle

Where V_{BW} is the volume consumed per BW, V_1 is the volume in the B2 tank at start, V_2 is the measured volume remaining in the B2 tank after N_{BW} number of BW cycles.

$$V_{SBW} = \frac{V_2 - V_1}{t_{BW} \times N_{BW}}$$

Equation 11: Calculation of consumed permeate volume per second of backwash

Where V_{SBW} is the volume of permeate consumed per second of backwash and t_{BW} is the duration of each BW.

The data could then be used to calculate how much permeate would be consumed for BW for different configurations by calculating the total time of backwashing during one hour of operation. By factoring in the size of the membrane, the reverse flux (LMH) was also possible to calculate. To measure the net flux was very time consuming since the whole B2-tank had to be emptied to measure the volume. The practicality of calculating the reverse flux was to be able to easily estimate the net flux when measuring the permeate flux at a given BW configuration.

3.4 The Dissolved Air Flotation unit

The DAF pressure chamber was filled with 1,8 liters of tap water which was saturated by air by applying a pressure of 5 bar for > 30 minutes (Figure 21). The valve was then opened, releasing the water into the bottom of a container under atmospheric pressure, filled with 15 liters of feed water mixed with a coagulant. After 3-6 seconds the valve was closed to let the sludge float to the top layer. This was repeated 3 times, spending approximately 1,5 liters of air-saturated water per 15-liter batch of wastewater.

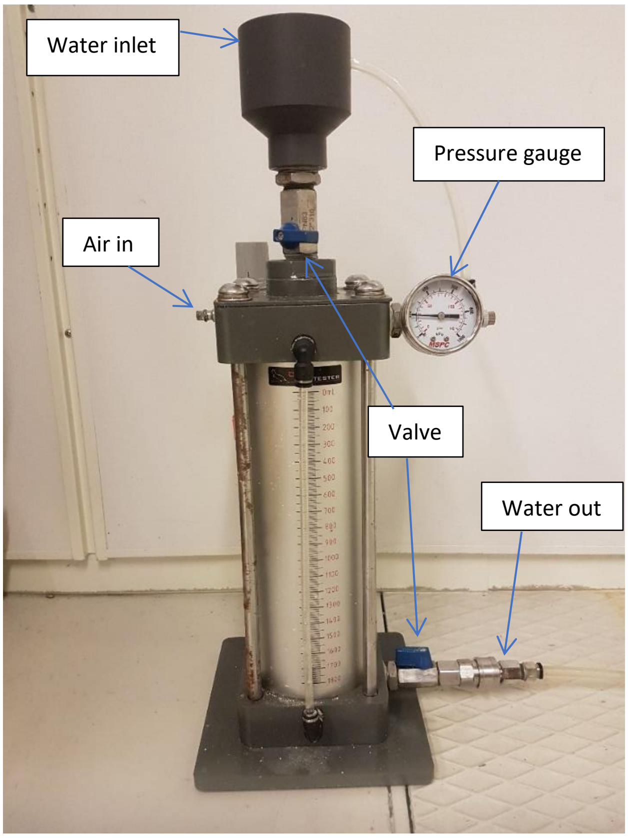

Figure 21: DAF pressure chamber

Figure 22: DAF setup

3.5 Analytical methods

In this subchapter the methods used for measuring turbidity, pH, total solids (TS), total suspended solids (TSS) and oil concentration in the feed and permeate water are described.

3.5.1 Turbidity

Turbidity was measured using a Hach 2100N turbidimeter. The apparatus was calibrated by standard solutions of >0,1, 20, 200, 1000 and 4000 NTU before sample measurements.

4.5.2 pH

pH measurements were performed with a VWR pH1100L apparatus which was calibrated by standard pH 4,01 and pH 7,00 solutions.

4.5.3 Energy consumption

Power consumption of the unit in standby mode (inactive pumps) was measured because this is the amount of energy the control center including the HMI of the unit requires to function, independently of filtration and BW pump energy consumption. In case of designing an upscaled version of the pilot unit, installing bigger pumps and larger membrane surface area, the HMI is not needed to be upscaled accordingly. Hence, upscaling the entire unit into industrial size, the energy consumption of the HMI will be negligible.

Energy consumption of the unit was measured using a “luxorparts” energy-meter which was connected to the power supply of the unit.

4.5.3 Solids classification

Total solids (TS) was found by evaporating a quantified volume of sample (V_{sample}) into complete dryness at 105°C in a bowl. The mass of the dried residue was analyzed by weighing the dry bowl (m_{bowl}) before adding the solution, and after drying ($m_{bowl + residue}$):

$$TS = \frac{m_{bowl+residue} - m_{bowl}}{V_{sample}}$$

Equation 10: Total solids

Total solids can be divided into total dissolved solids (TDS) and total suspended solids (TSS). TSS was found by filtration of a quantified sample (V_{sample}) using 0,45 µm pore size qualitative filters. The filter was dried for > 15 minutes at 105 °C and cooled in a desiccator before being weighed (m_{filter}) and placed on the vacuum flask for filtration. After filtration the filter was again evaporated into complete dryness at 105 °C for > 120 minutes, cooled in a desiccator and then weighted again ($m_{filter + residue}$) to find the suspended solids retained by the filter:

$$TSS = \frac{m_{filter+residue} - m_{filter}}{V_{sample}}$$

Equation 11: Total suspended solids

Total dissolved solids (TDS) can be found by subtracting the TSS concentration from the TS concentration (Equation 12):

$$TDS = TS - TSS$$

Equation 12: TDS concentration based on TS and TSS concentrations

4.5.4 Oil concentration measurement: Infrared spectroscopy (IR)

Infrared spectroscopy was used to determine the oil concentration in the samples, based on the standard method ASTM D7678-11 for oil in water measurement (Higgins, 2012). In the following section, analytical methods of IR experiments are presented. In preparation for analysis, organic compounds were extracted from the water phase and into the organic phase. Extraction is done to ensure other compounds in the analyte does not interfere with spectral regions of interest. The extractant used was cyclohexane as it has a sufficient spectral region in which to measure the hydrocarbon bending mode. Cyclohexane is also a relatively cheap extractant compared to other alternatives (Higgins, 2012).

In infrared spectroscopy, electromagnetic radiation is passed through a sample and then the fraction of absorbed radiation at particular energies is measured. The lacking part of the electromagnetic spectrum after passage corresponds to the vibration energy and concentration of different atoms in the analytical sample. Electromagnetic energy is absorbed/emitted by the atoms at quantized discrete energy levels, meaning that each atom has an associated electron excitation energy that is unique to that atom (Stuart, 2005). A software then creates an absorbance curve that is unique to that chemical compound and chemical composition can then be determined.

4.5.4.1 Extraction of organic compound

50 ml of cyclohexane were added to 900 ml of sample in a 1-liter bottle. The bottle was shaken for 5 minutes, and then set aside to allow the two phases to separate into organics and water. Pure water was then carefully added until the organic top layer was at the top of the bottle. The organic phase was then transferred into a 20 ml vial. 2 g of sodium sulphate (Na_2SO_4), as a drying agent and 2 g of

florisil were added to the vial and shaken vigorously for 2 minutes and then allowing the precipitate to settle for 5 minutes. In the final step, the top layer was filtered using a 0.45-micron nylon syringe filter with a 17 mm diameter.

4.5.4.2 Fourier transform infrared spectroscopy (FTIR)

The analyte was placed on the CARY 630 FTIR DialPath accessory window and the crystals were then cleaned using rectified ethanol. DialPath was then set to the appropriate 200 µm path length and MicroLab software were then used to create an IR spectrum over wavenumbers ranging from 500-5000 cm^{-1} as shown in Figure 23.

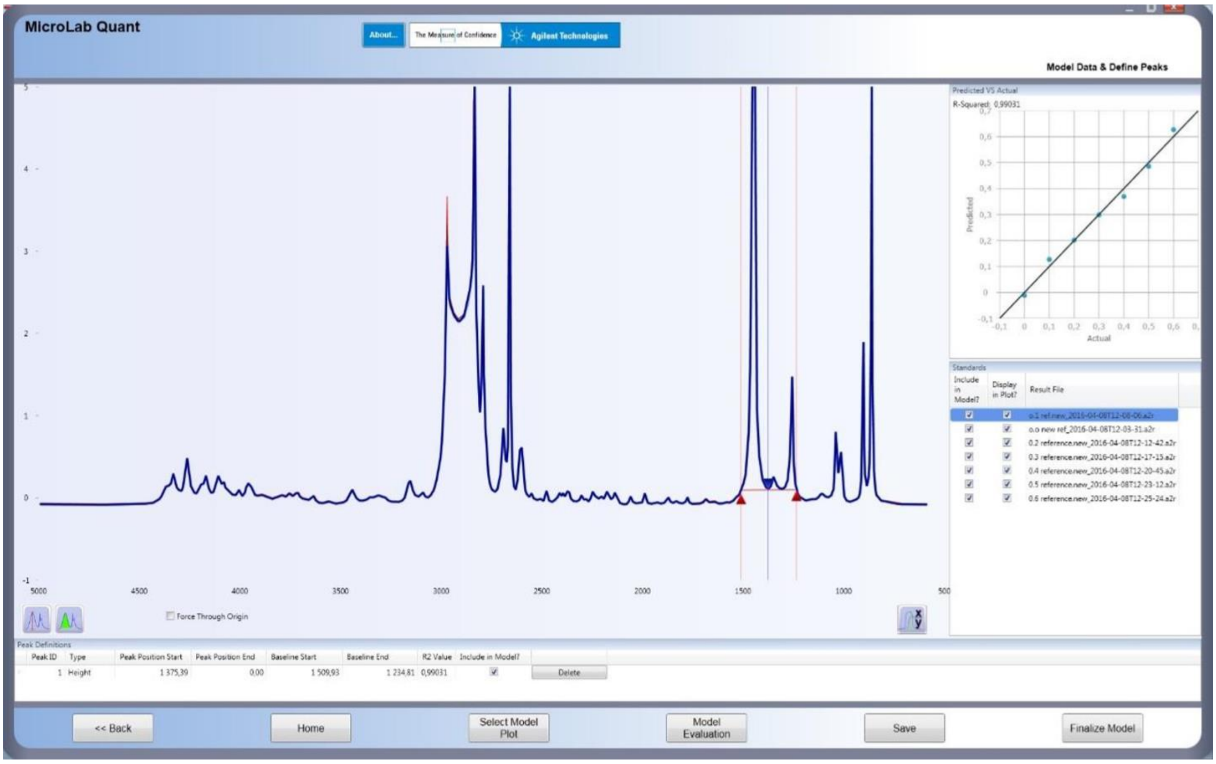

Standards

Include in Model?	Display in Plot?	Result File
☑	☑	0.1 ref.new_2016-04-08T12-08-06.a2r
☑	☑	o.o new ref_2016-04-08T12-03-31.a2r
☑	☑	0.2 reference.new_2016-04-08T12-12-42.a2r
☑	☑	0.3 reference.new_2016-04-08T12-17-15.a2r
☑	☑	0.4 reference.new_2016-04-08T12-20-45.a2r
☑	☑	0.5 reference.new_2016-04-08T12-23-12.a2r
☑	☑	0.6 reference.new_2016-04-08T12-25-24.a2r

Peak Definitions

Peak ID	Type	Peak Position Start	Peak Position End	Baseline Start	Baseline End	R2 Value	Include in Model?
1	Height	1 375,39	0,00	1 509,93	1 234,81	0,99031	☑

Figure 23: Total absorbance spectrum in MicroLab software

Range 1370-1380 cm^{-1}, the range of electromagnetic energy that is absorbed by the bending vibrations of methyl carbons in alkanes (Glagovich, 2013), was analyzed for variations in absorbance against a reference sample of pure cyclohexane for the different samples. The peaks seen in Figure 24 corresponds to the difference in concentration between pure cyclohexane (0.0 ml oil/l SW), 0.1, 0.2, 0.3, 0.4, 0.5 and 0.6 ml oil/l sample. The linearity between the reference concentrations were satisfactory, with an R^2-value (which describes correlation between data points and graph) of 0.99031 (Figure 25), which then was later used to calculate oil concentrations of samples.

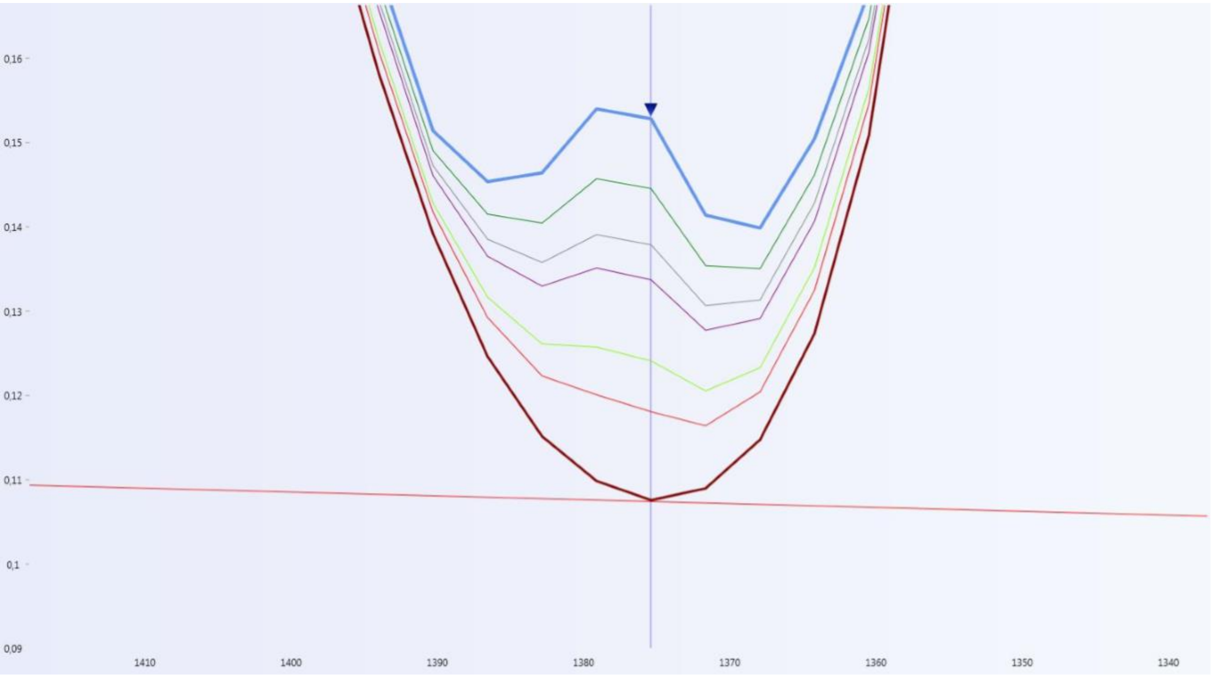

Figure 24: Reference concentration lines for 0,0 (dark brown), 0,1 (red), 0,2 (light green), 0,3 (purple), 0,4 (grey), 0,5 (green) and 0,6 (green) ml crude oil/liter sample

4.5.4.4 Calculation model of oil concentration

Calculation of the oil content in the samples was done using the constructed model in Figure 25:

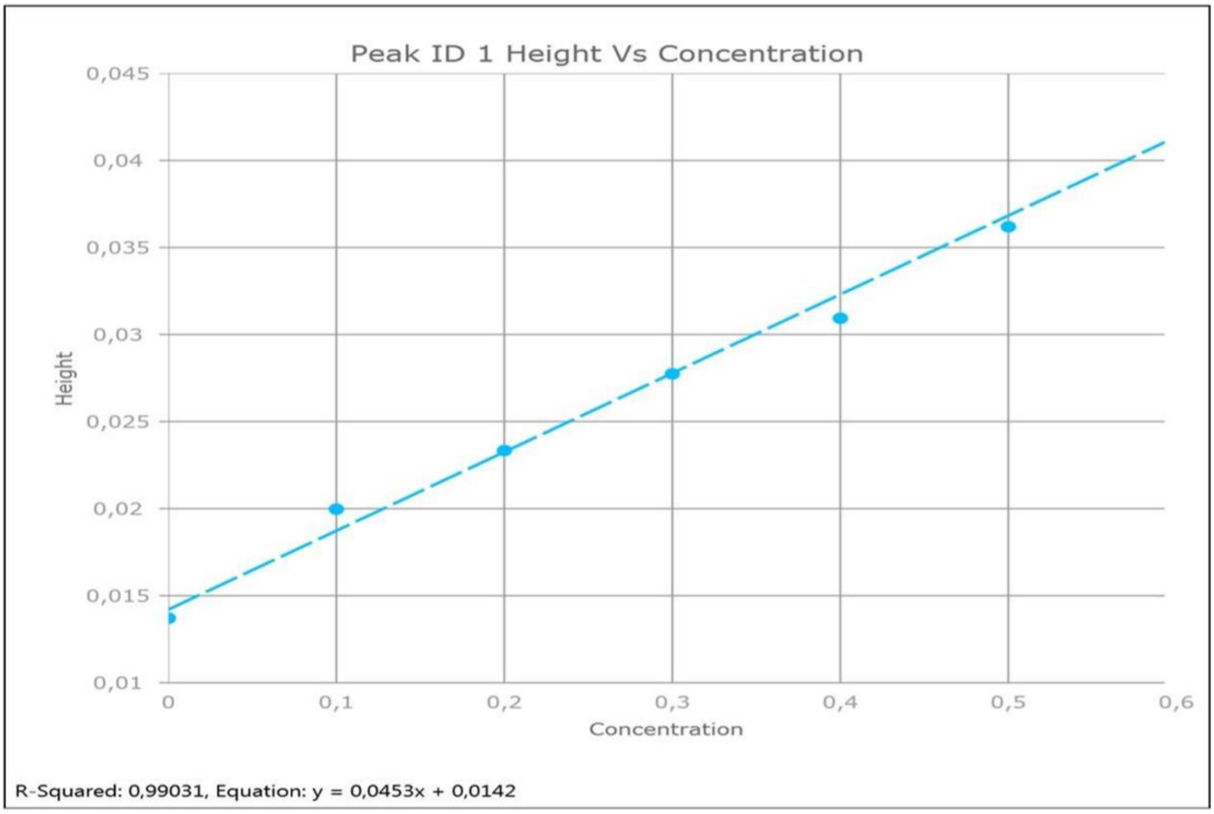

Figure 25: Model for predicting oil concentration

3.6 Wastewater used in the experiments

In this section the origin and characteristics of the four different wastewaters used in the experiments are described, respectively labelled as S1, S2, S3 and S4 and color coded (Table 9). The bioreactor wastewater (S1) was used to emulate "light" slop water and was mostly used in the initial testing from the beginning of the experiments. S2 and S3 are actual slop water with a typical degree of contamination. S4 is flowback water, chosen to emulate extra oily/dirty slop water. The different wastewaters are further described in the following sections.

Table 9: Color coded overview of the four different wastewaters used in the experiments

Label	Wastewater type
S1	Bioreactor effluent from Grødaland
S2	Stavanger Slop (tank 2, batch 1)
S3	Stavanger Slop (tank 2, batch 2)
S4	Flowback water from oil company

3.6.1 S1 - Bioreactor effluent

Secondary effluent from a municipal wastewater treatment plant at Grødaland (IVAR) was collected and used as feed. The sources for wastewater into this treatment plant consists of a mixture of animal destruction waste, municipal wastewater, food and dairy industry and chicken slaughtering. The wastewater had undergone the following treatment before it was collected:

- 3 mm bar screen
- Sand and grit removal
- Fat removal
- Dissolved air flotation
- Up-flow anaerobic sludge blanket (UASB) reactor

3.6.2 S2 - Slop water from tank 2, Stavanger slop (batch 1)

The S2 slop water was collected from the facilities of Stavanger Slop at Mekjarvik (From tank 2). The origins of the slop were not possible to trace, but as previously mentioned in the introduction, typical sources for the ingredients of slop are:

- Oily water from cleaning
- Drilling fluids
- Rain water
- Cleaning chemicals and other chemical residuals
- Water mixed with hydraulic oil from leakage. (McCosh et al., 2009; Sorbwater, 2014)

3.6.3 S3 - Slop water (batch 2)

A second batch was collected from the same tank as the S2 water. The tank content had been mixed with water of other characteristics.

3.6.4 S4 - Flowback water

Flowback water was collected from a customer of Norwegian Technology. The flowback water was used as feed to broaden the range of testing on the membrane and to emulate extra oily slop water.

Flowback water is a by-product of “well-fracking” where a mix of water, sand and various chemicals are pumped into the ground at high pressure to fracture slate formations to extract natural gas. The fracking water is transported back and blended with produced water from the formations, resulting in a high salinity wastewater stream typically containing:

- Soil and clay
- Oil
- Metals
- Fracking chemicals (Chilkoor, Shrestha, Soeder, & Gadhamshetty, 2018)

4 Results & Discussion: Slop water treatment with SiC flat sheet membranes

The results from the experimental part of the thesis are presented in this chapter, starting with base parameters (clean water flux and energy consumption without filtration) and the results from the feed water analysis, followed by membrane testing with separation efficiency and flux performance, grouped by wastewater type.

4.1 Clean water flux

Clean water flux was measured at temperatures of 14, 26, 34 and 44°C with a pressure of -0,02 bar (Figure 26). As expected, the flux increased significantly when the temperature was increased, mainly because of the decreased viscosity of the water at higher temperatures.

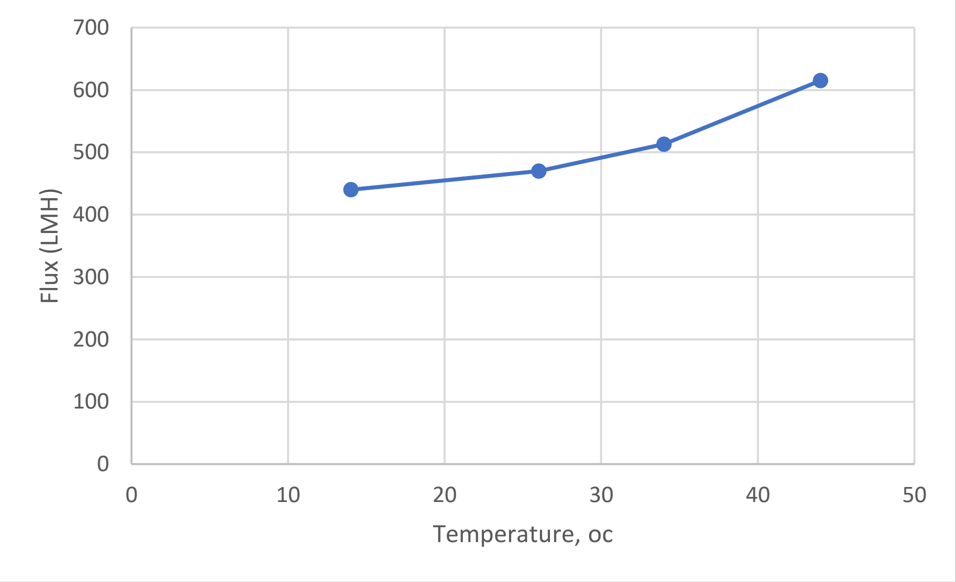

Figure 26: Clean water flux at increasing temperatures

4.2 Wastewater feed analysis of S1, S2, S3 and S4

4.2.1 S1 Feed analysis

The characteristics of the S1 wastewater are shown below in Table 9 and a visual representation is shown in Figure 27. The solution was observed to be containing small particles and had a light brown-yellowish color.

Table 9: Parameter values for the bioreactor effluent wastewater

Parameter	Unit	Value
TS	g/l	0,5
TSS	g/l	0,3
Turbidity (NTU)	NTU	28
Total VFA	mg CH_3COOH/l	180
pH	-	7,2

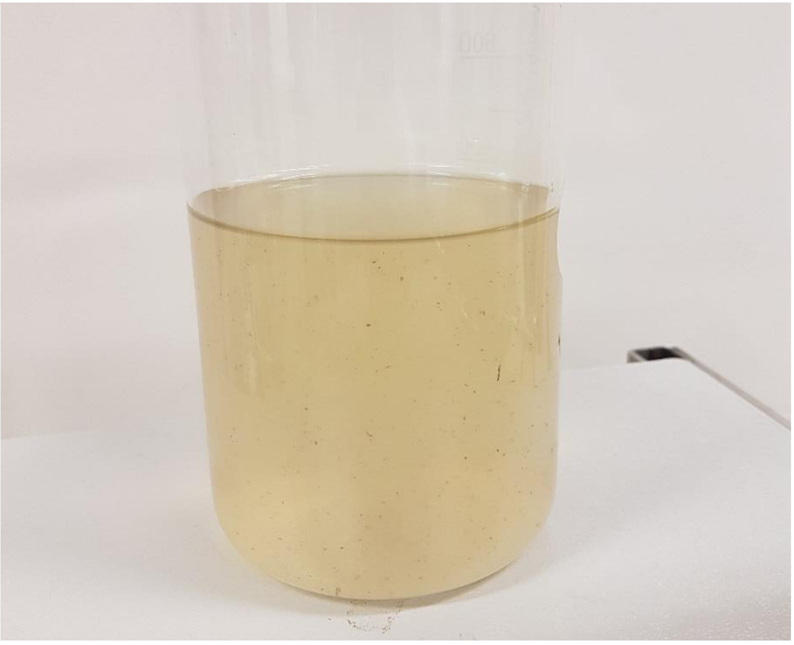

Figure 27: S1 – Bioreactor wastewater

4.2.2 S2 Feed analysis

The characteristics of the S2 wastewater are shown below in Table 10 and a visual representation is shown in Figure 28. The solution was observed to be clear, homogenous and with a dark brown-yellowish color. The big difference between TS and TSS content (using equation 12) shows that the solution had a high dissolved solids content, with only a small fraction of the solids being suspended.

Table 10: Measured characteristics of the S2 slop water

Parameter	Unit	Value
Oil concentration	ppm (vol.)	12
Total Solids (TS)	g/l	242
Total Suspended Solids (TSS)	g/l	0,4
Turbidity (NTU)	NTU	65
pH	-	2,9

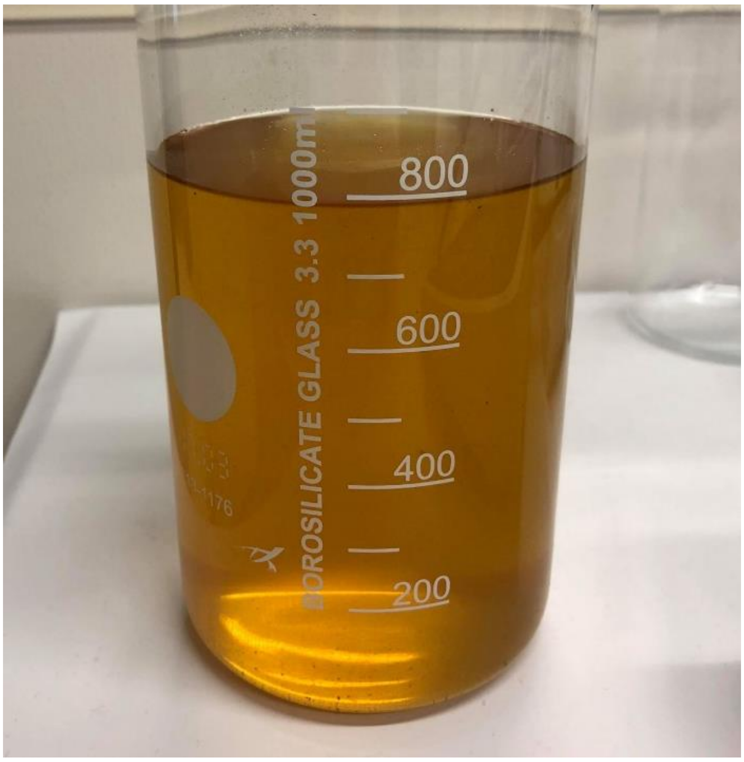

Figure 28: Visual representation of S2 - slop water

4.2.3 S3 Feed analysis

The characteristics of the S2 wastewater are shown below in Table 11 and a visual representation is shown in Figure 29. Visually, the S3 water was homogenous, but cloudier than the S1 and S2, which is reflected by the measured turbidity. Just as the S2 water, TS and TSS ratio implies that the solids are mainly dissolved in the solution.

Table 11: Measured characteristics of the S3 slop water

Parameter	Unit	Value
Oil concentration	Ppm (vol.)	12[1]
Total Solids (TS)	g/l	89,2
Total Suspended Solids (TSS)	g/l	0,4
Turbidity	NTU	1314
pH	-	3,3

1. *The S3 oil measurements failed, as the software was not able to give feedback on the measurement and only resulting in error in the measurement. It could be seen from the infrared spectrum during the analyzation on the software that there were a lot of disturbances on the sample, probably to complex dissolved structures, which is likely the reason of the software error. The error repeatedly occurred for multiple measurements. Stavanger Slop could report that the tank oil content should be mainly the same for the two batches. The oil content was therefore assumed to be the same as S2 (12 ppm).*

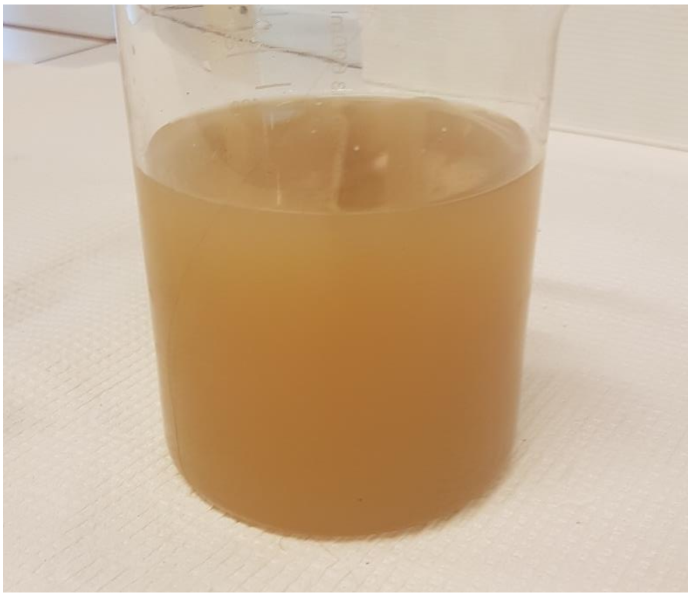

Figure 29: S3 - Slop water (batch 2)

4.2.4 S4 Feed analysis

The characteristics of the S4 wastewater are shown below in Table 12 and a visual representation is shown in Figure 30. The solution had a brown cloudy color with a visible top layer of organic phase with a distinctive smell of hydrocarbons. The TS and TSS ratio of S4 is similar to the S2 and S3 waters, with most of the solids in the solution being dissolved. The oil content was too high to be measured by the IR method, but was reported by Norwegian Technology that it was at least 400 ppm.

Table 12: Measured characteristics of the S4 Flowback water

Parameter	Unit	Value
Oil concentration	Ppm (vol.)	> 400
Total Solids (TS)	g/l	49,7
Total Suspend Solids (TSS)	g/l	0,75
Turbidity	NTU	2747
pH	-	7,4

Figure 30: S4 – Flowback water

4.3 - S1 Results

In this section the results from the membrane testing on S1 water is presented, starting with removal degree and followed by flux measurements.

4.3.1 Removal degree

Table 13: Parameter values of the wastewater before and after membrane separation

Parameters	**Unit**	**S1 - Feed**	**MF permeate**	**Removal (%)**
Total Solids (TS)	g/l	0,5	0,3	**40**
Total Suspended Solids (TSS)	g/l	0,3	0	**100**
Total VFA	mg CH_3COOH/l	182	12	**93**
COD_t	mg/l	0,5	0,32	**36**
NH_4^+	g/l	0,06	0,06	**0**
Alkalinity	g $CaCO_3$/l	0,7	0,7	**0**

As expected, the membrane completely removed TSS, resulting in a reduction of the total chemical oxygen demand (COD) and volatile fatty acids (VFA), but not the dissolved solids such as alkalinity and ammonium. Figure 31 below shows the removal degree of the removed compounds. The separation of TSS, VFA and total COD was 100%, 93% and 36%, respectively.

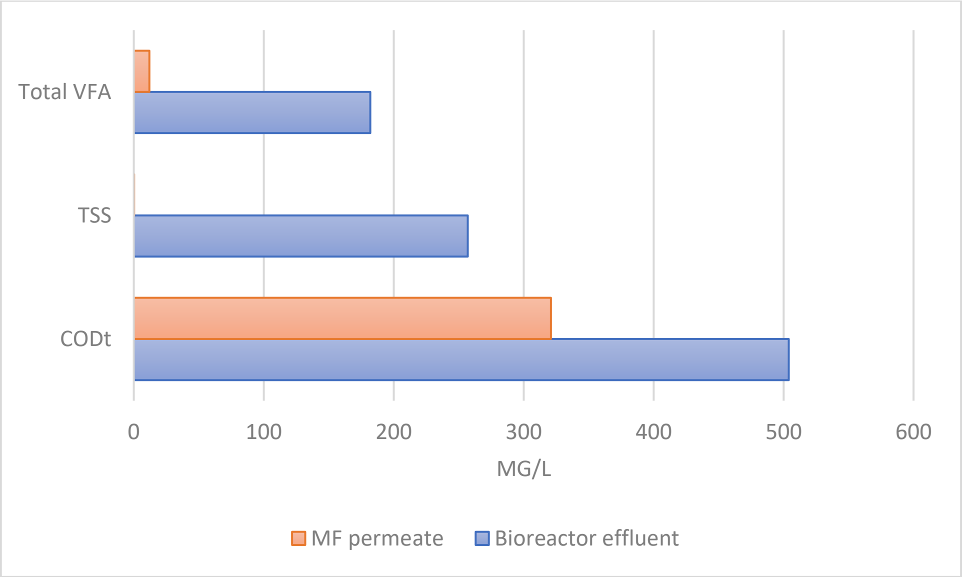

Figure 31: Graphical representation of the removed compounds (VFA, TSS and COD) from the S1 water

4.3.3 Backwash frequency and fouling

Average permeate flux was measured for each of the configurations in Table 7 are presented in Figure 32:

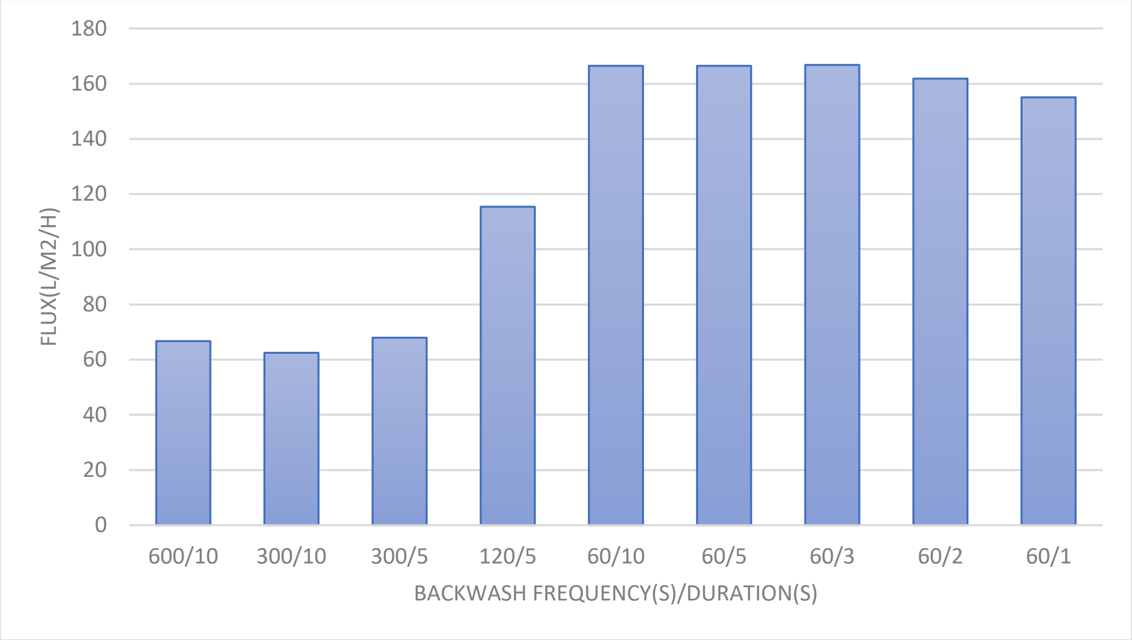

Figure 32: Average permeate flux for each of the performed backwashing frequencies and BW durations

It’s clear that shorter cycles of filtration are beneficial to maintain a high permeate flux. The configurations 600/10, 300/5 and 60/1 all have the same ratio of backwashing time and filtration time, but the 60 second BW frequency had a significantly higher average flux than 2, 5 or 10 minute, indicating that rapid decline in flux happened between 1-2 minutes after each backwash in the longer filtration cycles.

Permeate flux was then measured in three parts during the longest filtration cycles (10 and 5 minutes and two parts for the 2-minute cycle). Figure 32 shows that during 10 or 5-minute filtration cycle, the flux dropped by over 60%. However, the fouling was reversible as the flux was restored after each BW was performed.

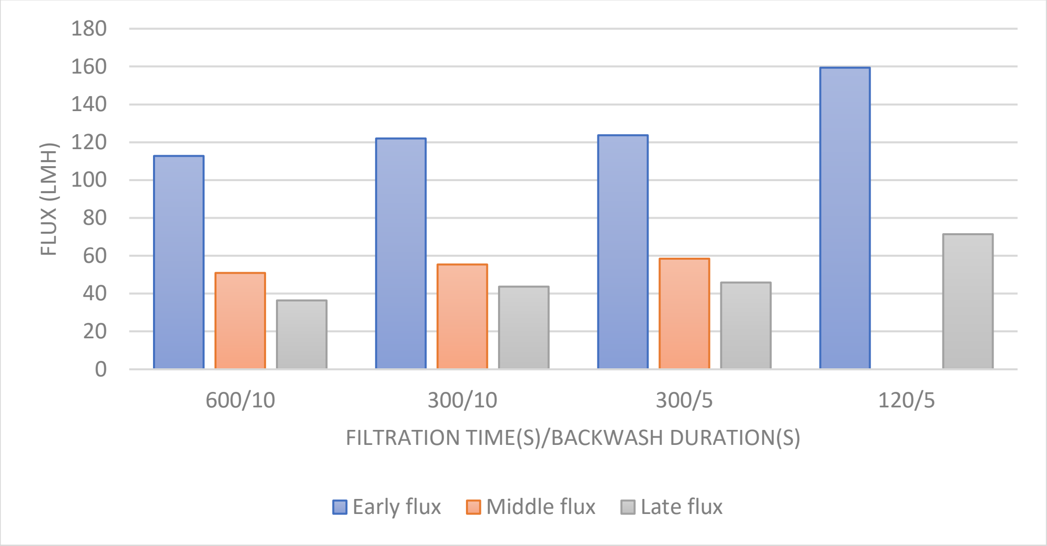

Figure 33: Flux decline in filtration cycles between each backwash, for different filtration/backwash frequencies (600/10, 300/10, 300/5 and 120/5)

The data indicate that relatively short backwash (BW) cycles are preferable to keep a high permeate flux over time. The effect of the backwash was decreased only slightly with decreased BW duration, even down to only one second (Fig. 31). However, after running the 60/1 configuration over 24 hours, the fouling was observed to be so severe that the flux was down to zero. By increasing BW to 3 seconds per minute, the flux was held stable over the same duration of operation.

4.3.5 Membrane relaxation

The effect of membrane relaxation was tested by running one-minute cycles of filtration followed by 10 seconds of relaxation. In addition to flux, pressure was monitored to get an indication of the degree of fouling. Results from the first ~40 minutes are shown in Figure 33 below:

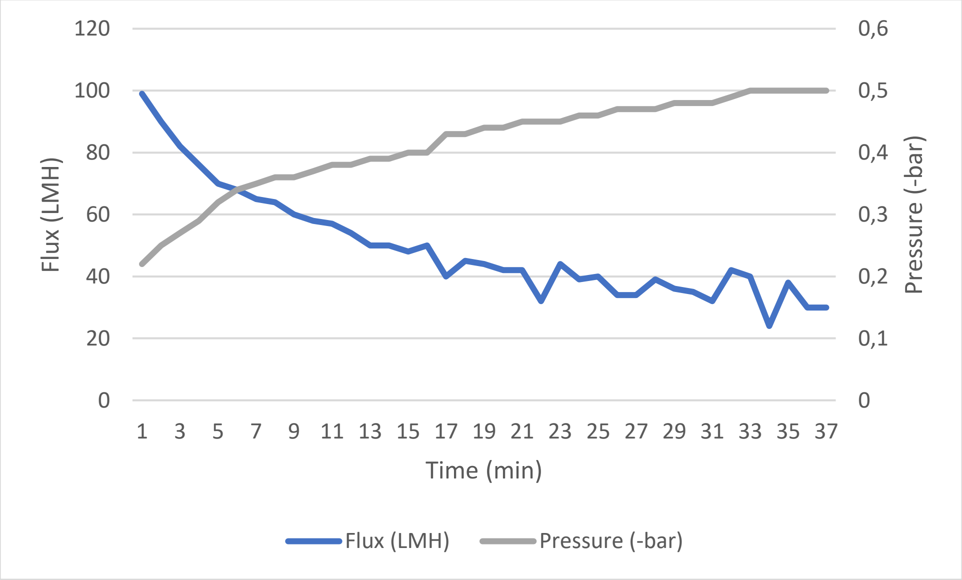

Figure 34: Membrane relaxation. Cycles of 60 seconds of filtration followed by 10 seconds of relaxation (filtration-stop), without BW

It was visually observed a slight increase in flux after each relaxing period during the test. As expected, the total membrane resistance continually increased according to the observed pressure increase. After almost 40 minutes the average permeate flux for each cycle was measured to be between 20-30 LMH but the flux was observed to be increasingly unstable, even periodically stopping completely in periods of 3-6 seconds.

The filtration was therefore continued with the same configuration, plus an additional 5 seconds of membrane relaxation every 30 second. After one additional hour, the flux and pressure had stabilized between 20-25 LMH and -0,56 bar, respectively (Figure 34).

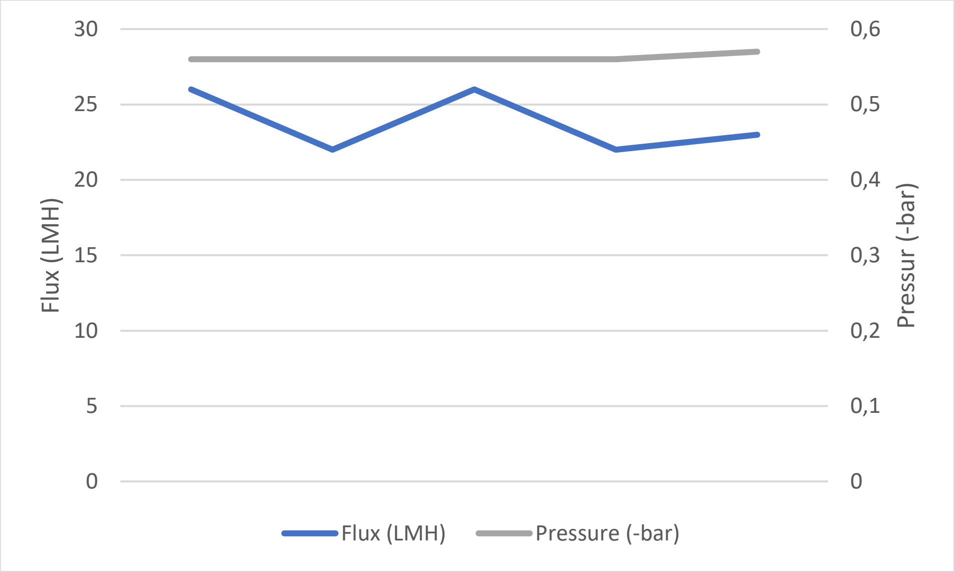

Figure 35: Flux and pressure measurements after 1 hour with 10 second of CWP each minute + 5 seconds of CWP every 30 second

An additional trial was done by applying 100 seconds of relaxation every 10 minutes, the result was quite similar, with an overall flux of 31 LMH after 2,5 hours of operation (Appendix 1). Regarding "light slop water" such as S1 with low turbidity and solids content, membrane relaxation could likely be useful in the long run in combination with backwashing. For wastewater with higher solids and hydrocarbon content, the effect is assumed to be limited, as the cake layer buildup happens more rapidly, hence more powerful cleaning will be preferred to limit the possibility for severe fouling in "heavier" slop water filtration.

4.3.4 Loss of permeate to backwashing

Permeate flux was measured and average net flux was calculated during a 300/10 filtration/BW configuration. Figure 36 shows the measured permeate flux and the calculated average net flux after reaching stable conditions.

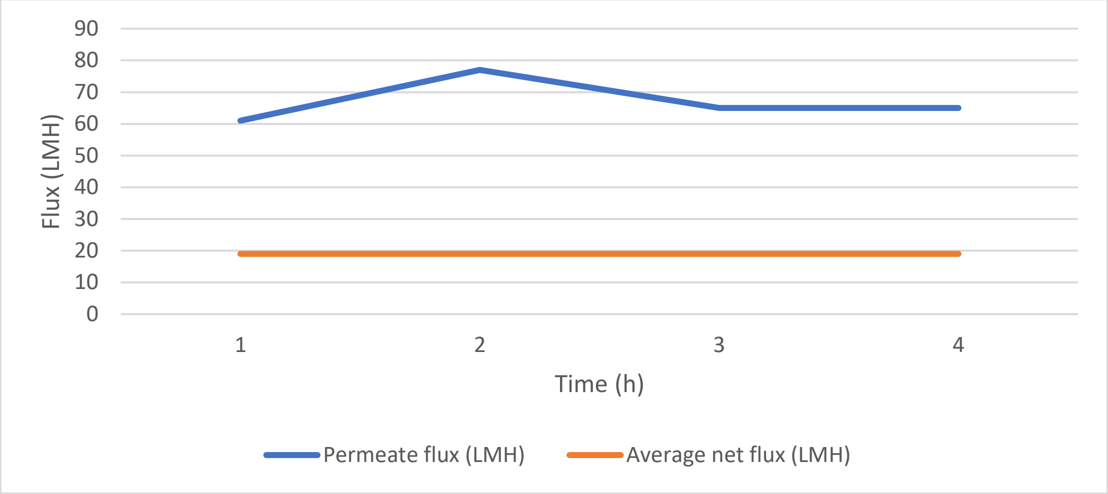

Figure 36: Graphical representation of the amount of permeate consumed by excessive backwashing, 300/10 configuration on S1 water

As shown in chapter 4.3.3, periodic backwashing is essential for maintaining high flux. However, too much of it will significantly reduce the overall net flux due to the loss of permeate to backwash. Flux measurements in Figure 35 show that very much (over 60%) of the produced permeate was transported back into the feed by backwashing, yielding an average net flux of 19 LMH.

Overall, the total collected data and experimental testing from the S1 trials show that frequent backwashing is important to maintain a good permeate flux. However, it but must be used with caution to not excessively spend produced permeate on high backwash volumes, resulting in a lowered net flux. Gaining knowledge of how to optimize net flux is considered essential, and trials for optimization of net flux was therefore further performed using a more representative feed water (S2) in chapter 4.2.

4.2 Results for S2 water

4.2.1 Removal rates

Parameter	Unit	Feed	Permeate	Removal (%)
Oil concentration	Ppm (vol.)	12	0	**100**
TS	g/l	242	125,5	**48**
TSS	g/l	0,4	0,026	**96**
Turbidity (NTU)	NTU	65	2	**97**

4.2.2 Model for predicting backwashing volume (50% BW pump intensity)

Based on experience from the S1-water initial testing, the amount of permeate consumed during backwashing was investigated using S2-water at different configurations to create a tabulated model for predicting permeate loss. This was done with BW-pump power intensity of 50% and 30% in accordance to the procedure described in chapter 3.3.5. Figure 35 and 37 show the amount of permeate consumed in one BW-cycle at 50% and 30% pump intensity, respectively.

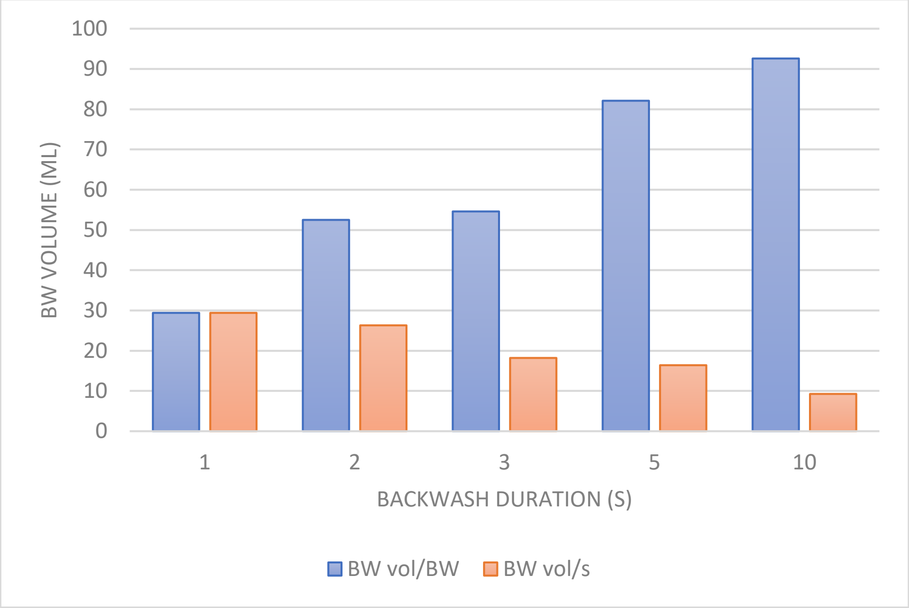

Figure 37: Backwash volume (ml) per backwash (blue) and per second (orange) for 1, 2, 3, 5 and 10 second BW durations with 50% applied BW-pump intensity.

Contradictory to the presumed outcome, backwashing volume consumed per second decreased as the backwash duration was increased (Figure 36 and Appendix 9). The consumption was over 200% higher per second during a one-second filtration than during 10 seconds, ranging from 9 ml/s for 10 seconds backwash duration to 29 ml/s at 1 second BW duration. There are several unknown parameters that could affect this since the system is partially automatic.

One possible reason could be due to the HMI program, which automatically controls the pumps. As the centrifugal BW pump must accelerate (and decelerate) the RPM (rounds per minute) magnitude, it will take a certain amount of time before the pump reaches its targeted RPM effect. It is possible that the HMI program only account the BW duration from when the pump has reached its targeted RPM, resulting in the flow generated in the acceleration process would be an addition to the programmed second. In that case, this extra volume would have a much larger impact in a 1 second BW than in a 10 second BW. So, what's programmed as 1 second BW, may possibly be practically longer.

Regardless of the reason behind the observed trend, the collected data is in Figure 37 scaled up as liter of permeate spent per hour of several different filtration/BW configuration processes. This is also converted into reverse flux (consumed permeate for BW) in the tabulated model in Table 15, to make it functional for the use of estimating the net flux for a given configuration when the permeate flux is measured. Baseline data for Table 15 and Figure 37 are can be found in Appendix 10.

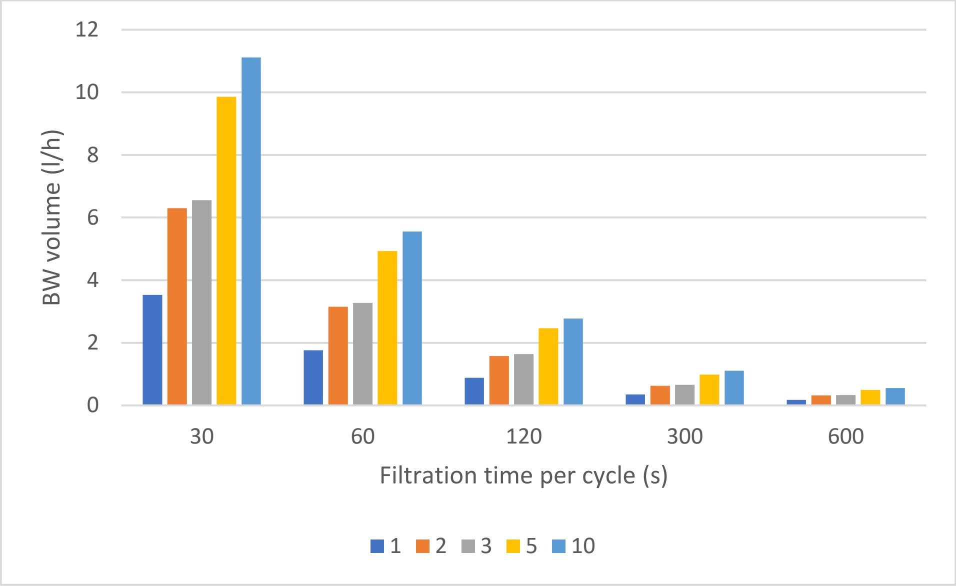

Figure 38: Liters of BW volume per hour of operation for different configurations at 50% BW pump intensity. Backwash durations (s) are represented by different colors at filtration time scenarios of 30, 60, 120, 300 and 600 seconds

Table 14: Model 1: Predicting BW-flux (permeate loss) (LMH) at different filtration/BW configurations (50% BW-pump intensity)

Filtration time (s)	**BW duration(s)**				
	1	**2**	**3**	**5**	**10**
30	54	97	101	152	171
60	27	48	50	76	85,5
120	13,6	24	25	38	42,7
300	5,4	10	10	15	17
600	2,7	4,8	5	7,6	8,6

>95 LMH
20 - 40 LMH
10 - 20 LMH
0-9 LMH

Logically, the model shows that if the BW duration is long and frequent, a lot of permeate is consumed for for BW. But given a reasonable choice of configuration, the model should be considered as a guiding tool when evaluating flux performance and choice of BW frequency. As an example, if the permeate flux is measured to be 100 LMH during a 600/10 configuration, the estimated net flux will be (100 – 8,6) LMH = 91,4 LMH.

The same measurements as the above was also performed with 30% BW pump intensity, presented in Figure 38, 39 and Table 16:

4.2.3 Model for predicting backwashing volume (30% BW-pump intensity)

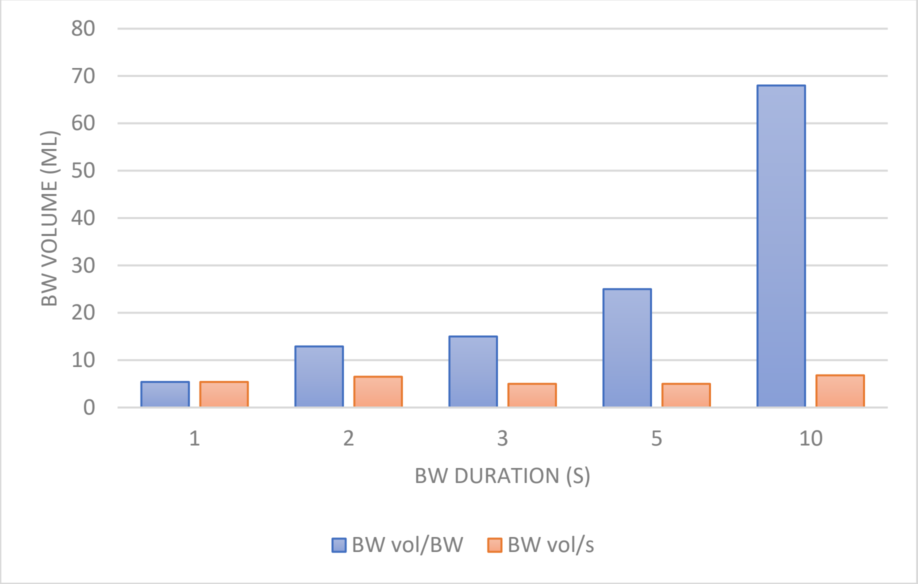

Figure 39: Backwash volume (ml) per BW cycle (blue) and per second of BW (orange) for 1, 2, 3, 5 and 10 second durations with 30% applied BW-pump intensity.

Reducing the pump intensity down to 30%, the amount of permeate consumed per second BW was relatively uniform, between 5 ml/s and 6,8 ml/s (Figure 37 & Appendix 9), showing no correlation between backwash volume per second and the duration of backwashing, as it did using 50% of the pump intensity (Figure 36). It was hypothesized that the HMI program does not "count" the programmed BW duration setting before it reaches its targeted intensity. The acceleration/deceleration process of the pump was audibly noticed to be significantly shorter at 30% than 50% power intensity, which is not proof, but a good indication that this is a contributing factor creating the non-uniform BW flow rate observed in Figure 36.

The data used in Figure 38 was scaled up as liter of permeate spent per hour of operation in several different filtration/BW configuration processes (Figure 39) and converted into consumed flux (LMH) in the tabulated model in Table 16.

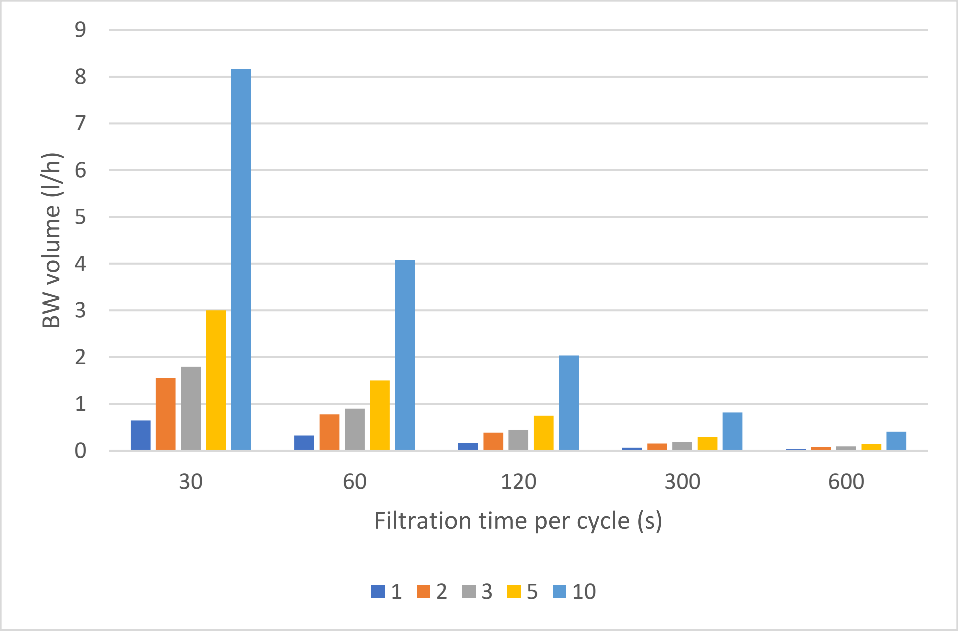

Figure 40: Graphical representation of the BW volume prediction model in liters per hour. Backwash durations are represented by different colors at filtration time scenarios of 30, 60, 120, 300 and 600 seconds.

Table 15: Model 2: Predicting BW-flux (LMH) at different filtration/backwash configurations (30% BW-pump intensity)

	Backwash duration (s)				
Filtration time (s)	**1**	**2**	**3**	**5**	**10**
30	10	23,8	27,7	46,2	125,5
60	5	11,9	13,8	23	62,8
120	2,5	6	6,9	11,5	31,4
300	1	2,4	2,8	4,6	12,6
600	0,5	1,2	1,38	2,3	6,3

>95 LMH
20 - 40 LMH
10 - 20 LMH
0-9 LMH

4.2.4 Flux performance

4.2.4.1 Configuration: 600/10

Based on the BW flux predictions in Model 1 (Table 15), it was decided to test slop water processed with filtration time of 10 minutes followed by 10 seconds of backwash (600/10 configuration), with a 50% power intensity of the BW-pump. Permeate flux and average net flux was measured for the first 3 hours (Figure 41).

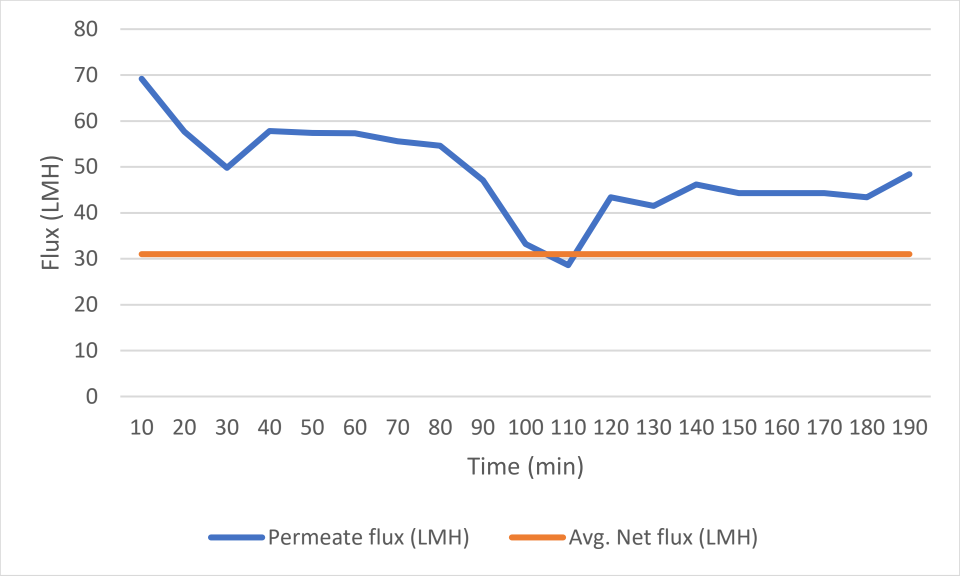

Figure 41: Permeate flux and pressure during a 600/10 configuration on S2-water

The permeate flux stabilized at slightly over 40 LMH and yielded an overall net flux of 31 LMH after 3 hours. Only slightly lower flux than estimated by the model, which indicated a flux loss of 8,6 LMH (Table 16).

The test was continued for almost 11 hours, monitoring the net flux and pressure in Figure 41:

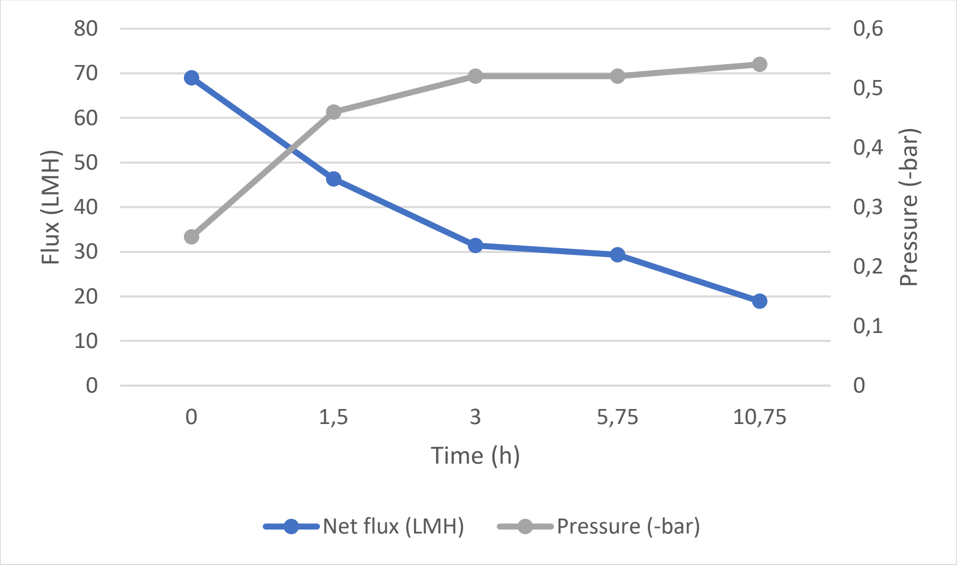

Figure 42: Net flux and pressure development in 600/10 configuration, 50% BW-pump intensity on S2 water

After 6 hours the net flux was 29 LMH and after additional 5 hours the net flux was 19 LMH after running almost 11 hours. Decrease in flux is reflected in the increased pressure, which indicates some fouling. In addition, the temperature was also steadily decreasing (from 22°C down to 16°C (Appendix 2)), which also has a negative effect on the flux, as shown in Figure 25 (Clean water flux).

4.2.4.2 Configuration: 60/3

More frequent backwashing was tested with a 60/3 configuration. Permeate flux was monitored and overall net flux was measured after the 7 hour process, shown in figure 43 below:

.

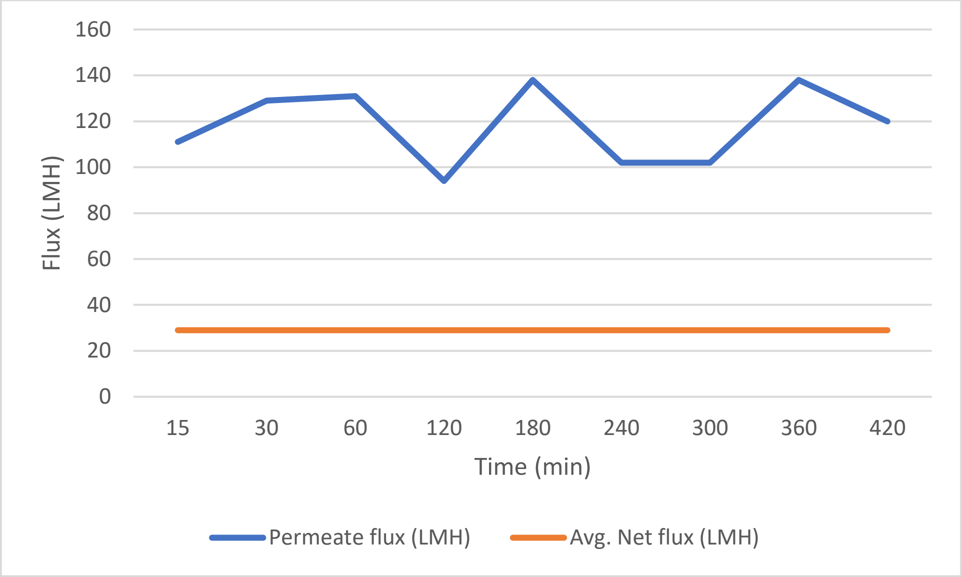

Figure 43: Permeate flux for S2 slop over 7 hours

The permeate flux was significantly increased compared to the 600/10 configuration, with an average permeate flux of 118 LMH. However, after measuring the net flux in the end of the experiment, it was found that over 70% of this was consumed for backwash, leaving a net flux of 29 LMH. Though the permeate flux was held relatively stable over 7 hours, the amount of permeate consumed to BW was considered too high. The backwash pump was therefore adjusted down to 30% intensity, continuing the same configuration (60/3).

After 5 hours of processing using lower backwashing power the results were almost similar as with 50% backwashing power, obtaining an average permeate flux of 126 and a net flux of 28 LMH. To further try to optimize, the BW duration was decreased down to 1 second per minute as described below.

4.2.4.3 Configuration: 60/1

The backwashing time was set to one second every minute and the BW pump was set to 50% intensity. After 3 hours, the net flux was 30 LMH, with a permeate flux of 122 LMH (Appendix 4)

As all the 3 configurations tested on the S2 water (600/10, 60/3 and 60/1) had similar output of net flux, approximately 30 LMH, two extra membranes were installed into the unit to observe if it would have an effect on the net flux. Also, this was not done sooner because of practical reasons as previously mentioned.

4.2.7 Increased membrane surface area

By adding two additional membranes in the filtration tank, the membrane surface area was expanded accordingly (from 0,065m^2 to 0,195 m^2). The filtration pump was still run at minimum speed, allowing a more stable filtration pressure because of the increased surface area.

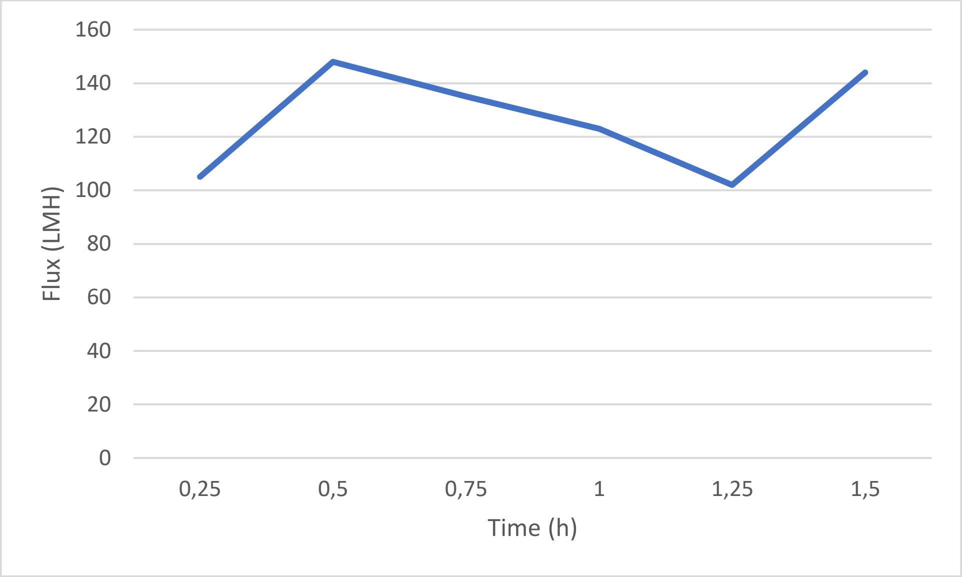

Figure 44: 60/3 configuration with increased membrane surface area on S2 filtration.

The result was a significant increase in net flux, yielding an average net flux of 114 LMH, with only 7 LMH lost to backwash from the permeate flux, slightly lower than model 1 predictions, which was 121 LMH on average. Filtration resistance in terms of pressure was very low, negative pressure down to only -0,06 bar at the end of the test.

This result show that the backwash pump probably is more suited for a larger membrane area. The permeate flux was maintained, and the backwash LMH (reverse flux) was significantly reduced.

The testing was continued with the same filtration/BW configuration, but on the second batch of slop from Mekjarvik (S3 water). Further testing using 3 membrane elements, continuing with the same filtration/BW configuration.

4.5 Results for S3 water

4.5.1 S3 Removal rates

Table 17 show the measured parameters after membrane filtration and pre-treatment.

Table 16: Removal efficiency in the S3 water

Parameter	Unit	Feed	Permeate	Removal (%)
Oil concentration	Ppm (vol.)	12[1]	0	**100**
TS	g/l	89,2	68	**24**
TSS	g/l	0,36	0,03	**92**
Turbidity	NTU	1314	1	**100**

The S3 water was visibly cloudier than S2, which was also reflected by the turbidity measurements, the S3 water had a turbidity (NTU) of over 20 times higher than the S2 water (Table 17)

4.5.2 Flux performance

The process in Figure 44 was continued using S3 water (60/3 configuration). Based on available information from Stavanger Slop, the new batch of slop water was not expected to be much of difference in filtration performance. However, the flux was significantly decreased, as shown in the results in Figure 44:

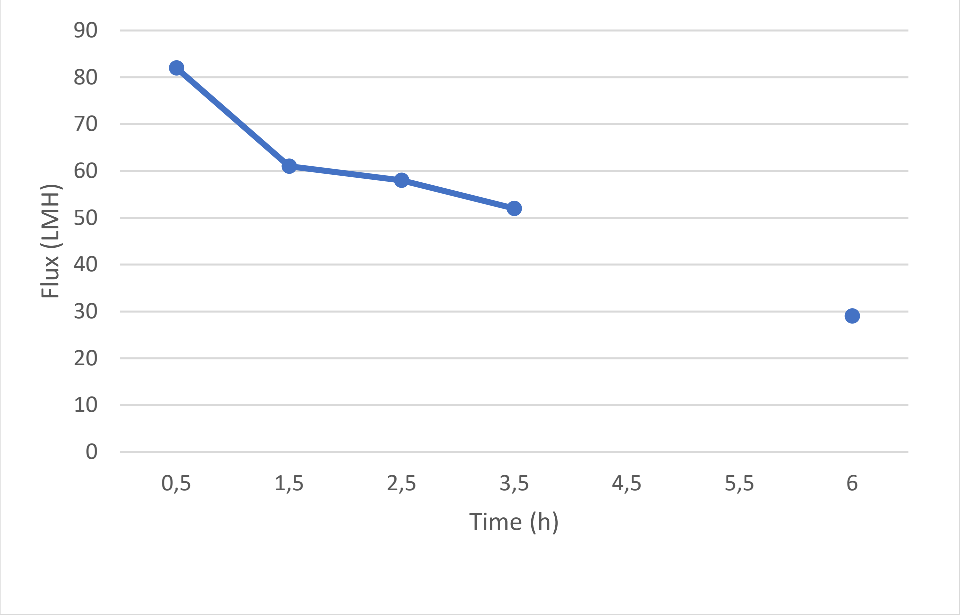

Figure 45: Permeate flux during a 60/3 configuration of S3 water

The flux rapidly declined after adding the S3 water to the feed tank. After 2 hours, the permeate flux had decreased by 48% compared to the average permeate flux in Figure 44, down to 64 LMH. The filtration was continued for a total of 6 hours. The permeate flux had then decreased down to 29 LMH, with an average net flux measured to be only 3 LMH. Therefore, it was decided to test the effect of dissolved air flotation as pre-treatment on the S3 water.

4.5.3 Dissolved air flotation as pre-treatment

The S3 water was treated using dissolved air flotation (DAF), according to the procedure described in chapter 3.4. After completing the DAF procedure, the sludge phase to clear phase ratio was measured to be approximately 1 to 5, as seen in Figure 46:

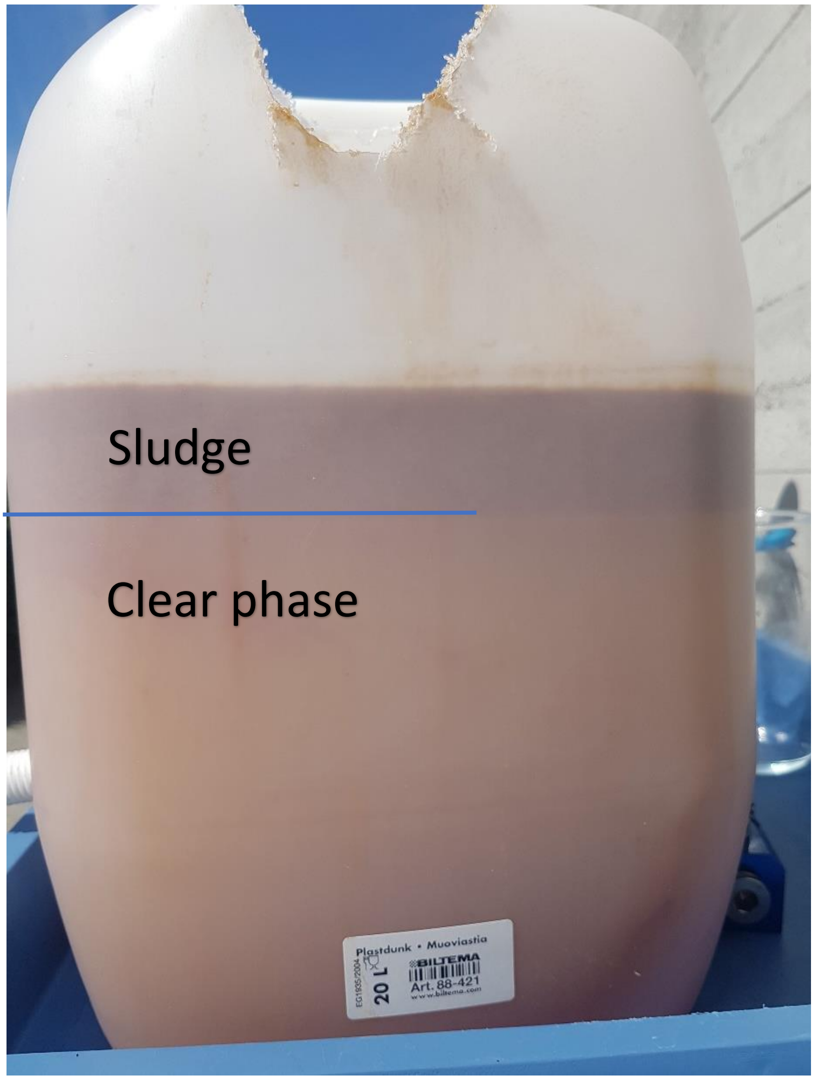

Figure 46: Sludge and clear phase after DAF treatment

4.5.4 Membrane performance after DAF pre-treatment

After treating the S3 water with DAF, the clear solution was placed in the feed tank of the membrane unit. From a visual perspective, the clear phase was significantly cleaner than the original feed, reflected by the turbidity which was down from 1314 in the original feed, to only 15 NTU after DAF. The DAF treated water was therefore considered to be relatively light to process and was run by a filtration/BW configuration of 600/10. The results are shown in Figure 47.

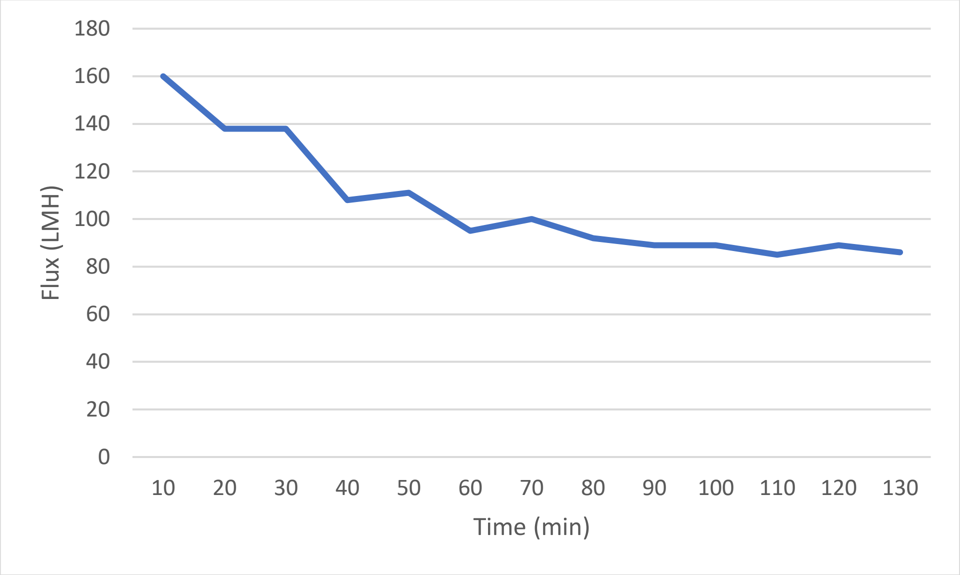

Figure 47: 60/10 configuration using DAF processed S3 water as feed

After two hours, the permeate flux stabilized around 90 LMH, an increase of 40% compared to Figure 45. The net flux was 79 LMH, which fits good with the predictions of from model 1 (Table 15). After running a total of 5 hours, the permeate flux was 65 LMH.

4.5.5 Sludge addition to feed

To get a view of how the membrane would react if there would be a problem with the DAF process (for example by operational error), the separated sludge seen in Figure 46 was mixed with the separated sludge and poured directly into the feed tank of the membrane unit while operating. It was expected that the membrane would experience rapid fouling as in Figure 45, therefore the filtration/BW configuration was set to 60/3, and the flux was monitored minute to minute, shown in Figure 48.

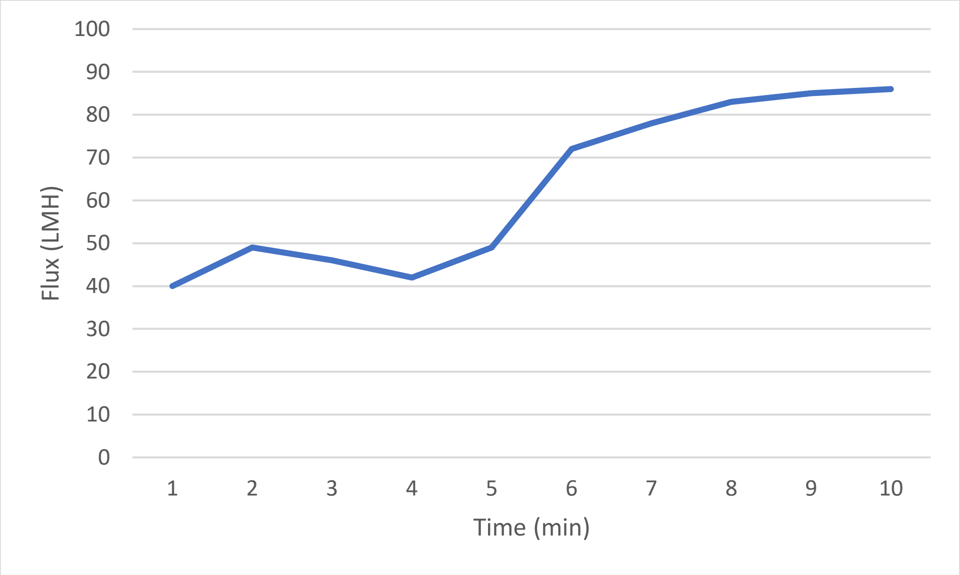

Figure 48: Permeate flux of the S3 water after mixing the sludge and clear phase from the DAF treatment, the first 10 minutes, 60/3 configuration

Right after the DAF-sludge was mixed with the membrane feed solution (DAF clear phase) the flux had a sudden drop from 65 LMH down to 40 LMH. But after 10 minutes the flux had increased to 86 LMH. The process was continued for 2 hours, shown in Figure 49

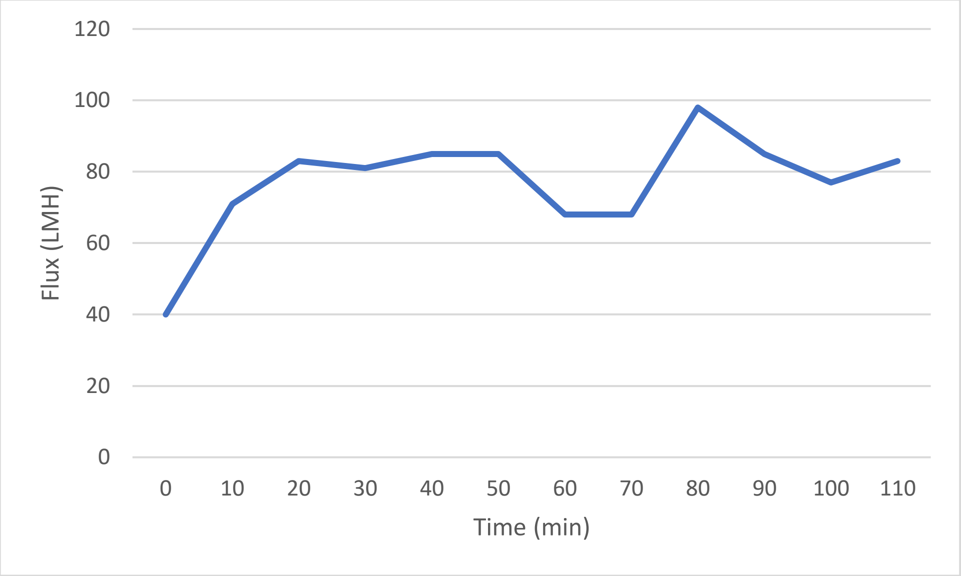

Figure 49: Extension of figure 48, continued filtration on sludge and clear phase from DAF, S3 water, 60/3 configuration

With a permeate flux stabilized around 80 LMH (Figure 49), which is an increase of 25% compared to the same configuration (60/3) prior to the pre-treatment (Figure 45).

This shows that the added mixture of coagulant ($FeCl_3$) from the DAF-process was beneficial to the efficiency of the filtration process, indicating that chemical enhancement using coagulant could be an effective tool for flux enhancement.

4.6 Results for S4 water

4.6.1 Removal rates

Table 17: Removal rates from the S4-water

Parameter	Unit	Feed	Permeate	Removal (%)
Oil concentration	ppm (vol.)	>400	-	-
TS	g/l	49,7	30,5	39
TSS	g/l	0,75	0,05	93
Turbidity (NTU)	NTU	2747	35	99

The S4 water was the most turbid water of the four wastewaters tested. Compared to the S2 water the turbidity was more than 42 times higher. This was also the only of the four wastewaters in which a visible organic phase was formed on the top of the solution, with a distinct smell of hydrocarbons. Two minor tests were performed on the S4 water, both with a 60/3 configuration. One with 50% BW-intensity (Figure 45) and one with 30% BW-intensity (Figure 46).

4.6.2 Flux performance

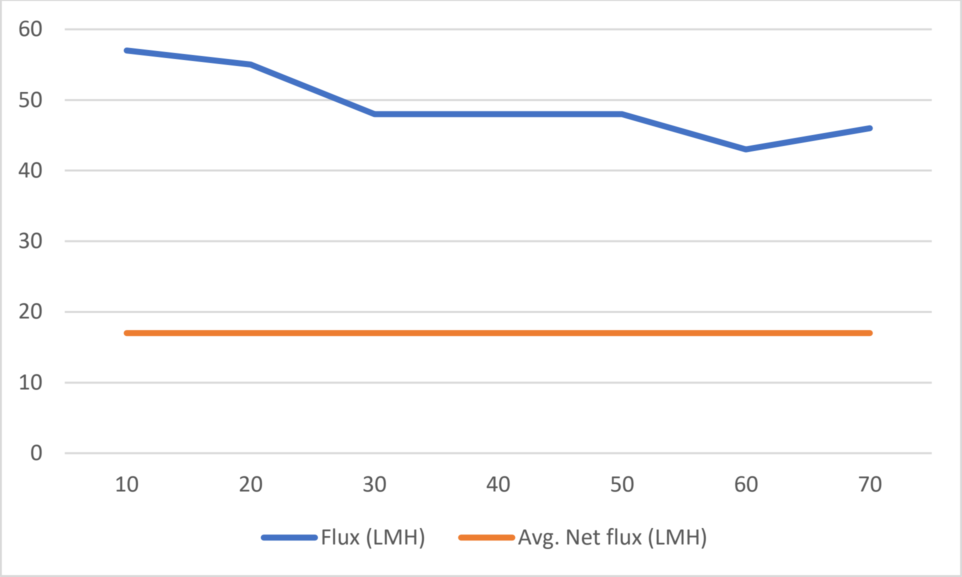

Figure 50: S4 permeate flux with a 60/3 configuration using 50% BW pump intensity

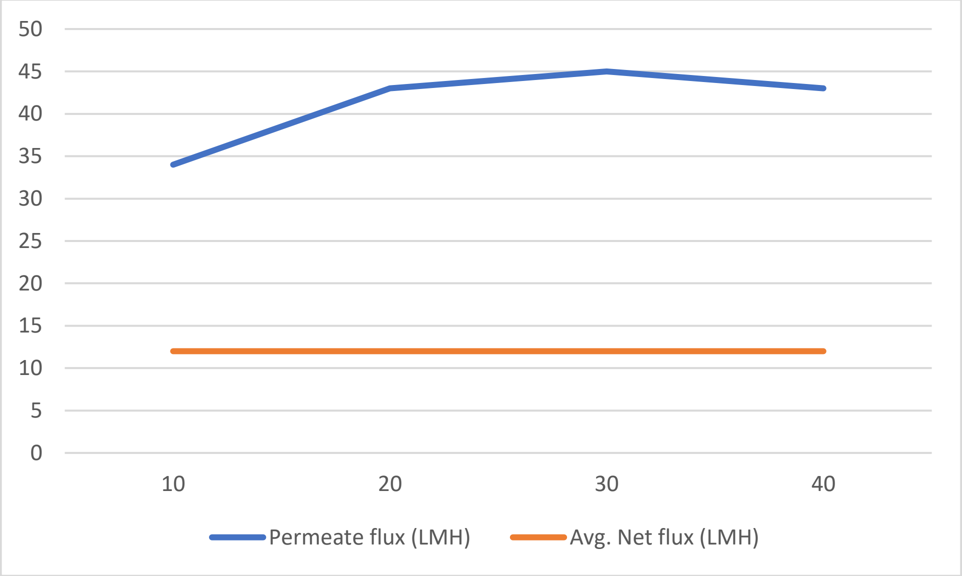

Figure 51: S4 permeate flux at 30% BW intensity, 60/3 configuration

The tests show that flowback water is fully capable of being treated by the flat sheet, even without pre-treatment. Average net flux measured in Figure 50 and 51 was 17 and 12, respectively.

4.7 Additional remarks

4.7.1 Cleaning

The membrane was cleaned both physically and chemically several times during the period of experiments. The membrane element to the right in Figure 52 shows how the membrane looks right after hydraulic backwashing. Flakes of the fouling layer have been repelled. It was observed during backwashing, that the maximum pressure provided from the BW-pump was only up to 0,7 bar. The information from the membrane manufacturer says that the maximum BW pressure is 2 bar. H

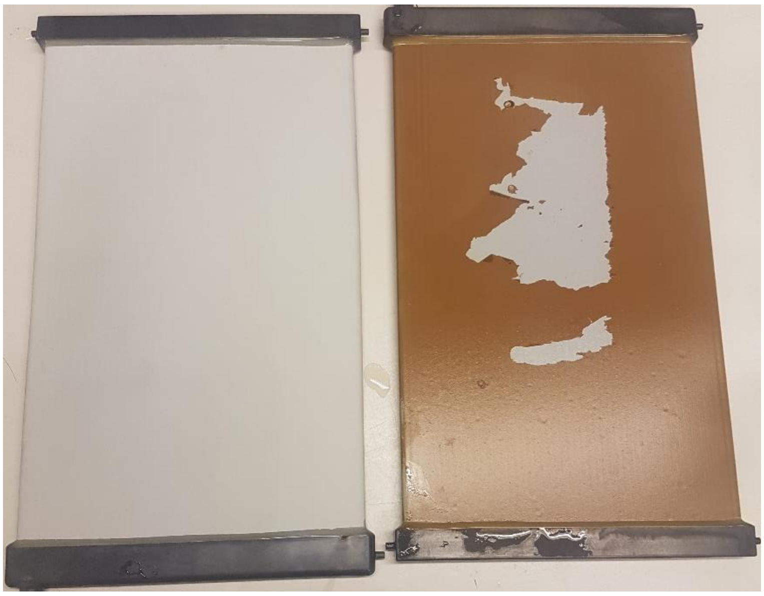

Figure 52: Clean membrane (left) and membrane with fouling layer, after hydraulic backwash

4.8 Energy analysis

The energy consumption during treatment of S2 water was measured and calculated as kWh consumed per liter of permeate produced without counting BW and net permeate produced (including BW-loss). The results are presented in Table 18 below:

Table 18: Energy consumption during 600/10, 60/1 and 60/3 configurations on the S2 water

Configuration		Permeate energy efficiency (kWh per liter permeate produced)	Total energy efficiency (kWh per liter net permeate produced)
Filtration duration (s)	***BW duration (s)***		
600	***10***	0,032	0,05
60	***1***	0,011	0,03
60	***3***	0,011	0,05

The numbers are considered unreasonably high. It is likely that since only one membrane was installed in the membrane unit when the measurements were made, the power consumption was excessive compared to the flowrate of produced permeate, because of oversized unit pumps, at least for only one membrane element. The data in Table 19 is therefore not considered as representable for the technology and should be further be investigated using maximum amount of membrane elements inserted in the unit before concluding.

5 Conceptual design: Development of a submerged flat-sheet slop water treatment unit

Based on the experiments in this thesis and other literature, a conceptual design for a slop water treatment unit is presented in this chapter.

The unit is designed as a complete wastewater purification system designed to recover contaminated water from offshore operational activity on rigs, floating production units, ships and other places where mobility and system flexibility is required.

The main purpose of the design is to have a practical look on this treatment technology, to see if it is suitable for offshore use in regards to treatment capability and footprint.

The unit is designed based on the need for:

1. *Automation*

   The need for trained personnel for operating this kind of unit is considered a major cost. The process should therefore be as easy as possible, preventing the need for excessive training and hiring of skilled personnel. The system has an easily operated HMI which is also controllable from onshore. An artificial neural network can also be integrated into the system, synchronized with available machine learning software pre-programmed to make adjustments to enhance the flux and limit fouling.

2. *Low footprint*

   Space is recognized to be limited. The flat sheet membranes are built in modules that can be stacked into towers into a standardized container. This will gain 132-396 m^2 of membrane surface area per container module.

3. *Easy replacement and extension of modules*

   Though the ceramic membranes are robust, the need for replacement of a single membrane is accounted for. The membrane module system is designed for easy access to every single membrane and can be replaced by any available personnel with basic mechanical experience by directions.

4. *Green technology*

   Membrane filtration requires no addition of chemicals. To enhance the filtration efficiency, chemicals such as surfactants, coagulants or flocculants may be added but the system does not require this to function.

Module framework

The unit consists of building blocks based on 1D ISO-containers (International Organization for Standardization), often referred to as 10-foot containers (Figure 43). The 1D containers internal dimensions are listed in Table 17.

Figure 53: Type 1D ISO-container (common name 10 foot container)

Table 19: Internal dimensions of a 1D container

Internal dimensions (mm)	
Height	2197
Width	2330
Length	2802

Table 20: Membrane module specifications retrieved from the manufacturer (Cembrane)

The container with its content is in this text considered as a part of the module unit system and referred to as a unit module, not to be confused with the membrane modules (Table 21).

Table 21: Membrane module/tower specifications retrieved from the manufacturer (Cembrane)

Membrane module/tower specifications	
Number of modules per single tower	1-15
Membrane surface area per module	6 m^2
Length	700 mm
Width	655 mm
Height of single module	450 mm
Extra height per module	160 mm
Cleaning options	Backpulse, pressure washing, sprinkler, CIP & CEP

The conceptual design of the modules is found in the following section. The membrane module is designed with an accurate container/membrane tower ratio based on a 1D ISO-container internal size (Table 17) and specifications from the membrane manufacturer (Cembrane) on the measurements of the membrane modules (Table 18). The DAF, NF/RO and Permeate-buffer container modules are for illustration only.

Membrane module

Figure 44 illustrates the main unit module, including the control center. The membrane tower is drawn in accurate size proportion relative to the container size. An empty sealed container have space for 3 times as many membranes (6 towers), and could be added as an alternative or as an extra module, given that pumps, control system and backpulsing tank can be placed externally.

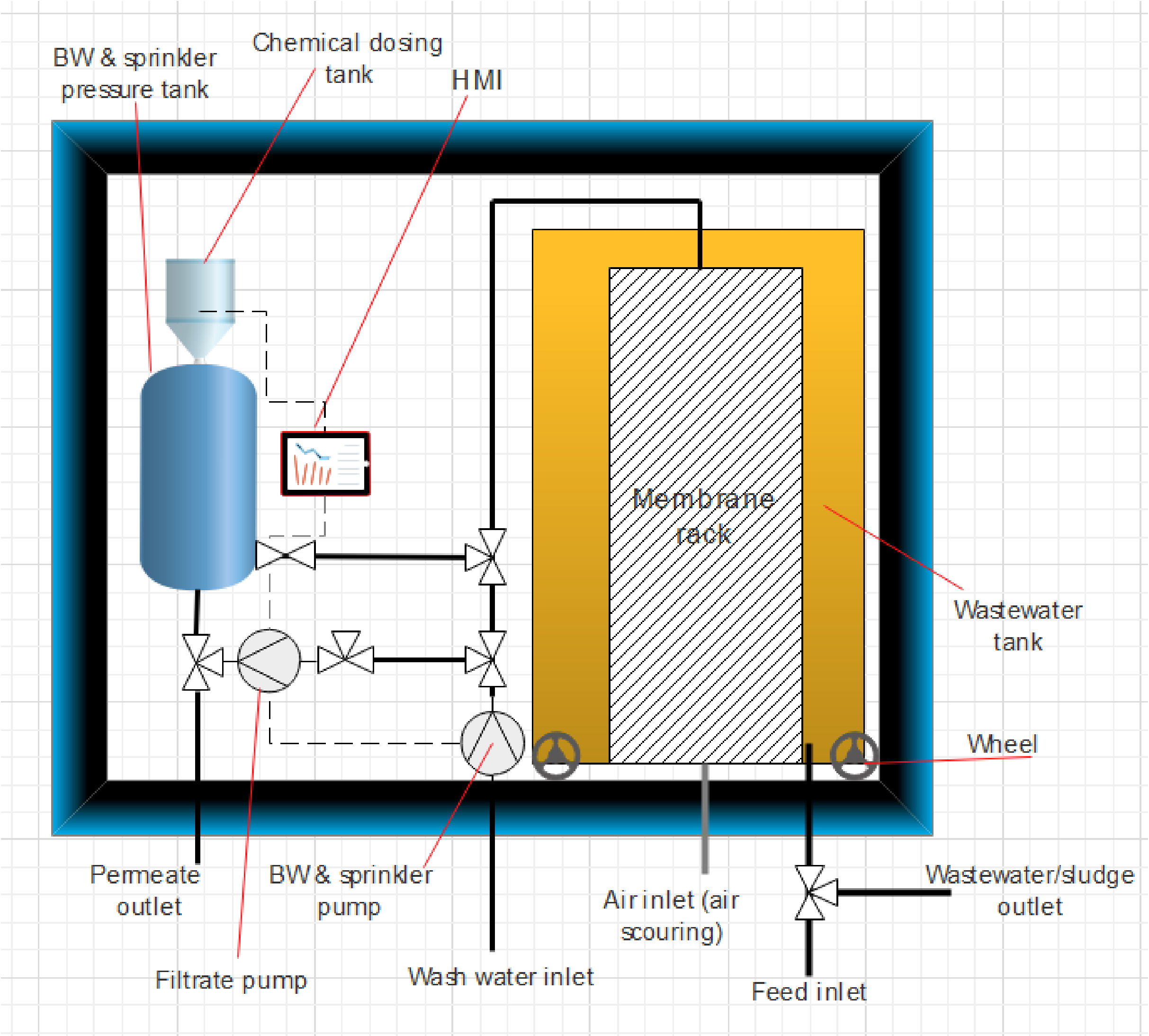

Figure 54: Concept of the membrane unit shown from the long side. Container/membrane tower ratio are drawn in scale relative to each other

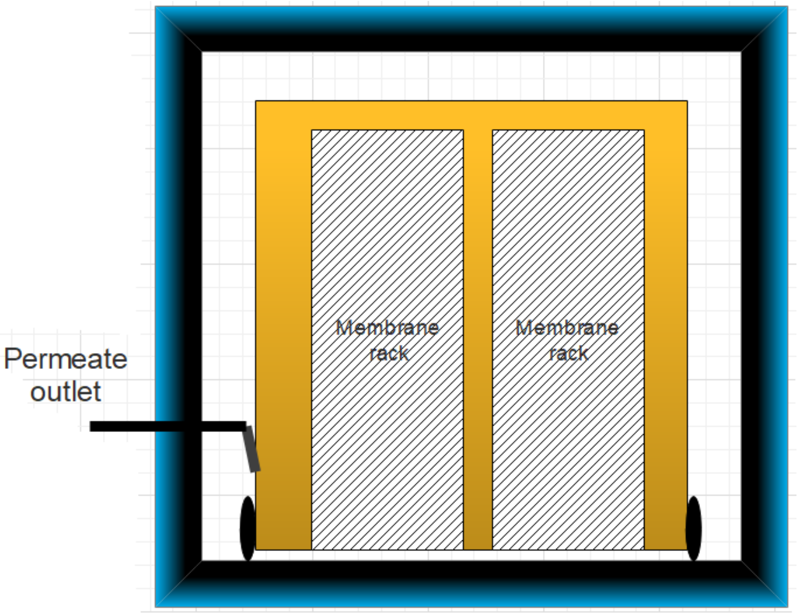

Figure 55: Membrane unit shown from short side. Container/membrane tower ratio are drawn in scale relative to each other.

Additional container modules

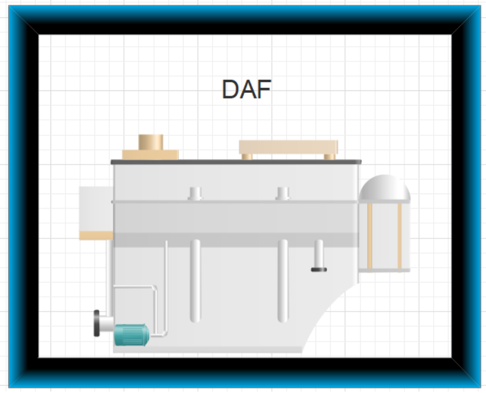

Figure 57: Dissolved air flotation module concept (not in scale)

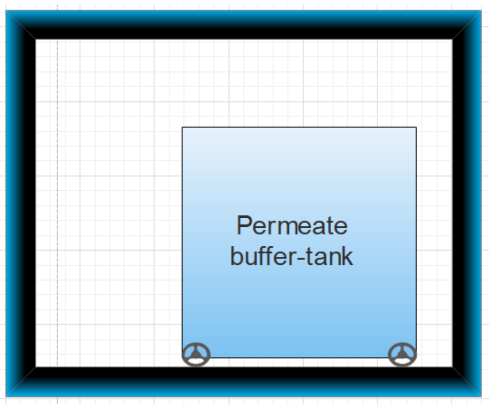

Figure 56: Permeate buffer tank container concept

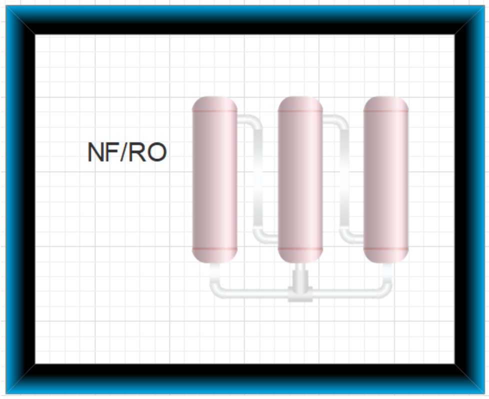

Figure 58: NF/RO (concept) separation container for complete purification (not in scale)

Module flowchart

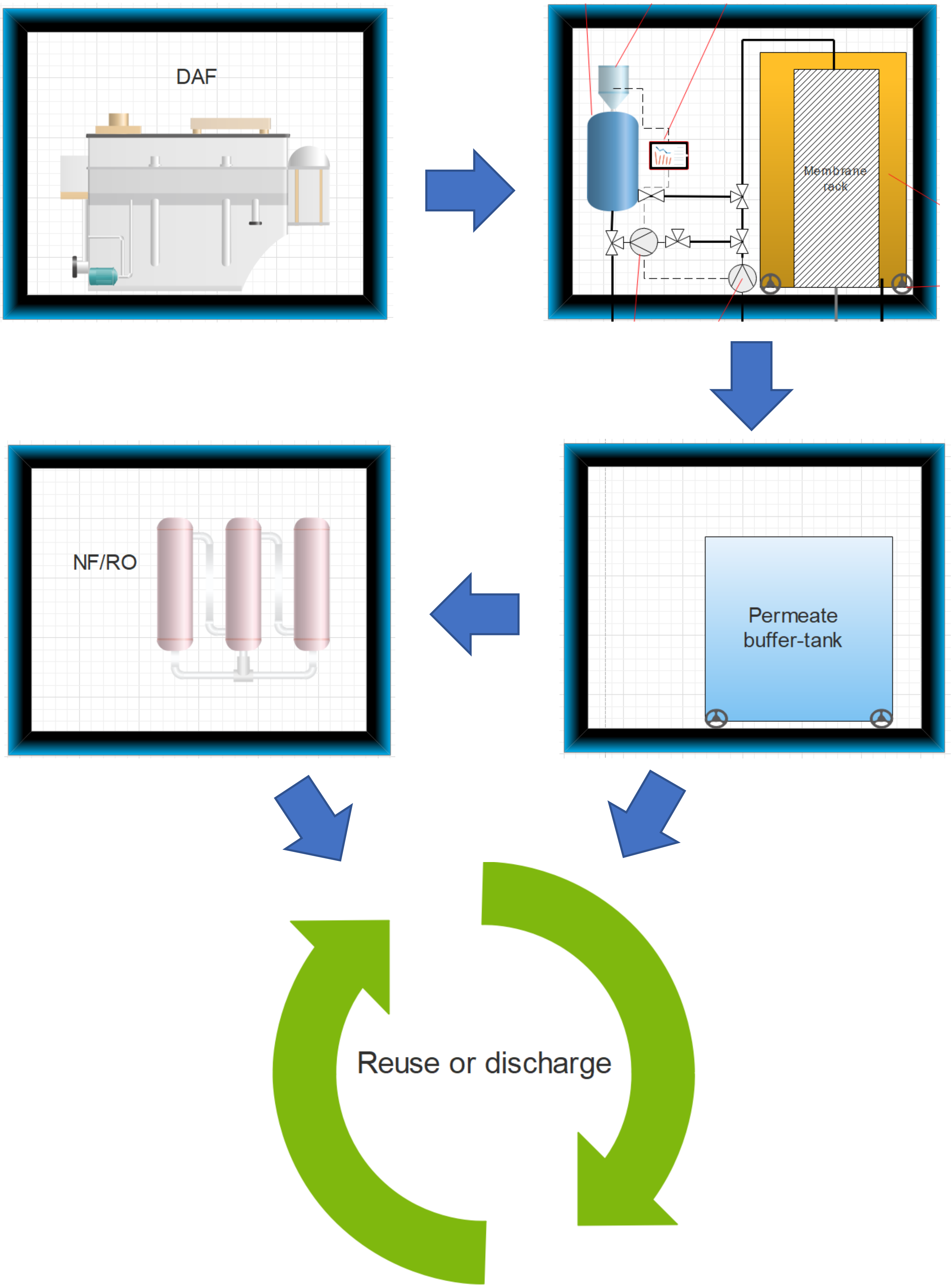

Flowrate

The membrane module container (Figure 54, 55) includes a total of 132 m^2 of membrane surface area, distributed by 22 membrane modules in two membrane towers. Given a net flux of 30 LMH, the output of the membrane container module will be $4m^3$/hour.

For extra high membrane treatment capacity, it is calculated that up to 6 membrane towers will fit in an extra module container of the same size (1D ISO), which can be controlled by the initial membrane container and powered by these pumps, given that the initial pumps and backpulse tank are dimensioned and adjusted accordingly. A module container with 6 towers will add an extra 396 m^2 of membrane surface area (528 including the initial 2 towers), which in theory will give a total net permeate flowrate of over 15 m^3 per hour, given a net flux of 30 LMH.

Cleaning

There are several options for cleaning the membrane unit. The following cleaning methods are suggested based on recommendations and possibilities available from the membrane manufacturer (Cembrane). Further testing is needed to evaluate the effect of the different membrane cleaning methods.

1. ***Pressure backpulsing***: The installed "BW & Sprinkler tank" can release small doses of pure permeate or permeate mixed with chemicals which can be rapidly released with a maximum pressure of 2 bar (maximum BW-pressure (Table 5). This reduces the amount of permeate spent for BW, by using rapid reverse pulsing into the system. This is done frequently during operation.
2. ***Traditional backwashing***: For longer cleaning durations, the permeate buffer tank (or other sources of clean water) can be connected to the BW pump. The BW water source can be infused with cleaning chemicals as well.
3. ***Sprinkler***: If the feed tank is emptied, the sprinklers can be activated. The water source is the "BW and sprinkler tank" and can also be enhanced by cleaning chemicals. The cleaning water is drained from the bottom of the feed tank.
4. ***Pressure washing***: The feed tank including the membrane module tower can be disconnected from the unit system and transported on the integrated wheels, out of the container. The membrane module tower is then lifted out of the tank and manually washed using pressure washers.

6 Conclusions

As a novel technology for offshore slop water treatment, a porous structured, submerged flat-sheet Silicon Carbide membrane with 0,1 µm pore size, installed in a pilot unit, was tested on four different slop waters. The wastewaters were labelled as S1, S2, S3 and S4, where S1 was considered representable for light slop, S2 was considered medium and S3 and S4 was considered as heavy slop based on flux overall flux performances. Special effort was put on how to optimize the membrane filtration process in terms of flux performance. Generally, the light slop water was able to be processed by the membrane unit with less frequent backwashing than the more contaminated water where the backwashing had to be performed more frequent to prevent fouling. A sustainable backwashing configuration for light slop was found to be 10 seconds of backwashing every 10 minutes (referred to as 600/10 configuration), while a good configuration for the heavier slop was found to be 3 seconds of backwashing every 1 minute (60/3).

Removal of contaminants by the membrane was considered satisfactory. Without any pre-treatment, the membrane removed oil in slop water by 100% when the feed concentration of oil was 12 ppm. The membrane also showed high removal of total suspended solids, which for the S1, S2, S3 and S4 water was removed by 100%, 96%, 93% and 92%, respectively.

In testing of S1 water, average permeate fluxes were found to be significantly higher with more frequent filtration/backwashing cycles, even when the filtration/backwashing ratio was overall the same. The permeate flux was more than 130% higher during 1 second of BW every minute (60/1), than for 10 second backwash every 10 minutes (600/10). It was also found that excessive amounts of permeate can be consumed by periodic backwash and that the frequency and duration should be chosen carefully depending on what needed to hold a stable flux.

Testing of the S2 water, two models (using 50% and 30% of the backwash pump intensity, respectively labelled as model 1 and model 2) were constructed as a foundation to determine backwash configurations. It was found that the volume of water consumed per second of backwash increased by over 200% as the filtration time decreased from 10 to 1 second of backwashing, when the backwashing pump was set to 50% intensity. When decreasing BW pump intensity down to 30%, the consumption was uniform for any duration of backwash. The model predictions were not found to be accurate enough for calculating net flux using measured permeate flux when 1-minute filtration cycles were performed. The model was more correct for the 10-minute filtration cycles and was an effective guiding tool for comparison and determining backwashing parameters.

The 60/3 and 60/1 configurations both gave a permeate fluxes on the S2 water of approximately 120 LMH, 3 times as high as the 600/10 configuration. However, the net flux was quite similar, around 30 LMH, for all the three configurations.

Expanding the membrane surface was beneficial. Running the 60/3 configuration on S2 water with 3 membrane elements instead of 1 gave a net flux of 114 LMH. However, the membrane fouled rapidly when the filtration was continued on the S3 water, with a 50% decrease in permeate flux after 2 hours, leaving a net flux of only 3 LMH after 6 hours of filtration.

Pretreatment was necessary for heavy slop. Filtration of the pretreated water using 600/10 configuration resulted in a 40% higher permeate flux than using the 60/3 configuration prior to pre-treatment. It was also found that by adding the separated sludge from the flotation process back to the membrane feed tank and using the 60/3 configuration, the permeate flux increased by over 40%

compared to the 600/10 configuration on the pre-treated water and increased 25% compared to running the 60/3 configuration prior to the pre-treatment. This indicates that skipping the dissolved air flotation process and adding the coagulant directly into the feed tank, also referred to as hybrid flotation, could be a viable option and a subject for further studies.

The membrane was also able to process highly oil-contaminated water. Indication testing performed on the S4 water resulted in an average permeate flux of 49 LMH and a net flux of 17 LMH, with 3 seconds BW per minute.

Energy consumption was measured using S2 water and it was found that permeate could be produced with an energy efficiency of 0,02 kWh per liter of permeate. This is however not considered representable as the pilot unit is not built for energy efficiency.

With the produced data from this research, a design of a mobile slop water treatment unit was suggested. The possibility for upscaling the membrane treatment method for slop water was considered feasible, though further studies on long-term durability is recommended. Experiments on up-concentration limits in the feed were not performed, but should be evaluated in further research, as this will certainly be a limiting factor for the technology. The effect of micelle enhanced filtration or hybrid filtration are considered as possible technologies for expanding this limitation, as well as enhancement of the dissolved air flotation process.

The submerged membrane technology offers a high packing density when stacked into modules and towers, with a membrane surface area of over 190 m^2 per m^2 of floor space when stacked to full height (2,7m). It was shown in a conceptual design that 396 m^2 of membrane surface area was possible to pack into a standardized 1D ISO-container (14 m^3), excluding pumps and control unit (132 m^2 if pumps and control unit integrated in the container/module). Even with a net flux down to 15 LMH, a maximum stacked module would result in a flowrate of 6 m^3 per hour. Most of the observed net fluxes from the experiments is therefore considered high enough due to the available packing density.

For achieving optimal net flux, configuration for backwash should not be constant, but adjusted according to wastewater quality and membrane behavior and performance. Novel technologies such as artificial neural network software should therefore be investigated further and possibly be implemented to the design of the unit to gain optimized efficiency.

Overall, the air-scouring submerged silicon carbide membrane is a technology that is compact, and suited for lightly contaminated slop without pre-treatment, and also for more heavy slop in combination pre-treatment such as dissolved air flotation.

Further testing is needed before realization of design, but the overall impression based on the results, the technology showed to be promising. Considering the obtained fluxes throughout the testing, the compactness of the technology makes it a promising technology for oily wastewater treatment.

References

Aarestrup, T. (2018). [Notes from MLJ630, Separation Technology].

Abadi, S. R. H., Sebzari, M. R., Hemati, M., Rekabdar, F., & Mohammadi, T. (2011). Ceramic membrane performance in microfiltration of oily wastewater. *Desalination, 265*(1-3), 222-228.

Abderrazak, H., & Hmida, E. S. B. H. (2011). Silicon carbide: Synthesis and properties. In *Properties and applications of Silicon Carbide*: InTech.

Aktivitetsforskriften, § 60a (2010).

Al-Zoubi, H., Al-Thyabat, S., & Al-Khatib, L. (2009). A hybrid flotation–membrane process for wastewater treatment: an overview. *Desalination and Water Treatment, 7*(1-3), 60-70.

Biesheuvel, P. M., & Verweij, H. (1999). Design of ceramic membrane supports: permeability, tensile strength and stress. *Journal of membrane science, 156*(1), 141-152.

Boch, P., & Niepce, J.-C. (2010). *Ceramic Materials: Processes, Properties, and Applications* (Vol. 98): John Wiley & Sons.

Carlin, E. M. (2002). Oil pollution from ships at sea: The ability of nations to protect a blue planet. *Environmental regime effectiveness: confronting theory with evidence*, 331.

Castricum, H. L., Kreiter, R., van Veen, H. M., Blank, D. H., Vente, J. F., & Johan, E. (2008). High-performance hybrid pervaporation membranes with superior hydrothermal and acid stability. *Journal of membrane science, 324*(1-2), 111-118.

Cembrane. Retrieved from http://cembrane.com/wp-content/uploads/Cembrane-Company-Brochure1.pdf

Cerafiltec. Break-through performance in Ground water Middle East. Retrieved from http://cembrane.com/2018/04/14/break-through-performance-in-ground-water-middle-east/

Cheryan, M. (1998). *Ultrafiltration and microfiltration handbook*: CRC press.

Chilkoor, G., Shrestha, N., Soeder, D., & Gadhamshetty, V. (2018). Corrosion and environmental impacts during the flowback water disposal associated with the Bakken shale. *Corrosion Science, 133*, 48-60.

De Vos, R. M., & Verweij, H. (1998). High-selectivity, high-flux silica membranes for gas separation. *Science, 279*(5357), 1710-1711.

Deriszadeh, A., Husein, M. M., & Harding, T. G. (2010). Produced water treatment by micellar-enhanced ultrafiltration. *Environmental science & technology, 44*(5), 1767-1772.

DNV-GL. (2017). *Oil & Gas forecast to 2050 - Energy transition outlook*. Retrieved from

El–Safty, S. A., & Hoa, N. D. (2012). Organic–Inorganic Mesoporous Silica Nanotube Hybrid Anodic Alumina Membranes for Ultrafine Filtration of Noble Metal Nanoparticles. In *Noble Metals*: InTech.

Ghali, E., Sastri, V. S., & Elboujdaini, M. (2007). *Corrosion prevention and protection: practical solutions*: John Wiley & Sons.

Gillot, J. (1991). The developing use of inorganic membranes: A historical perspective. In *Inorganic Membranes Synthesis, Characteristics and Applications* (pp. 1-9): Springer.

Gitis, V., & Rothenberg, G. (2016). *Ceramic Membranes,*

New Opportunities and Practical Applications: Wiley-VCH.

Glagovich, N. (2013). IR absorptions for representative functional groups. *Accessed on April, 11*.

Griffin, J. (2003). Pompeii, by Robert Harris. *SPECTATOR-LONDON-WEEKLY-, 293*, 53-53.

Higgins, F. (2012). Environmentally friendly oil in water analysis by FTIR spectroscopy, based on ASTM 7678-11. In: Agilent Technologies, Danbury, CT, USA.

Howell, J., Chua, H., & Arnot, T. (2004). In situ manipulation of critical flux in a submerged membrane bioreactor using variable aeration rates, and effects of membrane history. *Journal of membrane science, 242*(1-2), 13-19.

Hwang, K.-J., Chan, C.-S., & Tung, K.-L. (2009). Effect of backwash on the performance of submerged membrane filtration. *Journal of membrane science, 330*(1-2), 349-356.

Jones, D. S., & Pujadó, P. P. (2006). *Handbook of petroleum processing*: Springer Science & Business Media.

Kekre, K., Ang, W. S., Niwa, T., Yamashita, T., Shiota, H., & Noguchi, H. (2015). Production of Industrial Grade Water for Reuse from Industrial Used Water using UASB+ CMBR Process. *Proceedings of the Water Environment Federation, 2015*(16), 150-158.

Koltuniewicz, A. B. (2015). Submerged Membrane. In. Encyclopedia of Membranes: Springer Link.

Körting-Hannover. Retrieved from https://www.koerting.de/en/jet-pumps-for-pressurised-dissolved-air-flotation.html

Lenntech. Retrieved from https://www.lenntech.com/microfiltration-and-ultrafiltration.htm

Li, X., & Li, J. (2015). Critical Flux. In E. Drioli & L. Giorno (Eds.), *Encyclopedia of Membranes* (pp. 1-3). Berlin, Heidelberg: Springer Berlin Heidelberg.

Lin, Y., Kumakiri, I., Nair, B., & Alsyouri, H. (2002). Microporous inorganic membranes. *Separation and Purification Methods, 31*(2), 229-379.

Liqtech. Retrieved from https://www.liqtech.com/our-technology/

Loeb, S., & Sourirajan, S. (1962). Sea water demineralization by means of an osmotic membrane. In: ACS Publications.

Management agency revised basin management plan project. (2003). Retrieved from https://books.google.no/books?id=cgozAQAAMAAJ&printsec=frontcover&hl=no#v=onepage&q&f=false.

Mazille, & Spuhler. Coagulation-Flocculation. Retrieved from http://archive.sswm.info/category/implementation-tools/water-purification/hardware/semi-centralised-drinking-water-treatmen-7

McCosh, K. L., Kapila, M., Dixit, R., Way, P. W., & Phipps, J. (2009). Continuous improvement in slop-mud treatment technology. *SPE Drilling & Completion, 24*(03), 418-423.

McNaught, A. D., & Wilkinson, A. (1997). International Union of Pure and Applied Chemistry. *Compendium of chemical terminology: IUPAC recommendations, 2*.

Meidensha. Wastewater Treatment Facility on Campus of Guilin University of Technology in China. Retrieved from http://www.meidensha.com/products/case/prod_03/prod_03_02/prod_03_02_01/1210639_4256.html

Metcalf, E., & Eddy, M. (2014). Wastewater engineering: treatment and Resource recovery. *Mic Graw-Hill, USA*.

Miljødirektoratet. (2017). *OSPAR*. http://www.miljodirektoratet.no/no/Tema/Olje_og_gass/OSPAR/.

Miyahara, S., Sugimoto, M., Takaya, H., Watanabe, Y., Soejima, N., & Ishikawa, T. (2015). Silicon carbide semiconductor device. In: Google Patents.

Nath, K. (2017). *Membrane separation processes*: PHI Learning Pvt. Ltd.

OSPAR. (2015). Principles. Retrieved from https://www.ospar.org/about/principles

Owoeye, F., Olokode, O., Aiyedun, P., & Anyanwu, B. (2012). *Preparation and Characterization of Ceramic Microfiltration Membrane for Water Treatment.* Paper presented at the 4th International Conference on Engineering Research and Development (ICERD 2012), paper number ICERD.

Pabby, A. K., Rizvi, S. S., & Requena, A. M. S. (2008). *Handbook of membrane separations: chemical, pharmaceutical, food, and biotechnological applications*: CRC press.

Pentair. Retrieved from https://xflow.pentair.com/en/technologies/membrane-technology-in-general

Process-Technology, M. a. Retrieved from http://www.mediaandprocess.com/products/products01.html

Rahimi, M., Madaeni, S., Abolhasani, M., & Alsairafi, A. A. (2009). CFD and experimental studies of fouling of a microfiltration membrane. *Chemical Engineering and Processing: Process Intensification, 48*(9), 1405-1413.

Schmitt, F., & Do, K.-U. (2017). Prediction of membrane fouling using artificial neural networks for wastewater treated by membrane bioreactor technologies: bottlenecks and possibilities. *Environmental Science and Pollution Research, 24*(29), 22885-22913.

Sengur, R., Deveci, G., Kaya, R., Turken, T., Guclu, S., Imer, D. Y., & Koyuncu, I. (2015). CFD modeling of submerged membrane bioreactors (sMBRs): a review. *Desalination and Water Treatment, 55*(7), 1747-1761.

Shackleton, R. (1987). The application of ceramic membranes to the biological industries. *Journal of Chemical Technology and Biotechnology, 37*(1), 67-69.

Sorbwater. (2014). Slop Water. Retrieved from http://www.sorbwater.com/slop-water.html

Stuart, B. (2005). *Infrared spectroscopy*: Wiley Online Library.

Tianjin-Motimo. Retrieved from http://www.motimo.com/OTHER/en/about/?127.html

Van Gestel, T., Vandecasteele, C., Buekenhoudt, A., Dotremont, C., Luyten, J., Van der Bruggen, B., & Maes, G. (2003). Corrosion properties of alumina and titania NF membranes. *Journal of membrane science, 214*(1), 21-29.

Yacou, C., Wang, D., Motuzas, J., Zhang, X., Smart, S., & Diniz da Costa, J. C. (2013). Thin-Film Ceramic Membranes. *Encyclopedia of Membrane Science and Technology*.

Ødegård, H. (2014). *Vann- og avløpsteknikk* (H. Ødegård Ed. 2nd ed.): Norsk Vann.

Appendices

1)

Backwash duration (s)	BW frequency (s)	Time (h)	Produced V_p(l)	Net flux (LMH)
100	600	2,5	5,1	31

Figure 59: Permeate production with 100 s relaxation of membrane and 600 s filtration cycles

2)

S2 600/10 configuration

time (h)	flux	net flux (LMH)	T	P end
0	69	69	22	0,25
1,5	47,1	46,3	20	0,46
3	43,4	31,4	17	0,52
5,75		29,3	19	0,52
10,75	39,7	18,9	16	0,54

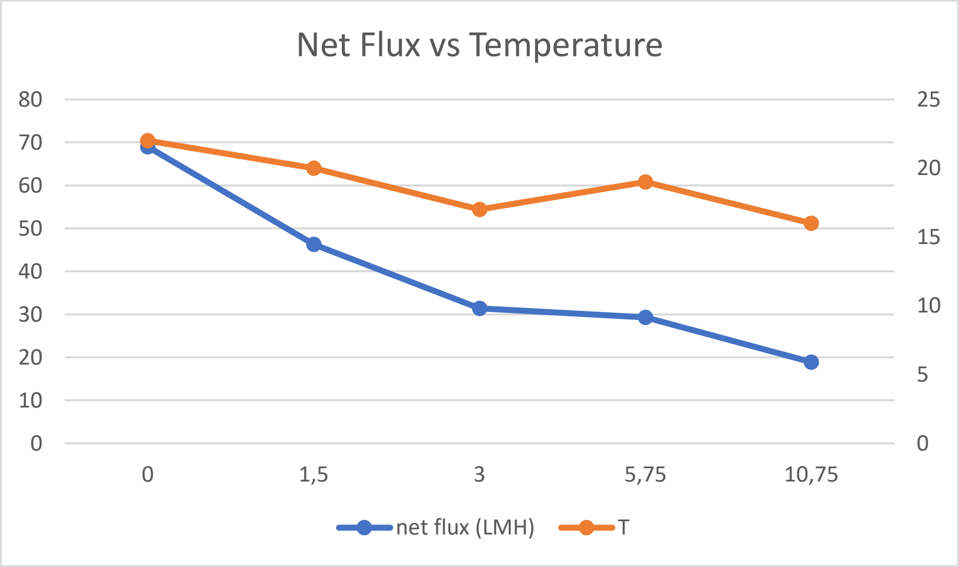

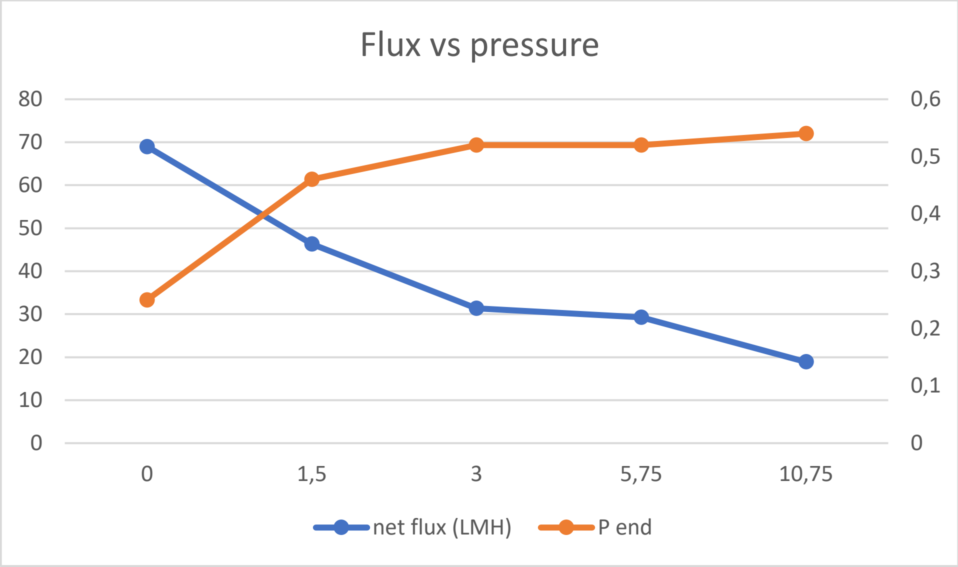

3)

60/1 Slop

Time (min)	T	P	Volume/10 min	Flux (LMH)	Accumulated net volume (l)	Net flux
10	22	0,22	1,52	140,3	1,52	
30	22	0,25	1,554	143,4		
60	22	0,28	0,315/2 min	145	4,62	60,9

4)

	50% pump	flux	pressure	temp
60/1				
start vol: 3,5 l				
0,5	3,35	103	0,35	25
1	3,8	117	0,25	24
1,5	4,1	126	0,26	23
2	4,1	126	0,26	23
2,5	4,1	126	0,26	23
3	4,25	131	0,25	22
end vol: 9,4				
akkumulert end vol: 9,4 - 3,5 = 5,9 liter				
net flux: 30,3 LMH				
power consumption: 0,35 kWh = 0,059 kWh/l				

5)

3 membraner = 0,065 x 3 = 0,195 m2

60/3	set P: 0,01 bar=> 25% pump					
time h						
0,25	5,1	105	0,01	23	4,9	
0,5	7	148	0,03	23	5	
0,75	6,6	135	0,05	23	3,8	
1	6	123	0,05	23	6	
1,25	5	102	0,05	22	5	
1,5	7	144	0,06	21	7	
end vol: 5,65					sum: 31,7	
accumulated: 1,65						
totalt produsert: 31,7 + 1,65 = 33,35 liter						
net flux: 114 LMH						
brutto flux: 121						
BW flux: 7 LMH						

6)

start vol: 4l

time (hours)	permeate vol	permeate flux	T	P (-bar)
0,5	8	82	19	0,15
1,5	11,9	61	18	0,17
2,5	11,4	58	18	0,18
3,5	10,1	52	18	0,18
6	13,9	29	18	0,19
end vol: 7,6				
accumulated vol: 3,6				
net flux: 3 LMH				
power consumption: 0,71 kWh				

7)

tilsetter ny slop		**start vol: 4l**		
0,5	8	82	0,15	19
1			0,17	18

1,5	11,9	61	0,18	18
2,5	11,4	58	0,18	18
3,5	10,1	52	0,19	18
6	13,9	29	0,2	18
end vol: 7,5 -4 = 3,5 l				
net flux = 3 LMH				
brutto flux = 47 LMH				

8)

Backwash	**cleaning wp**	**set flow control**	**temperature**	**turbidity**
600/10	30s/300s	15 l/h is equal to pump at 25%	16 oC	28 FNU
time(h)	Vp, total (l)	Vbw (l), lost		
1	4,75	1,57		
2	8	3,14		
3	11,75	4,71		
4	14,25	6,28		
5	16,8	7,85		
6	19	9,42		

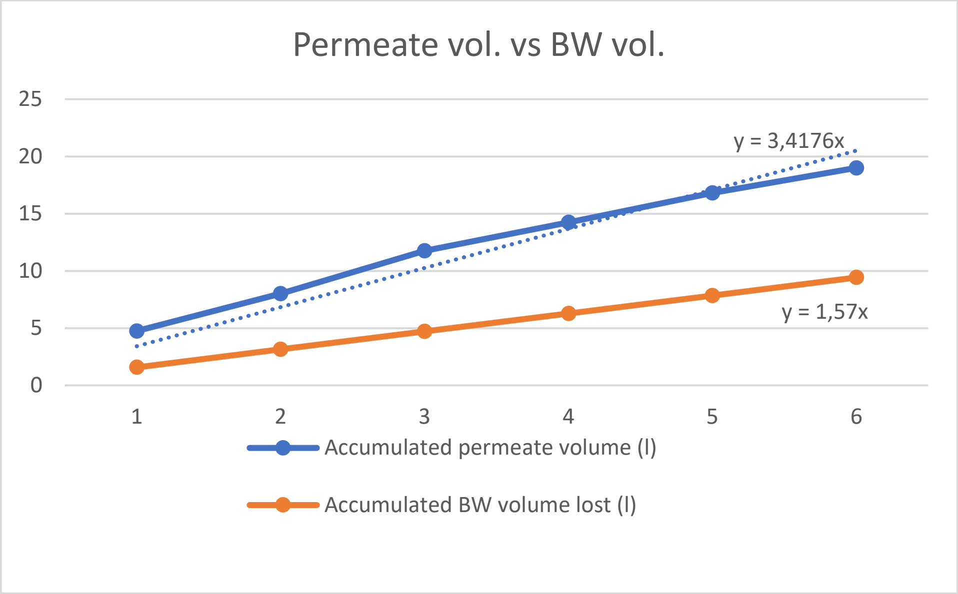

Figure 60: Accumulated volume of permeate vs. Accumulated volume of permeate consumed for BW

Table 22: Collected data in Figure 42 used to calculate the amount of backwash consumed

Total permeate vol. (l)	Total vol. lost in BW	net permeate vol. (l)	Permeate flux (LMH)	net flux (LMH)
19	9,4	9,6	48,7	24,6

Lost in BW (l)	Per sec BW	Per min BW	Per h BW
	0,026	1,57	94

9)

Table 23: : Volume of BW (ml) per backwash cycle and per second in each BW configuration at 50% BW pump intentsity

BW duration (s)	BW vol (ml) per BW	BW vol/s
1	29,4	29,4
2	52,5	26,3
3	54,6	18,2
5	82,1	16,4
10	92,6	9,26

Table 24: Volume of BW (ml) per backwash cycle and per second in each BW configuration at 30% BW pump intentsity

BW time	BW vol (ml) per BW	BW vol/s
1	5,4	5,4
2	12,9	6,5

3	15	5
5	25	5
10	68	6,8

10)

Table 25: Baseline for the BW model (50% pump intensity)

1s BW

Filtration time	Cycles per hour	BW vol/h (l)
30	120	3,529
60	60	1,764
120	30	0,882
300	12	0,353
600	6	0,177
2s BW		
Filtration time	Cycles per hour	BW vol/h (l)
30	120	6,3
60	60	3,15
120	30	1,575
300	12	0,63
600	6	0,315
3s BW		
Filtration time	Cycles per hour	BW vol/h (l)
30	120	6,552
60	60	3,276
120	30	1,638
300	12	0,656
600	6	0,328
5s BW		
Filtration time	Cycles per hour	BW vol/h (l)
30	120	9,852
60	60	4,926
120	30	2,463
300	12	0,986
600	6	0,493
10s BW		

Filtration time	Cycles per hour	BW vol/h (l)
30	120	11,112
60	60	5,556
120	30	2,778
300	12	1,111
600	6	0,556

Table 26: Baseline for the BW model (30% pump intensity)

1s BW

Filtration time	Cycles per hour	BW vol/h (l)
30	120	0,648
60	60	0,324
120	30	0,162
300	12	0,065
600	6	0,0324

2s BW

Filtration time	Cycles per hour	BW vol/h (l)
30	120	1,548
60	60	0,774
120	30	0,387
300	12	0,155
600	6	0,0774

3s BW

Filtration time	Cycles per hour	BW vol/h (l)
30	120	1,8
60	60	0,9
120	30	0,45
300	12	0,18
600	6	0,09

5s BW

Filtration time	Cycles per hour	BW vol/h (l)
30	120	3
60	60	1,5
120	30	0,75
300	12	0,3
600	6	0,15

	10s BW			
	Filtration time	Cycles per hour		BW vol/h (l)
	30	120		8,16
	60	60		4,08
	120	30		2,04
	300	12		0,816
	600	6		0,408

11)

Table 27: S2 water, 600/10

Cycle (a 10min)	**(-)P(@end)**	**T (oC)**	**Permeate flux (LMH)**	**net flux (LMH)**	**net vol. (l)**	**Vp**	**power consumption**
1	0,25	22	69,2			750	
2	0,32	22	57,7			625	
3	0,35	21	49,8			540	
4	0,39	20	57,8			626	
5	0,42	20	57,4			622	
6	0,43	21	57,3			621	
7	0,45	20	55,6			602	
8	0,46	20	54,6			591	
9	0,46	20	47,1	46,3	4,51	510	
10	0,46	20	33,2			360	
11	0,48	20	28,6			310	
12	0,48	19	43,4			470	
13	0,5	19	41,5			450	
14	0,5	19	46,2			500	
15	0,51	18	44,3			480	
16	0,51	18	44,3			480	
17	0,51	18	44,3			480	
18	0,52	17	43,4			470	
19		18	48,4	31,4	6,46	524	0,42 kWh